THE UNIVERSITY OF CALGARY

The Tube Method for Extremes of 2-D Random Fields

by

Xing Wei

A THESIS

SUBMITTED TO THE FACULTY OF GRADUATE STUDIES

IN PARTIAL FULFILLMENT OF THE REQUIREMENTS FOR THE

DEGREE OF MASTER OF SCIENCE IN CIVIL ENGINEERING

DEPARTMENT OF CIVIL ENGINEERING

CALGARY, ALBERTA

JUNE, 1998

Abstract

The extreme value distributions of random fields are critically important in reliability and safety analysis and they are generally approximated using point-process methods, which have their own limitations.

In this thesis, the tube method, an alternative approach first suggested by Sun (1993), is improved and an asymptotic approximation for the maxima of a 2D differentiable non-homogeneous Gaussian random field is developed. This method is based on geometrical concepts and it provides the approximation directly without any assumption about the random field and with little computational effort.

The relationship between geometrical concepts and the extreme value distribution of a random field is discussed. Then the development of the proposed tube method is demonstrated in detail, followed by comparisons between the proposed method and existing methods. The extreme value distribution associated with boundaries and endpoints of the random field are also studied and the corresponding formulas are given.

The accuracy and the efficiency of the proposed method are verified by simulation and compared with other existing methods for 2D differentiable Gaussian random fields, homogeneous and not. The application to practical problems is demonstrated by an application to air pollutant concentrations, during which, the complete analysis procedure of the tube method is outlined and the application of the discretization methods of random fields to the tube method is discussed. The verifications, comparisons and applications show that the proposed method is accurate, efficient and flexible in its application to any type of Gaussian random field.

Acknowledgements

I would like to express my sincere thanks to all of those contributed in some way to the development of this research and my education.

I am particularly indebted to the chairman of the thesis committee Professor M. A. Maes for his caring guidance and continuing encouragement throughout the period of this research. His resourcefulness knowledge and constructive criticisms expand the limits of my own capacity. I was exceedingly fortunate to have been able to learn from him.

I also owe an enormous debt of gratitude to my former supervisor, Professor Jie Li, for his guidance on my study.

My appreciation is also extended to the remaining members of the thesis committee and my fellow students: Ingrid Farasyn and Luc Husye.

This research was made possible by a University of Calgary Graduate Teaching Assistantship and the support from the secretaries in the Department of Civil Engineering.

I am also extremely grateful to my wife, parents and the family of my sister for their encouragement, love and inspiration.

Table of Contents

List of Tables

List of Figures

Nomenclature

$a_i(t)$	i^{th} discretization function of a ground motion process
a_0	area of a random field with rectangular domain
a_i	i^{th} deterministic parameter
c_1	square root of the absolute value of the metric tensor matrix $\mathbf{M}$
c_2	coefficient related to the sencod derivatives of $\mathbf{h(t)}$
c_3	equal to $c_2 + 1$
$c(t)$	c_1 for the one-dimensional case
$\mathbf{C}$	covariance matrix of the nodal values of the random field $Z(\mathbf{t})$
$Cov[X, Y]$	covariance of the random variables X and Y
$COV_{\widehat{P}}$	coefficient of variation of $\widehat{P}$
$\mathbf{E}_i$	i^{th} unit coordinate vector related to the manifold M
$\mathbf{E}_i^*$	i^{th} unit coordinate vector related to the manifold M^*
$\widetilde{\mathbf{E}}_i$	i^{th} unit coordinate vector related to the neighborhood $N(M)$
$\mathbf{E}_a$	tangential vector of boundary a at endpoint i of the random field $Z(\mathbf{t})$
$\mathbf{E}_b$	tangential vector of boundary b at endpoint i of the random field $Z(\mathbf{t})$
$\mathbf{G}_i$	$k \times k$ matrix with components $g^i_{j\nu}$
$\mathbf{h(t)}$	vector listing the normalized discretization function of the random field $Z(\mathbf{t})$
$h_i(\mathbf{t})$	i^{th} normalized discretization function of the random field $Z(\mathbf{t})$
$\mathbf{h}^*(\mathbf{t})$	vector listing the discretization function of the random field $Z(\mathbf{t})$

$h_i^*(\mathbf{t})$	i^{th} discretization function of the random field $Z(\mathbf{t})$
$\mathbf{h}_{lj}$	second derivatives of $\mathbf{h}(\mathbf{t})$
$\mathbf{H}$	$k \times k$ matrix with components $\mathbf{h}_{lj}$
$\widetilde{\mathbf{h}}_{lj}$	vector defined in equation (3.66)
$\widetilde{\mathbf{H}}$	$k \times k$ matrix with components $\widetilde{\mathbf{h}}_{lj}$
$\mathbf{h}_{lj}^+$	vector defined in equation (3.109)
$h_f(t)$	unit-impulse response function of the second order linear filter representing the local soil
$f_Z(z)$	probability density function (p.d.f.) of $Z(\mathbf{t})$
$F_Z(z)$	cumulative distribution function (c.d.f.) of $Z(\mathbf{t})$
$f_{\chi_n}(r)$	probability density function of a χ_n-random variable
$\mathbf{I}_k$	$k \times k$ unit matrix
i	imaginary unit
$j_0(\theta)$	function defined in equation (3.26)
$j_2(\theta)$	function defined in equation (3.27)
k	the dimension of the random field $Z(\mathbf{t})$
M	k-dimensional manifold on the surface of the unit sphere S^n
M^*	$(n-1)$-dimensional manifold on the surface of the unit sphere S^n
$\mathbf{M}$	metric tensor matrix of the manifold M or M^*
$m(\mathbf{t})$	mean value function of a random field
$m_{ij}(\mathbf{t})$	the metric tensor coefficient, the scalar product of $\mathbf{E}_i$ and $\mathbf{E}_j$, component of $\mathbf{M}$
$\mathbf{n}_l$	l^{th} coordinate vector normal to the space spanned by $\mathbf{E}_i$

n	the dimension of the unit sphere S^n
n_b	number of the boundaries of the random field $Z(\mathbf{t})$
n_e	number of the endpoints of the random field $Z(\mathbf{t})$
n_z	number of samples of the random field $Z(\mathbf{t})$
n_{ex}	number of samples of the random field $Z(\mathbf{t})$ that exceed the threshold β
$N(M)$	the neighborhood of the manifold M
$N_\beta(T)$	number of upcrossings of β by $Z(t)$ in $[0,T]$
$\widehat{P}$	estimated $P(\beta)$
$\mathbf{P}$	projection matrix onto the space spanned by $\mathbf{n}_1, \mathbf{n}_2, ..., \mathbf{n}_m$
$\mathbf{P}^*$	projection matrix onto the space spanned by $\mathbf{E}_1, \mathbf{E}_2, ..., \mathbf{E}_k, \mathbf{y}$
$P(\beta)$	probability that the maximum of a random field is greater than β
$q_k(t)$	modulation function of the k^{th} filter representing the local soil
$r(\mathbf{t})$	the distance between the endpoints of $\mathbf{U}$ and $\mathbf{h}(\mathbf{t})$
r	$r(\mathbf{t})$ at a specified $\mathbf{t}$
r_c	radius of curvature of the manifold M
R_n	random variable having a χ_n-random variable with probability density function
r_n	a sample of R_n
$R(\boldsymbol{\tau})$	autocorrelation function of a homogeneous random field
$R(\mathbf{s},\mathbf{t})$	autocorrelation function of a random field
$R_{ZZ}(\mathbf{t}_1,\mathbf{t}_2)$	
or $R(\mathbf{t}_1,\mathbf{t}_2)$	autocorrelation function of the random field $Z(\mathbf{t})$
R^n	n-dimensional space

S	intrinsic scalar curvature of the manifold M
S^n	n-dimensional unit sphere
$S(\omega)$	power spectral density of a wide-sense homogeneous random field
$\mathbf{t}$	time vector
t_i	i^{th} component of the vector $\mathbf{t}$
$\mathbf{T}$	domain of the random field $Z(\mathbf{t})$
$\ddot{u}_f(t)$	acceleration of the soil layer relative to the bedrock
$\mathbf{U}$	vector with uniform distribution on the n-dimensional unit sphere
$V(\mathbf{t})$	nodal value of a random field at time point $\mathbf{t}$
$V_{n-1}(N)$	the volume of the $n-1$-dimensional neighborhood of the manifold M
W_i	i^{th} component of the random pulse train representing the discretized white noise $W(t)$
$W(t)$	stationary white noise process
x	a sample of a random variable
X	a ramdom variable
$\mathbf{x}$	a sample of a random vector
$\mathbf{X}$	a random vector
X_i	i^{th} component of the random vector $\mathbf{X}$
$\mathbf{y}$	vector of endpoints of $\mathbf{h}(\mathbf{t})$
$Z(\mathbf{t})$	a random field
Z_i	a sequence of random variables
z_i	a sample of Z_i
α_i	angle between two boundaries at point i

β	a specified threshold level
$\beta(\mathbf{t})$	variable level to be considered in the case of a non-zero-mean random field
$\Gamma(\cdot)$	Gamma function
δ_{ij}	Kronecker delta
$\Delta\mathbf{t}$	time interval
λ_{ij}	spectral moment of a stochastic process, defined by equation (2.31)
λ_i	i^{th} eigenvalue of the covariance function $R(\mathbf{t}_1, \mathbf{t}_2)$
$\lambda_\beta(t)$	number of upcrossings of β by $Z(t)$ per unit time
$\Psi_0(\beta)$	function defined in equation (3.127)
$\Psi_2(\beta)$	function defined in equation (3.128)
Φ_0	intensity of the white noise $W(t)$
$\Phi(\cdot)$	standard normal distribution function
Φ_i	i^{th} eigenvector of the covariance matrix $\mathbf{C}$
σ	constant standard deviation of a random field
$\sigma(\mathbf{t})$	standard deviation function of a random field
$\sigma_Z^2(\mathbf{t})$	variance of the random field $Z(\mathbf{t})$
τ	time vector difference $\mathbf{t}_2 - \mathbf{t}_1$
ω	frequency vector
ω_n	the volume of the surface area of a n-dimensional unit sphere
ω_f	natural frequency of the second order linear filter representing the local soil
ξ_f	damping ratio of the second order linear filter representing the local soil
θ	angle between the vectors $\mathbf{U}$ and $\mathbf{h}(\mathbf{t})$
$\mathbf{\Lambda}_{11}$	a matrix defined by equation (2.30)

$\mathbb{E}\{g(X)\}$	expected value or mean value of the arbitrary function $g(x)$
ρ_{ij}	dimensionless coefficient of correlation of two random variables
$A \cap B$	the intersection of sets A and B
$\#\{A\}$	number of occurrence of event A
$\langle \mathbf{x}, \mathbf{y} \rangle$	scalar product of two vectors $\mathbf{x}$ and $\mathbf{y}$
$\lvert\mathbf{X}\rvert$	length of the vector $\mathbf{X}$: $\lvert\mathbf{X}\rvert = \sqrt{\langle \mathbf{X}, \mathbf{X} \rangle}$
$P_r(A)$	probability that the event A occurs

Chapter 1

Introduction and Objective

1.1 Introduction

Traditionally, structural analysis is based on deterministic methods: all loading parameters, material and geometric properties are considered to be known with certainty. To quote Lin (1963): "since no material is perfectly homogeneous, no beam is perfectly uniform, and no rivet perfectly fits a hole, etc., it is clear that the probabilistic viewpoint is more realistic".

The simpler deterministic approach may of course be satisfactory if uncertainties regarding material properties are small and loads and load effects can be predicted precisely. In reality however, loads (especially dynamic ones such as loads due to earthquake, blast, wind loads, sea waves) are usually difficult to predict and the uncertainties in geometric parameters, material properties (especially in the case of composite materials), and boundary conditions may be large, depending on different situations. Therefore, it is often more reasonable and accurate to use a probabilistic model in structural analysis.

In the last two decades, much effort has been devoted to the research and applications of probabilistic theory in the general area of engineering mechanics and structural engineering and probabilistic design requirements have been incorporated in most building codes. In practice, the uncertainties or responses in the analysis models are often represented by 1- or 2-dimensional random fields (see section 2.2). Those

dependent only on continuous time, such as earthquake ground motion, dynamic response at a specified point, and those dependent on one-dimensional space, such as structural parameters of bar elements, are 1-dimensional random fields, whereas 2-dimensional random fields usually have domains such as space-space or time-space, for instance, wind load on a high-rise building or space-space (boundary conditions or parameters of a plate).

In many engineering problems, particularly in the area of reliability and safety analysis of structures, it is always necessary and important to evaluate the extreme value distribution of random fields. Two main failure mechanisms can be considered in the probabilistic structural analysis (Sólnes, 1997): 1. the system may fail due to the maxima response exceeding a certain threshold once (first-passage); 2. the system may tolerate several response exceedances of a certain limit (cumulative damage). In both cases, the extreme value distribution of the response plays an important role. Similarly, the maxima of other random fields are also of major concerns in probabilistic structural analysis and it is concluded by several authors (e.g. Yao and Wen, 1996) that a common feature of structural reliability techniques is the reformulation of the problem into a time-invariant one using the extreme value distribution of the random fields in some time domain.

The development of extreme value theory of random fields dates back to the early work of Rice (1944, 1945) in the 1940's. Subsequent progress and applications can be found in several papers and books by Powell (1958), Gumbel (1958), Leadbetter (1967, 1983), Adler (1981), Vanmarcke (1983) and others. For stationary random fields, considerable methodology is derived in Cramer and Leadbetter (1967) and Leadbetter (1983) and for non-stationary sequences in Leadbetter (1983). Approxi-

mation equations for the extreme value distributions of homogeneous random fields can be found in Adler (1981) and Vanmarcke (1983), whereas those for stationary Gaussian vector processes can be found in Breitung (1994). Bounds are derived for univariate non-stationary Gaussian processes and for non-stationary Gaussian vector processes in Breitung (1990).

A common feature of these widely used methods is that they are approximation methods based on point process theory of exceedances or upcrossings. According to Adler (1981), there are only six exact formulas for the extreme value distributions of random processes, corresponding to six covariance functions of random processes. For k-dimensional random fields and other random processes ($k = 1$), we are forced to turn to asymptotic results in order to obtain any information at all about these distributions. This may be enough for most engineering problems since they usually deal with the upper tail probabilities of one or two-dimensional random fields. However, problems may occur in the applications of traditional methods to practical situations. First, one should verify that the obtained approximations are not only bounds, but asymptotically exact, by proving that the approximating point process converges to a Poisson process which involves much more complicated mathematics than the derivation of the approximation itself (Breitung and Maes, etc., 1995). Second, traditional methods for the extreme value distributions of random fields are mostly limited to the homogeneous cases, while practical problems are often non-homogeneous.

A different approach named the 'tube method' was first recommended by Sun in 1993. This method calculates the approximations directly so that it avoids the verification of the convergence of the point process of exceedances to a Poisson pro-

cess. Furthermore, it can easily be extended to non-homogeneous random fields. As described by the name 'tube', this new approach is based on geometric concepts. By analyzing the problems of the maxima of random fields, one can find that they are related to the volume of neighborhoods of a manifold on the surface of a unit sphere. For a one-dimensional case, the manifold is a curve on the surface of the unit sphere, whereas the neighborhood, consisting of the points contributing to the extreme value distribution, looks like a tube around the curve. This leads to the name of the tube method.

As early as 1930's, formulas for the volume of neighborhoods of a k-dimensional manifold embedded in an n-dimensional unit sphere have been suggested. Hotelling (1939) derives a formula for the one-dimensional case, followed by a formula derived by Weyl (1939) for the general k-dimensional case. Weyl's formula is applicable to any finite dimensional manifold. However, as shown in Chapter 3, it involves the scalar curvature in its higher term corresponding to higher dimensional manifolds ($k \geq 2$), which is difficult to evaluate directly.

In Sun (1993), Weyl's formula is used directly in the derivation of the extreme value distribution of a differential non-homogeneous Gaussian random field with constant variance and no boundary. Without listing the details of the derivation, Sun gives a two-term approximation formula. Following Sun's footsteps, Maes and Breitung (1996) extend the tube method to random fields with time dependent variance and propose an improved two-term equation similar to Sun's formula (Sun, 1993) but more general. Farasyn (1997) investigates, tests and improves the tube method mainly for one-dimensional random fields. By combining Hotelling's formula (Hotelling, 1939) for the volume of neighborhoods with the problem of the maxima

of stochastic processes, Farasyn (1997) derives approximations for the maxima of one-dimensional non-stationary Gaussian processes, and also develops a formula for the probability associated with the endpoints of the stochastic processes.

Since Sun's two-term formula, as well as Maes and Breitung's extended formula are both derived directly using Weyl's volume formula (Weyl, 1939), the second terms of both formulas involve the scalar curvature. In an application of the tube method to a practical problem, Sun (1991) used a simulation method to obtain the scalar curvature in a special case that the metric tensor matrix (equation (3.28)) is diagonal, in order to avoid calculating it directly. But this method is not suitable for practical problems since it consumes too much computational effort in addition to the fact that the special condition is not always satisfied in practical situations. Therefore, in order to enhance the feasibility of the tube method, the formula for the volume of neighborhoods has to be improved to get rid of the scalar curvature. It will be shown in Chapter 3 that the scalar curvature is generated in the evaluation of an integration involved in the calculation of the volume of neighborhoods. So the focus is to find a different way to evaluate that integral.

An effective effort in this direction, is the projection method, introduced by Breitung (1997). A scalar vector product, which is much easier to evaluate, is derived to substitute the term involving the scalar curvature in Weyl's formula. Although it will be shown that this particular scalar vector product is incorrect, the projection method will prove to be an effective method to improve the volume formula in Chapter 3.

1.2 Objectives

The main objective of this thesis is to develop a practical algorithm for the approximation of the extreme value distributions of 2D differentiable Gaussian random fields by improving the tube method.

This is achieved using Breitung's projection method (1997). Comparisons between the proposed formula and the Monte Carlo simulation method, other existing methods, together with practical applications show that the tube method is applicable to general classes of 2D differentiable Gaussian random fields and it is accurate and efficient.

This thesis is organized as follows: following the introduction, Chapter 2 summarizes basic concepts of random fields and traditional extreme value theory, then discretization methods of random fields are discussed and two efficient discretization methods are introduced, since the tube method requires that random fields must be expressed in a discrete form in terms of a set of random variables. Chapter 3 is devoted to the investigation of the tube method. A formula for the volume of neighborhoods of a 2D manifold on the surface of an n-dimensional unit sphere is developed using Breitung's projection method. Based on this, an approximation of the extreme value distribution of a 2D Gaussian random field is derived. The details of the derivation are demonstrated. In Chapter 4, the analysis procedure of the tube method will first be outlined. Then a simulation method is performed to test the accuracy of the proposed formula. Furthermore, comparisons between the tube method and other existing methods are made. Lastly, the tube method is applied to a practical problem in order to verify its feasibility in practical situations.

Conclusions and recommendations are given in Chapter 5.

Chapter 2

Random Fields and Extremes

2.1 Introduction

Random fields and extreme value theory are introduced in this chapter. In section 2.2, the basic concepts of random fields in civil engineering are summarized. Traditional extreme value theory is outlined in section 2.3. In section 2.4, two efficient discretization methods of random fields are discussed in detail, as the discretization of a random field is an important step in practical problems involving random media.

2.2 Basic Concepts of Random Fields

Many engineering problems are typified by temporal or spatial random variations. Often, it is not precise enough to represent them by random variables only. Continuous or discrete random field models are the only way to accurately reflect those realities and they are fundamental for design or prediction purposes.

The theory of random fields was first introduced in the 1970s. Significant advances and applications have been made in recent years, especially with the development of the stochastic finite element method and reliability analysis. In this section, the basic concepts of random fields are introduced.

The random field is a natural extension of the one-dimensional stochastic process to a multi-dimensional Euclidean space. It can be regarded as a random variable

system defined on the parameterized space in which each point is corresponding to a random variable. Examples of stochastic processes are market fluctuations on the stock exchange, earthquake ground motion, etc., whereas sea waves, structural parameters, wind loads and soil properties are examples of random fields. A detailed study of the properties of stochastic processes can be found in many well known books, for instance Lin (1967) or Papoulis (1991), whereas clear descriptions of properties related to random fields can be found in Adler (1981) or Vanmarcke (1983). Since stochastic processes can be regarded as special one-dimensional cases of random fields, it is only necessary to introduce the properties of the general case of random fields.

Let $Z(\mathbf{t})$, $\mathbf{t} = (t_1, t_2, ..., t_k) \in \mathbf{T}$, denote a random field defined within the domain $\mathbf{T}$, where k is the dimension of the random field. The value $k = 1$ means that $Z(t)$ is a stochastic process and $k = 2$ means $Z(\mathbf{t})$ a plane random field. For any value of the deterministic parameter $\mathbf{t}$, $Z(\mathbf{t})$ is a random variable $Z = Z(\mathbf{t})$ whose value is described only by the probability laws that govern the random field. For an observed value $z = z(\mathbf{t})$, assume event $A = \{Z \leq z\}$, with $\Pr(A)$ denoting the probability that A occurs which is defined by the cumulative distribution function (c.d.f.) of Z:

$$\Pr[A] = \Pr[Z \leq z] = F_Z(z) \tag{2.1}$$

$F(z)$ increases monotonically from 0 to 1 as z increases from -∞ to +∞. The probability density function (p.d.f.) of Z is defined by the derivative of $F_Z(z)$:

$$f_Z(z) = dF_Z(z)/dz \tag{2.2}$$

The c.d.f. and the p.d.f. may not completely reflect the probability laws that define a random field. In a strict probability sense, the probability laws are finite dimensional distributions which are represented by the joint cumulative distribution function of random variables at fixed point $\mathbf{t}_i$ $(i = 1, 2, ..., m)$,

$$\begin{aligned} & F_Z(z_1, z_2, ..., z_m; \mathbf{t}_1, \mathbf{t}_2, ..., \mathbf{t}_m) \\ = \; & \Pr[Z(\mathbf{t}_1) < z_1 \cap Z(\mathbf{t}_2) < z_2 \cap ... \cap Z(\mathbf{t}_m) < z_m] \end{aligned} \tag{2.3}$$

for finite m. However, in practical situations, it is almost impossible to evaluate the probability structure of a random field by means of the finite dimensional distributions since they can hardly be determined. Instead, the first two order moments, expected value function $m(\mathbf{t})$ and autocorrelation function $R(\mathbf{t}, \mathbf{t}')$ can be used to represent the probability structure of a random field, where $\mathbf{t}$ and $\mathbf{t}'$ are two distinct points in the domain $\mathbf{T}$.

The expected value function $m(\mathbf{t})$ and autocorrelation function $R(\mathbf{t}, \mathbf{t}')$ of the random field $Z(\mathbf{t})$ are defined separately as,

$$m(\mathbf{t}) = \mathbb{E}\{Z(\mathbf{t})\} \tag{2.4}$$

$$R(\mathbf{t}, \mathbf{t}') = \mathbb{E}\left\{Z(\mathbf{t})\, Z(\mathbf{t}')\right\} \tag{2.5}$$

in which $\mathbb{E}\{\cdot\}$ is the expected value operator, defined as,

$$\mathbb{E}\{g(X)\} = \int_{-\infty}^{+\infty} g(x)\, f(x)\, dx \tag{2.6}$$

in which X is a random variable with the p.d.f. $f(x)$ and $g(x)$ is an arbitrary function of x. The variance of $Z(\mathbf{t})$ is,

$$Var\left[Z(\mathbf{t})\right] = \mathbb{E}\left\{\left[Z(\mathbf{t}) - m(\mathbf{t})\right]^2\right\} = \sigma^2(\mathbf{t}) \tag{2.7}$$

whose square root $\sigma(\mathbf{t})$ is referred to as the standard deviation function of $Z(\mathbf{t})$.

It is the homogenous property of a random field that corresponds to the stationarity of a stochastic process. Similar to a stochastic process, a random field is called strict-sense homogeneous when its finite distribution function is not dependent on $\mathbf{t}$ or wide -sense homogeneous when the first two moments are invariant to $\mathbf{t}$. For the wide-sense situations, $m(\mathbf{t}), \sigma(\mathbf{t})$ are constants and the autocorrelation function is not a function of $\mathbf{t}$ either but a function of $\boldsymbol{\tau}$, which denotes the time interval $\mathbf{t} - \mathbf{t}' = (t_1 - t_1', t_2 - t_2', ..., t_n - t_n') = \boldsymbol{\tau} = (\tau_1, \tau_2, ..., \tau_n)$ between $\mathbf{t}$ and $\mathbf{t}'$, then

$$R(\boldsymbol{\tau}) = R(\mathbf{t} - \mathbf{t}') = \mathbb{E}\left\{Z(\mathbf{t})Z(\mathbf{t} + \boldsymbol{\tau})\right\} \tag{2.8}$$

For a Gaussian random field, all finite dimensional distributions are normal distributions and completely determined by the first two moments. This means that all the probability structures of a Gaussian random field depend only on $m(\mathbf{t})$ and $R(\mathbf{t}, \mathbf{t}')$. Therefore, a Gaussian random field is strictly homogeneous if it is weakly homogeneous and the estimation of the first two moments is sufficient. In this thesis, we mainly deal with the Gaussian random field.

For the two random variables $Z_1 = Z(\mathbf{t}_1)$ and $Z_2 = Z(\mathbf{t}_2)$ with mean values m_1, m_2 and standard deviations σ_1 and σ_2, respectively, the covariance of them is defined

as the expected value of the product of the deviations from their respective means,

$$\begin{aligned} Cov\,[Z_1, Z_2] &= \mathbb{E}\{(Z_1 - m_1)\ (Z_2 - m_2)\} \\ &= \mathbb{E}\{Z_1\, Z_2\} - m_1 m_2 \qquad (2.9) \\ &= R(\mathbf{t}_1, \mathbf{t}_2) - m_1 m_2 \qquad (2.10) \end{aligned}$$

according to equation (2.5).

Dividing the above covariance by σ_1 and σ_2 leads to the dimensionless coefficient of correlation between Z_1 and Z_2 :

$$\rho_{12} = \frac{Cov\,[Z_1, Z_2]}{\sigma_1 \sigma_2} \qquad (2.11)$$

$\rho_{12} = 0$ means Z_1 and Z_2 are uncorrelated. Independence between two random variables implies lack of correlation, but not vice versa except for those of normally distributed random variables.

The above definitions are all limited to the time domain. In the analysis of the frequency domain of a homogeneous random field $Z(\mathbf{t})$, one of the most useful definitions is the power spectral density, which is the Fourier transform of the autocorrelation function $R(\boldsymbol{\tau})$ of $Z(\mathbf{t})$:

$$S(\boldsymbol{\omega}) = \frac{1}{2\pi} \int_{-\infty}^{+\infty} R(\boldsymbol{\tau})\ e^{-i\boldsymbol{\omega}\boldsymbol{\tau}} d\boldsymbol{\tau} \qquad (2.12)$$

where $\boldsymbol{\omega} = (\omega_1, \omega_2, ..., \omega_n)$ is a vector of frequencies and i is the imaginary unit: $i = \sqrt{-1}$.

2.3 Extremes

As introduced in Chapter 1, research about maxima of random fields has mostly been limited to the one dimensional case. The existing higher dimensional approaches are generalizations of the well established one-dimensional theory. In this section, traditional one-dimensional extreme theory is first outlined, followed by the introduction of Vanmarcke's and Adler's approaches as the examples of the few studies of maxima of higher dimensional random fields. Most of the approaches are based on the following concepts of point process theory.

A point process generally refers to a series of discrete events occurring in time, or space, or both of them, according to some statistical law. Of major concern is when the events are the occurrences of upcrossings of a high level β by a stochastic process or a random field and exceedances of a high level β by a sequence of random variables.

2.3.1 Level Upcrossings of Stochastic Processes

Given is a differentiable stochastic process $Z(t)$ with derivative process $Z'(t)$ and defined in the interval $[0, T]$. Then the event

$$Z(t_0) = \beta \text{ and } Z'(t_0) > 0 \tag{2.13}$$

means that a path $Z(t)$ crosses the level β from below at a time point t_0, which is called an upcrossing as shown in Figure (2.1). The upcrossings define a point process

with the number $N_\beta(T)$ of upcrossings of β by $Z(t)$ in $[0,T]$ equal to:

$$N_\beta(T) = \#\left\{t \in [0,T], Z(t) = \beta \text{ and } Z'(t) > 0\right\} \tag{2.14}$$

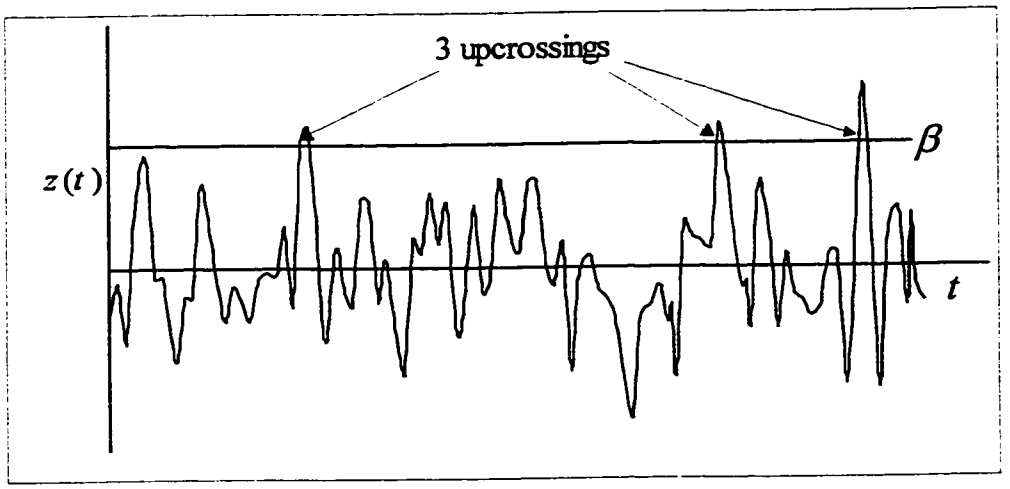

Figure 2.1: Upcrossings of the Level β by a Sample of the Stochastic Process $Z(t)$

Our major concern is the upper tail probability of the maximum of $Z(t)$, which can be expressed as,

$$\begin{aligned} P(\beta) &= P\left(\max_T Z(t) > \beta\right) \\ &= P\left(Z(0) > \beta\right) + P\left(N_\beta(t) > 0\right) - P\left(Z(0) > \beta, N_\beta(t) > 0\right) \end{aligned} \tag{2.15}$$

For large β, only the second term is important,

$$P(\beta) \sim P\left(N_\beta(t) > 0\right) \tag{2.16}$$

since

$$P(Z(0) > \beta) \to 0, \qquad \text{as } \beta \to \infty \tag{2.17}$$

In order to evaluate equation (2.16), the following assumptions are usually made (Li, 1992):

1. In the interval $(t, t+dt)$, $dt \to 0$, there is at the most one upcrossing.

2. The numbers of up-crossings in disjoint intervals are independent.

Assume that the expected number of β-upcrossings by $Z(t)$ per unit time at time t is $\lambda_\beta(t)$, then the expected number of β-upcrossings by $Z(t)$ in the interval dt is $\lambda_\beta(t)dt$.

The point process of β-upcrossings that satisfies the above two assumptions is asymptotically a Poisson process with intensity $\lambda_\beta(t)$. Therefore, these assumptions are usually called Poisson assumptions. On the basis of them, we can obtain,

$$\begin{aligned} P(\beta) &\sim P(N_\beta(t) > 0), \qquad \text{as } \beta \to \infty \\ &= 1 - \exp\left(-\int_0^T \lambda_\beta(t)\, dt\right) \end{aligned} \tag{2.18}$$

where $\lambda_\beta(t)$ has been given by Rice (1944, 1945):

$$\lambda_\beta(t) = \int_0^{+\infty} Z'(t)\, f_{ZZ'}\left(\beta, Z', t\right)\, dZ' \tag{2.19}$$

in which $f_{ZZ'}\left(\beta, Z', t\right)$ is the joint probability density function of $Z(t)$ and its derivative $Z'(t)$.

The above representation for the probability of the maximum is widely used for stochastic processes. However, since it is based on the Poisson assumptions, there is

always a need to prove that the approximating point process converge to a Poisson process. This involves much more complicated mathematics than the calculation of the probability of the maximum itself and it always imposes a great limitation upon practical applications. One of the properties of the method we will propose is that it successfully avoids making these assumptions.

2.3.2 Exceedances of Sequences

A sequence is a set of ordered observations or random variables with a discrete domain, for instance, the temperatures at specified time intervals and structural parameters at described points. Therefore, the domain of a sequence can be time as well as other dimensions such as space.

Let $\{Z_i;\ i = 1, 2, ..., n\}$ be a sequence of random variables, defined as follows:

$$Z_i = m_i + X_i \tag{2.20}$$

where m_i is a bounded sequence and X_i is a stationary normal sequence with zero mean, variance σ^2. Let the coefficient of correlation between X_i and X_{i+k} be ρ_k (2.11),

$$\mathbb{E}\left(X_i X_{i+k}\right)/\sigma^2 = \rho_k \tag{2.21}$$

ρ_k satisfies,

$$\sum_{k=1}^{\infty} \rho_k < \infty \tag{2.22}$$

The exceedance of a level β by this sequence means,

$$\max_{i=1,2,...,n} X_i \geq \beta \tag{2.23}$$

which is shown in Figure 2.2.

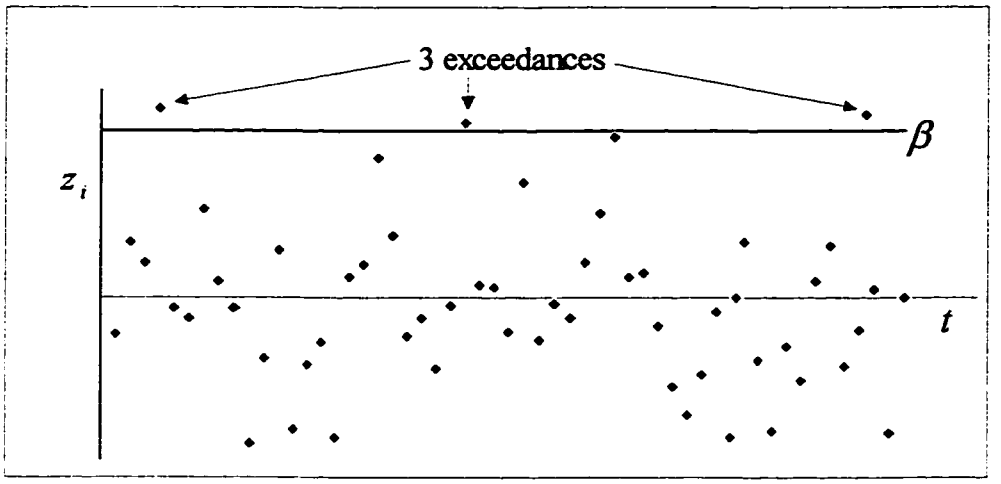

Figure 2.2: Exceedances of the Level β by a Sequence z_i $(i = 1, 2, ..., n)$

Based on the Poisson assumptions similar to those made for maxima of stochastic processes, the extreme value distribution of the sequence (with coefficients of correlation satisfying equation (2.22))can be proven to be asymptotically (Horowitz, 1980):

$$P(\max X_i \geq \beta,\ i = 1, 2, ..., n) \sim 1 - \exp\left[-\exp(-\frac{\beta - c_n - m^*}{d_n})\right] \ ,n \to \infty \tag{2.24}$$

with,

$$c_n = (2\log n)^{1/2} - (1/2)(2\log n)^{-1/2} \times (\log\log n + \log 4\pi) \tag{2.25}$$

$$d_n = (2\log n)^{-1/2} \tag{2.26}$$

$$m^* = d_n \log\left[n^{-1}\sum_{i=1}^{n}\exp(m_i/d_n)\right] \tag{2.27}$$

Equation (2.24) is an extension of the corresponding extreme value formula for sequences of independently and normally distributed variables and is suitable for sequences of normally distributed variables with coefficients of correlation satisfying equation (2.22). Since it is based on the convergence of the point process of exceedances to the Poisson process, the verification of the Poisson assumptions should, strictly speaking, be made for all applications.

2.3.3 Extremes of Random Fields

a. Vanmarcke's Approach

Vanmarcke's approach (1983) for the extreme value distribution of random fields include a basic formula and an improved formula.

For a 2D differentiable homogeneous random field $Z(t_1, t_2)$ with zero-mean, standard deviation σ and domain $\mathbf{T}$, the basic formula is asymptotically exact as the threshold β is relatively large:

$$P_{vm1}(\beta) = P\left(\max_{\mathbf{T}} Z(t_1,t_2) \geq \beta\right) \sim 1 - \exp(-\mu_\beta a_0) \approx a_0\mu_\beta,\ \beta \to \infty \tag{2.28}$$

in which a_0 is the area of the time domain $\mathbf{T}$ and μ_β is defined by,

$$\mu_\beta = \frac{1}{2\pi}\cdot\frac{[f_Z(\beta)]^2}{1-F_Z(\beta)}\cdot|\mathbf{\Lambda}_{11}|^{1/2} \tag{2.29}$$

where $f_Z(z)$, $F_Z(z)$ are the marginal probability density function and the cumulative

distribution function of $Z(t_1, t_2)$ respectively, defined by equations (2.2) and (2.1), $\mathbf{\Lambda}_{11}$ is a matrix with components as follows,

$$\mathbf{\Lambda}_{11} = \begin{bmatrix} \lambda_{20} & \lambda_{11} \\ \lambda_{11} & \lambda_{02} \end{bmatrix} \tag{2.30}$$

where λ_{ij} $(i, j = 0, 1, 2)$ are the spectral moments of the spectral density function $S_{Z_1 Z_2}(\omega_i, \omega_j)$ defined by equation (2.12):

$$\lambda_{ij} = \int \omega_i \omega_j S_{Z_1 Z_2}(\omega_i, \omega_j)\, d\boldsymbol{\omega} \tag{2.31}$$

in which $\boldsymbol{\omega} = (\omega_i, \omega_j)$, Z_i $(i = 1, 2)$ denote $Z(t_1, t_2)$ considering that only t_i is a variable.

Based on (2.28), Vanmarcke develops the improved formula,

$$P_{vm2}(\beta) = P\left(\max_{\mathbf{T}} Z(t_1, t_2) \geq \beta\right) = 1 - F_Z(\beta) \cdot \exp\left\{-\frac{\mu_\beta a_0}{F_Z(\beta)}\left[1 - \exp\left(-\frac{\mu_{\beta,R}}{\mu_\beta}\right)\right]\right\} \tag{2.32}$$

where β, $F_Z(z)$, μ_β and a_0 are the same as those in the basic formula. The value $\mu_{\beta,R}$ is defined by:

$$\mu_{\beta,R} = \frac{1}{2\pi} \cdot \frac{[f_R(\beta)]^2}{1 - F_R(\beta)} \cdot \sigma_{Z_1'} \sigma_{Z_2'} \cdot |\mathbf{\Delta}_{11}|^{1/2} \tag{2.33}$$

in which Z_i' $(i = 1, 2)$ are the first derivatives of Z_i and $\sigma^2_{Z_i'}$ are the variances of the derivative field. $f_R(x)$, $F_R(x)$ are the p.d.f. and the c.d.f. of the envelope (Vanmarcke, 1983) of the random field respectively. If the random field is Gaussian,

we have (Vanmarcke, 1983):

$$f_R(x) = \frac{x}{\sigma^2}\exp\left(-\frac{x^2}{2\sigma^2}\right), \quad x \geq 0 \tag{2.34}$$

$$F_R(x) = 1 - \int_x^\infty f_R(x)\,dx = 1 - \exp\left(-\frac{x^2}{2\sigma^2}\right), \quad x \geq 0 \tag{2.35}$$

And $\mathbf{\Delta}_{11}$ in equation (2.33) is a 2×2 matrix with components,

$$\Delta_{11}^{(ij)} = \frac{\lambda_{ij}}{\sigma_{Z_1'}\sigma_{Z_2'}} - \left(1 - \left[\varepsilon^{(i)}\right]^2\right)^{1/2} \cdot \left(1 - \left[\varepsilon^{(j)}\right]^2\right)^{1/2} \tag{2.36}$$

where $(i, j = 1, 2)$ and $\varepsilon^{(i)}$ are the spectral band widths and they are defined by,

$$\varepsilon^{(1)} = \sqrt{1 - \frac{\lambda_{20}^2}{\lambda_{00}\lambda_{40}}} \tag{2.37}$$

$$\varepsilon^{(2)} = \sqrt{1 - \frac{\lambda_{02}^2}{\lambda_{00}\lambda_{04}}} \tag{2.38}$$

The improved formula (2.32) is more accurate than the basic one (2.28) when the threshold is small. Both the basic and improved formulas are conjectures and based on an extrapolation of one-dimensional results obtained using Poisson point-process theory. Note also that Vanmarcke's approach is limited to homogenous random fields.

b. Adler's Approach

Based on the research of Belyaev and Piterbarg (1972a, 1972b), Adler (1981) proposed a general formula for the k-dimensional differentiable homogeneous Gaussian

random field $Z(\mathbf{t})$ with zero-mean, unit variance and domain $\mathbf{T}$:

$$\lim_{\beta\to\infty} \frac{P\left(\max_{\mathbf{T}} Z(\mathbf{t}) > \beta\right)}{\Psi(\beta)(\beta)^k} = (2\pi)^{-k/2} |\mathbf{\Lambda}|^{1/2} a_0 \tag{2.39}$$

where β, a_0 are the threshold and the area of the domain $\mathbf{T}$, respectively. $\mathbf{\Lambda}$ is a matrix similar to $\mathbf{\Lambda}_{11}$ in Vanmarcke's formulas but a $k \times k$ one. $\Psi(x)$ is defined by,

$$\Psi(x) = (\sqrt{2\pi}x)^{-1} \exp(-\frac{1}{2}x^2) \tag{2.40}$$

Adler's approach is also based on an extrapolation of one-dimensional results obtained using Poisson point-process theory. It will be shown in Chapter 4 that both Vanmarcke's and Adler's formulas are special cases of the more general result developed in this thesis.

2.4 Discretization of random fields

2.4.1 Introduction

In most applications, the representations of random fields themselves cannot be used directly. Instead, representations consisting of random variables are achieved using discretization methods.

Since our interest lies in the maxima of random fields, it is important to choose an accurate and efficient discretization method with respect to tail probabilities. In this section, two different discretization methods are discussed.

2.4.2 Extension Optimal Linear Discretization Method

In practical situations, the transformation of a random field into random variables plays an important role. We should try to keep as much information as possible about the random field during discretization. There are seven widely used transformation methods which include the midpoint method (Der Kiureghian and Ke, 1988), the spatial averaging method (Vanmarcke and Grigoriu, 1983), the shape function method (Liu, 1986), the optimal linear discretization method (Li and Der Kiureghian,1993), the weighted integral method (Takada, 1990) and the truncated Karhunen-Loève expansion method (KLE) (Spanos and Ghanem, 1989). Of all these methods, KLE is the most efficient one, provided that the exact eigenvalues and eigenfunctions of the autocovariance function of the random field can be obtained. However, such a condition cannot always be met in practical problems. According to Li and Der Kiureghian (1993), the most useful discretization approach is the Extension Optimal Linear Discretization Method (EOLD). It is proved to be more efficient than most of other existing methods and it is more practical than KLE for the reason mentioned above. Therefore, this method is introduced in this section and it will be applied to the subsequent analysis in this thesis.

a. Optimal Linear-estimation (OLE)

For a Gaussian random field $Z(\mathbf{t})$, $\mathbf{t} = (t_1, t_2, ..., t_n) \in \mathbf{T}$, the information we have is the first two moments $m(\mathbf{t})$ and $R(\mathbf{t}, \mathbf{t}')$. The objective is to find the representation of the random field in terms of random variables according to the basic rule that such a representation should have a probability structure as close as possible to that of the original random field.

For every discretization method, the first step is to divide the random field into finite elements. The smaller the element size, the more precise the discretization will be. Infinitely small elements are required for exact discretization. However, practical considerations dictate a finite number. In the divided random field, each nodal point is a fixed point, $\mathbf{t}_i$, at which the corresponding nodal value, $V(\mathbf{t}_i)$, is a random variable.

Assume that the number of the nodal points is n, then the random field $Z(\mathbf{t})$ can be described by a linear function of nodal values as follows,

$$\widehat{Z}(\mathbf{t}) = a(\mathbf{t}) + \sum_{i=1}^{n} b_i(\mathbf{t}) V(\mathbf{t}_i) = a(\mathbf{t}) + \langle \mathbf{b}(\mathbf{t}), \mathbf{V}(\mathbf{t}) \rangle \, , \mathbf{t} \in \mathbf{T} \tag{2.41}$$

in which $a(\mathbf{t})$ is a scalar function of $\mathbf{t}$, while $\mathbf{b}(\mathbf{t})$, $\mathbf{V}(\mathbf{t})$ are functions of $\mathbf{t}$ with elements of $b_i(\mathbf{t})$ and $V(\mathbf{t}_i)$ respectively. The next step is to determine the expressions of $a(\mathbf{t})$ and $\mathbf{b}(\mathbf{t})$ according to the basic rule. Li and Der Kiureghian (1993) achieved this by employing the basic notions of optimal linear-estimation (OLE) theory (Vanmarcke, 1983), that is, by minimizing the variance of the difference between $Z(\mathbf{t})$ and $\widehat{Z}(\mathbf{t})$ subject to the latter being an unbiased estimator of the former in the mean:

$$\text{Minimize} \quad Var\left[Z(\mathbf{t}) - \widehat{Z}(\mathbf{t})\right] \tag{2.42}$$

subject to

$$E\left\{Z(\mathbf{t}) - \widehat{Z}(\mathbf{t})\right\} = 0 \tag{2.43}$$

The solution is,

$$a(\mathbf{t}) = m(\mathbf{t}) - \langle \mathbf{b}(\mathbf{t}), \mathbf{m} \rangle \tag{2.44}$$

$$\mathbf{b}(\mathbf{t}) = \mathbf{C}^{-1} \cdot \mathbf{d}(\mathbf{t}) \tag{2.45}$$

where $\mathbf{m}$ is the vector of mean values of $\mathbf{V}(\mathbf{t})$, while $\mathbf{d}(\mathbf{t})$ is a vector consisting of the covariances of $Z(\mathbf{t})$ with the elements of $\mathbf{V}(\mathbf{t})$,

$$\mathbf{d}(\mathbf{t}) = \begin{pmatrix} \mathbb{E}\{Z(\mathbf{t}) \cdot V(\mathbf{t}_1)\} \\ \mathbb{E}\{Z(\mathbf{t}) \cdot V(\mathbf{t}_2)\} \\ \vdots \\ \mathbb{E}\{Z(\mathbf{t}) \cdot V(\mathbf{t}_n)\} \end{pmatrix} = \begin{pmatrix} R(\mathbf{t}, \mathbf{t}_1) \\ R(\mathbf{t}, \mathbf{t}_2) \\ \vdots \\ R(\mathbf{t}, \mathbf{t}_n) \end{pmatrix} \tag{2.46}$$

and $\mathbf{C}$ is the covariance matrix of $\mathbf{V}(\mathbf{t})$ which is assumed to be non-singular,

$$\mathbf{C} = \begin{bmatrix} R(\mathbf{t}_1, \mathbf{t}_1) & R(\mathbf{t}_1, \mathbf{t}_2) & \cdots & R(\mathbf{t}_1, \mathbf{t}_n) \\ R(\mathbf{t}_1, \mathbf{t}_2) & R(\mathbf{t}_2, \mathbf{t}_2) & & \vdots \\ \vdots & & \ddots & \\ R(\mathbf{t}_1, \mathbf{t}_n) & \cdots & & R(\mathbf{t}_n, \mathbf{t}_n) \end{bmatrix} \tag{2.47}$$

Hence, the discretized random field is,

$$\widehat{Z}(\mathbf{t}) = m(\mathbf{t}) + \mathbf{d}(\mathbf{t})^T \mathbf{C} \cdot [\mathbf{V}(\mathbf{t}) - \mathbf{m}], \quad \mathbf{t} \in \mathbf{T} \tag{2.48}$$

Note that the discretized random field has the same mean value as that of the original random field. On the other hand, OLE theory took into account the correlation structure of the random field by minimizing the variance of the error in (2.42) at every nodal point. That is why such a method is comparatively more accurate than most of the other discretization methods which do not account sufficiently for

the correlation structure.

Furthermore, it is seen that, although the random field is successfully represented by a set of random variables, the elements of $\mathbf{V(t)}$ are all dependent. In most of the practical problems, independent random variables are generally preferred. Therefore, Li and Der Kiureghian (1993) extended the OLE method by means of the spectral decomposition method.

b. Spectral Decomposition Method

The spectral decomposition method was first introduced by Liu and Belytschko (1986) by using the fact that any non-singular covariance matrix can be brought in a diagonal form.

Since the covariance matrix $\mathbf{C}$ is an $n \times n$ non-singular symmetric matrix, there must exist eigenvalues λ_i and eigenvectors $\mathbf{\Phi}_i$ $(i = 1, 2, ..., n)$, that satisfy:

$$\mathbf{C\Phi}_i = \lambda_i \mathbf{\Phi}_i \tag{2.49}$$

They can easily be obtained by any eigenvalue method such as the QR method (Burden, et al., 1978).

The eigenvectors are normalized such that

$$\langle \mathbf{\Phi}_i, \mathbf{\Phi}_j \rangle = \delta_{ij} \tag{2.50}$$

Then the vector $\mathbf{V(t)}$ can be expressed in terms of a vector $\boldsymbol{\eta}$ with independent

elements,

$$\mathbf{V(t)} = \mathbf{m} + \mathbf{\Phi} \cdot \boldsymbol{\eta} \tag{2.51}$$

where $\mathbf{\Phi}$ is the $n \times n$ eigenvector matrix with elements $\mathbf{\Phi}_i$. It is easy to verify that the covariance matrix of $\boldsymbol{\eta}$ is a diagonal matrix with diagonal elements $\lambda_1, \lambda_2, ..., \lambda_n$. Therefore, η_i can be presented as,

$$\eta_i = \sqrt{\lambda_i} X_i \tag{2.52}$$

where X_i are uncorrelated random variables and obviously independent when they are normally distributed.

Now the equation (2.51) can be rewritten as,

$$\mathbf{V(t)} = \mathbf{m} + \sum_{i=1}^{n} \sqrt{\lambda_i} X_i \mathbf{\Phi}_i \tag{2.53}$$

Assume that the eigenvalues in (2.53) are ordered in decreasing magnitude and recall the fact that the information contained in the covariance matrix is concentrated in the larger eigenvalues and eigenvectors. Therefore, at a given level of accuracy, $\mathbf{V(t)}$ can be represented by $r \leq n$ terms of the largest eigenvalues and the number of random variables X_i needed can be reduced as well. Hence,

$$\mathbf{V(t)} = \mathbf{m} + \sum_{i=1}^{r} \sqrt{\lambda_i} X_i \mathbf{\Phi}_i \tag{2.54}$$

c. Extension Optimal Linear Discretization Method (EOLD)

Substituting equation (2.54) in (2.48) yields the random field approximation,

$$\widehat{Z}(\mathbf{t}) = m(\mathbf{t}) + \sum_{i=1}^{r} \frac{X_i}{\sqrt{\lambda_i}} \Phi_i^T \mathbf{d}(\mathbf{t}), \mathbf{t} \in T \tag{2.55}$$

$$= m(\mathbf{t}) + \sum_{i=1}^{r} X_i h_i^*(\mathbf{t}) \tag{2.56}$$

The combination of OLE with the spectral decomposition method is called the extension optimal linear discretization method (EOLD). As outlined, its efficiency lies in the use of an optimal shape function and the representation in terms of a smaller number of independent random variables. The number of random variables always determines the computational efficiency in many practical situations.

In the application of EOLD, enough attention should be paid to the accuracy of the discretization, since both the transformation from the random field to dependent random variables and the use of a smaller number of random variables could cause errors, while the results of many applications are sensitive to the errors, especially with regards to tail probabilities.

As discussed in Li and Der Kiureghian (1993) and Wei (1995), the errors in the discretization mainly depend on:

1. l, the size of each element
2. a, the correlation length
3. the autocorrelation function of the random field
4. r, the number of random variables used

For a random field to be discretized, the correlation length and the autocorrelation function are fixed. It is appropriate to scale the element size l and to choose r in

such a way as to attain a given level of accuracy. Since correlation lengths and autocorrelation functions of different random fields can be different, the optimal l and r for these fields depend on the required level of accuracy. Even for specified l and r, the errors may vary along the domain of the random field. Therefore, both the global accuracy and the accuracy at selected points should be verified when discretizing a random field.

2.4.3 Discretization by Earthquake Ground Motion Model

a. Basic concept

This discretization method was originally developed by Der Kiureghian and Li (1996) for modeling earthquake ground motions. Since it achieves the representation consisting of independent random variables by a very simple procedure, it is suitable to almost any kind of non-stationarity to be modeled or discretized. Similar to the EOLD method, it also minimizes the variance of the error between the original random field and its approximation to obtain the optimal shape functions. The major difference between them lies in the fact that the ground motion model does not require eigenvalue solutions, which may be a huge computation problem when the number of nodal points is large. Therefore, the present method is introduced and compared with the EOLD method in the applications in Chapter 4.

In practical applications for design or prediction purposes, earthquake ground motions should be modeled as stochastic processes since there is no way to deterministically estimate the ground motion at a site during a future earthquake.

We can consider an earthquake ground motion as a ground surface response of the local soil system or wave propagation path subject to the movement of the

bedrock (Der Kiureghian and Li, 1996; Farasyn, 1997). Therefore, the corresponding dynamical model can be constructed by assuming that the local soil system is a linear filter, the movement of bed rock is a broad-band white noise excitation and the response is the absolute acceleration:

$$\ddot{u}_f(t) + 2\zeta_f\omega_f\dot{u}_f(t) + \omega_f^2 u_f(t) = -W(t) \tag{2.57}$$

in which $W(t)$ is a white noise excitation, ζ_f represents the damping ratio of the soil system and ω_f its natural frequency. $\ddot{u}_f(t), \dot{u}(t)$ and $u_f(t)$ are the acceleration, velocity and displacement of the soil layer relative to the bedrock, respectively. Our interest lies in the ground motion which is the absolute acceleration at the ground surface. It is defined by,

$$Z(t) = \ddot{u}_f(t) + W(t) \tag{2.58}$$

The above concepts are illustrated in Figure 2.3.

According to Clough and Penzien (1975), the exact solution of a filter that responds to a white noise input, the ground motion, is equal to,

$$Z(t) = \int_0^t W(\tau)\, h_f(t-\tau)\, d\tau \tag{2.59}$$

in which $h_f(t)$ is the unit-impulse response function of the filter which is given by,

$$h_f(t) = -\left(C_1 \sin(\omega_d t) + C_2 \cos(\omega_d t)\right) \exp(-\zeta_f\omega_f t) \tag{2.60}$$

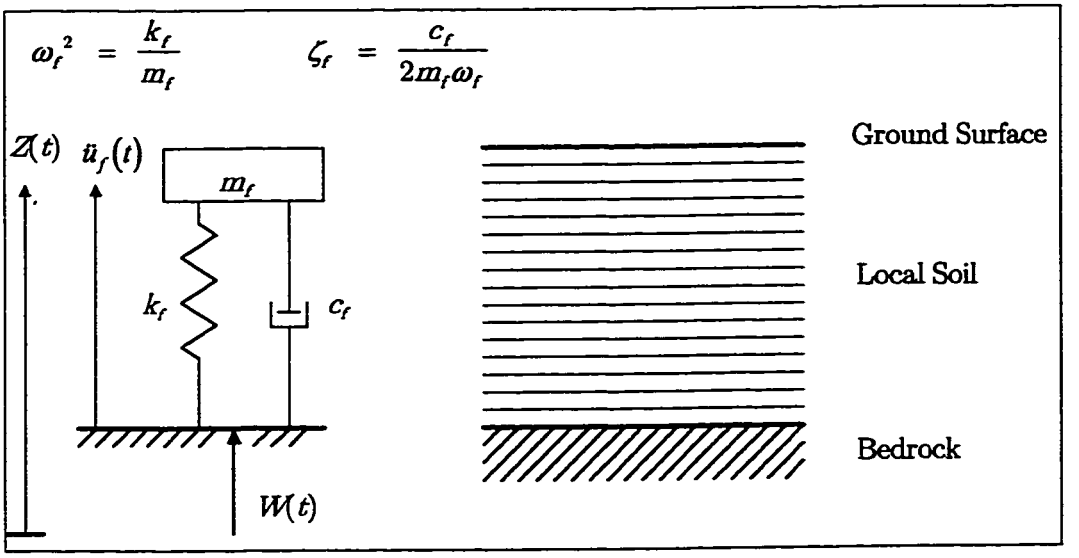

Figure 2.3: Model Used to Discretize Earthquake Signals and Other Stochastic Processes

with

$$\omega_d = \omega_f\sqrt{1-\zeta_f^2} \tag{2.61}$$

$$C_1 = \frac{\omega_f\left(1-2\zeta_f^2\right)}{\sqrt{1-\zeta_f^2}} \tag{2.62}$$

$$C_2 = 2\zeta_f\omega_f \tag{2.63}$$

b. Discretization

Similar to other problems dealing with random media, the earthquake ground motion $Z(t)$ must be represented as a discretized form in terms of random variables as follows,

$$\widehat{Z}(t) = \sum_{i=1}^{n} W_i a_i(t) \tag{2.64}$$

where n is the nodal number, W_i $(i = 1, 2, ..., n)$ are Gaussian random variables with zero mean and variances σ_i^2, and $a_i(t)$ are the discretization shape functions which are deterministic.

The objective of any discretization method just is to estimate σ_i^2 and $a_i(t)$. Firstly, the random variables can be expressed by discretizing the white noise excitation since it only originates from the randomness in equation (2.57). That is,

$$W_i = \int_{t_{i-1}}^{t_i} W(t)\, dt \qquad i = 1, 2, ..., n \tag{2.65}$$

where t_i $(i = 0, 1, ..., n)$ denote a set of closely and equally spaced time points at intervals $\Delta t = t_i - t_{i-1}$. Therefore, the sequence W_i represents $W(t)$ in the discrete form of a random pulse train. It is easy to show (Clough and Penzien, 1975) that W_i are statistically independent Gaussian random variables with zero mean and constant variance,

$$\sigma_i^2 = \sigma^2 = 2\pi\Phi_0\Delta t \tag{2.66}$$

in which the intensity Φ_0 is the constant power spectral density (2.12) of the white noise $W(t)$.

The natural choice for $a_i(t)$ is the unit-impulse response function given by equation (2.60) but it is not the best. Similar to the EOLD method, the better choice is obtained by minimizing the variance of the discretization error between $Z(t)$ and $\widehat{Z}(t)$. The solution is given by Der Kiureghian and Li (1996),

$$a_i(t) = \frac{1}{\Delta t} \int_{\min(t,t_{i-1})}^{\min(t,t_i)} h_f(t - \tau)\, d\tau \tag{2.67}$$

where $h_f(t)$ is defined by (2.60). For detail about the derivation, one refers to Farasyn (1997). Insertion of (2.60) in (2.67) gives the following expression for $a_i(t)$:

$$a_i(t) = \begin{cases} 0 & t < t_{i-1} \\ \frac{1}{\Delta t\sqrt{1-\zeta_f^2}} \{\exp(-\zeta_f\omega_f(t-t_{i-1}))\sin(\omega_d(t-t_{i-1})-\theta)\} & \\ +\frac{1}{\Delta t} & t_{i-1} \le t \le t_i \\ \frac{1}{\Delta t\sqrt{1-\zeta_f^2}} \{\exp(-\zeta_f\omega_f(t-t_{i-1}))\sin(\omega_d(t-t_{i-1})-\theta) & \\ -\exp(-\zeta_f\omega_f(t-t_i))\sin(\omega_d(t-t_i)-\theta)\} & t_i < t \end{cases} \tag{2.68}$$

with

$$\theta = \arccos(\zeta_f) \tag{2.69}$$

Note that $a_i(t)$ is equal to zero until $t = t_{i-1}$ and it attains a peak value at $t = t_i$. The magnitude of the peak value depends on the damping ratio ζ_f and the frequency ω_f.

So far, the ground motion is successfully discretized in terms of independent random variables. But such a discretization only defines a stationary process while the ground motions are typically non-stationary in both the time and frequency domain.

The temporal non-stationary can be taken into account by multiplying (2.64) by a deterministic modulation function $q(t)$. This gives,

$$\widehat{Z}(t) = \sum_{i=1}^{n} W_i q(t_i) a_i(t) \tag{2.70}$$

To account for spectral non-stationarity, we can consider the ground motion as

the summation of several independent absolute accelerations of different filters. The corresponding natural effect is that the soil system has several soil layers, each having its own natural frequency. The discrete representation can then be rewritten as,

$$\widehat{Z}(t) = \sum_{i=1}^{n} W_i \sum_{j=1}^{k} q_j(t_i) a_{ij}(t) \tag{2.71}$$

where k is the number of the filters, $q_j(t_i)$ denotes the modulation function of the j-th filter and $a_{ij}(t)$ is the shape function corresponding to the i-th random variable and j-th filter.

Recall that W_i are independent random variables with zero mean and variance σ^2 defined by equation (2.66), so that normalizing gives,

$$X_i = \frac{W_i}{\sigma} \tag{2.72}$$

Therefore, X_i are standard normal random variables. Substituting the above equation in (2.71) results in the general discretized form,

$$\widehat{Z}(t) = \sigma \sum_{i=1}^{n} X_i \sum_{j=1}^{k} q_j(t_i) a_{ij}(t) \tag{2.73}$$

$$= \sum_{i=1}^{n} X_i h_i^*(t) \tag{2.74}$$

Although the above representation is developed originally for modeling earthquake ground motions, it allows almost any kind of non-stationary processes to be modeled, simply by selecting the parameters in filter properties and modulation functions. Similarly, when it is used for a discretization purpose, it is necessary to

estimate the suitable filter properties and modulation functions to attain a given level of accuracy. Such a method is much more convenient than the EOLD method since it does not require eigenvalue solutions. However, if the estimated parameters can reflect precisely the original probability structures, the ground motion method can be as efficient as the EOLD method. On the other hand, as indicated by the applications in Chapter 4, it may sometimes be difficult to obtain the optimal set of parameters.

Chapter 3

The Tube Method for 2D Random Fields

3.1 Introduction

In this chapter, the method of the 'tube' is discussed in detail. A formula for the extreme value distributions of 2D Gaussian random fields is developed. The method we propose is slightly different from other methods for random fields, and the differences are pointed out in detail.

In the first two sections, the relationship between the problem of the maxima of random fields and purely geometric principles is discussed. It is shown that extremes are related to the volume of neighborhoods of a manifold on the surface of a unit sphere. Section 3.3 describes the volume of neighborhoods corresponding to a 2D random field. It is related to the problem of the maxima of random fields in section 3.4. This leads to a formula for the extreme value distribution of a 2D Gaussian random field with zero mean. The formulas developed in section 3.3 and section 3.4 do not consider the total volume of neighborhoods that make contributions to the extreme value distribution. Approximations of the probabilities associated with endpoints and boundaries of the random field are discussed in section 3.5. A summary is given in section 3.6. Finally, in section 3.7, it is shown that the tube method can easily be applied to random fields with non-zero mean and variable correlation structure.

3.2 Geometry and Maxima of Random Fields

3.2.1 Introduction

As explained in the previous chapters, our prime interest lies in the maxima of random fields. Let a k-dimensional differentiable zero mean Gaussian random field on a set $\mathbf{T} \subset R^k$ be defined by $Z(\mathbf{t})$, $\mathbf{t} = (t_1, t_2, ..., t_k) \in \mathbf{T}$. Then the complementary cumulative distribution function of the maxima of the random field can be written as:

$$P(\beta) = P(\max_{\mathbf{T}} Z(\mathbf{t}) \geq \beta) \tag{3.1}$$

where β is the threshold.

In traditional extreme theory, such a problem is generally solved by an asymptotic approximation of $Z(\mathbf{t})$ by a Poisson point process which involves checking and verifying the use of Poisson distribution. It is shown in this chapter that this problem can, instead, be interpreted on the basis of purely geometric concepts.

3.2.2 Geometrical Representation of A Random Field

In practice, the expression of a random field, $Z(\mathbf{t})$, cannot directly be used in a practical problem and it needs to be transformed into a format consisting of random variables and deterministic functions as follows,

$$Z(\mathbf{t}) = \sum_{i=1}^{n} X_i h_i^*(\mathbf{t}) \tag{3.2}$$

where X_i $(i = 1, 2, ..., n)$ is a sequence of independent standard normal random variables and the functions $h_i^*(\mathbf{t})$ are a set of twice continuously differentially deter-

ministic functions. As discussed in section 2.4, many discretization methods can be used to transform random fields into such a format, for instance, the EOLD method, the ground motion model method, the KLE method, etc.

Due to the independence of X_i, the correlation function $R_{ZZ}(\mathbf{t}_1, \mathbf{t}_2)$ and the variance $\sigma_Z^2(\mathbf{t})$ of a random field $Z(\mathbf{t})$ can be expressed as:

$$R_{ZZ}(\mathbf{t}_1, \mathbf{t}_2) = \sum_{i=1}^{n} h_i^*(\mathbf{t}_1)\, h_i^*(\mathbf{t}_2) \tag{3.3}$$

and

$$\sigma_Z^2(\mathbf{t}) = R_{ZZ}(\mathbf{t}, \mathbf{t}) = |\mathbf{h}^*(\mathbf{t})|^2 = \sum_{i=1}^{n} [h_i^*(\mathbf{t})]^2, \tag{3.4}$$

respectively. Notice that X_i and $h_i^*(\mathbf{t})$ $(i = 1, 2, ..., n)$ can be expressed in vector format with $\mathbf{X} = (X_1, X_2, ..., X_n)$ a vector of independent standard normal random variables and $\mathbf{h}^*(\mathbf{t}) = (h_1^*(\mathbf{t}), h_2^*(\mathbf{t}), ..., h_n^*(\mathbf{t}))$ a vector of time dependent deterministic functions. Therefore, the random field can be rewritten as the scalar product of these two vectors:

$$Z(\mathbf{t}) = \langle \mathbf{X}, \mathbf{h}^*(\mathbf{t}) \rangle \tag{3.5}$$

This is the starting point for introducing the geometric concepts.

Introducing,

$$R_n = \sqrt{|\mathbf{X}|^2} = |\mathbf{X}| \tag{3.6}$$

$$\mathbf{U} = \frac{\mathbf{X}}{|\mathbf{X}|} \tag{3.7}$$

We obtain:

$$\mathbf{X} = R_n \cdot \mathbf{U} \tag{3.8}$$

It can be seen that R_n^2 is a χ^2-random variable with n degrees of freedom so that R_n is a χ_n-random variable with probability density function:

$$f_{\chi_n}(r_n) = \begin{cases} 0 & r_n < 0 \\ \frac{2^{1-\frac{n}{2}} \cdot (r_n)^{n-1}}{\Gamma\left(\frac{n}{2}\right)} \exp\left(-\frac{r_n^2}{2}\right) & r_n \geq 0 \end{cases} \tag{3.9}$$

Since $\mathbf{X}$ is a standard normal distributed vector, $\mathbf{U}$ must be a unit length vector with uniform distribution so that all samples of $\mathbf{U}$ form an n-dimensional unit sphere S^n in the n-dimensional space R^n. The sphere S^n is defined by:

$$S^n = \left\{ \mathbf{z} : \mathbf{z} = (z_1, z_2, ..., z_n), \sum_{i=1}^{n} z_i^2 = |\mathbf{z}|^2 = 1 \right\} \tag{3.10}$$

Furthermore, it can be proven that the random vector $\mathbf{U}$ is independent of $R_n = |\mathbf{X}|$.

Rewriting the expression of $Z(\mathbf{t})$ (3.5) by inserting equation (3.8) and using the independence property, we get:

$$\begin{aligned} Z(\mathbf{t}) &= \langle \mathbf{X}, \mathbf{h}^*(\mathbf{t}) \rangle \\ &= R_n \cdot |\mathbf{h}^*(\mathbf{t})| \cdot \langle \mathbf{U} \cdot \mathbf{h}(\mathbf{t}) \rangle \end{aligned} \tag{3.11}$$

with,

$$\mathbf{h}(\mathbf{t}) = \frac{\mathbf{h}^*(\mathbf{t})}{|\mathbf{h}^*(\mathbf{t})|} \tag{3.12}$$

This time, the geometric meaning of such a random field expression is clearer. Note that, at a given $\mathbf{t}$, $\mathbf{h(t)}$ is a deterministic n-dimensional vector with unit length in the n-dimensional space R^n. Then for $\mathbf{t} = (t_1, t_2, ..., t_k) \in \mathbf{T}$, endpoints of $\mathbf{h(t)}$ form a manifold M, with domain $\mathbf{T}$, embedded on the surface of the n-dimensional unit sphere S^n (3.10):

$$M = \{\mathbf{h(t)} : \mathbf{t} \in \mathbf{T},\ \mathbf{h(t)} = (h_1(\mathbf{t}), h_2(\mathbf{t}), ..., h_n(\mathbf{t}))\} \tag{3.13}$$

For the case of $k = 1$, M describes a t dependent curve on the surface of S^n. While for $k = 2$, it is a two-dimensional area on the $n-1$-dimensional unit sphere surface. On the other hand, $\mathbf{U}$ denotes a vector with endpoint on the surface; the endpoint of each realization of $\mathbf{U}$ corresponds with one point on the surface of the unit sphere.

Assume that the angle between the vectors $\mathbf{U}$ and $\mathbf{h(t)}$ is θ, while the distance between the endpoints of $\mathbf{U}$ and $\mathbf{h(t)}$ is $r(\mathbf{t})$. Using elementary trigonometry, we have,

$$\theta = \arccos(1 - \frac{r(\mathbf{t})^2}{2}) \tag{3.14}$$

$$r(\mathbf{t}) = \sqrt{2(1 - \cos\theta)} \approx \tan\theta,\ \theta \to 0 \tag{3.15}$$

Figure 3.1 shows the relationships between θ and r ($r(\mathbf{t})$ at a fixed $\mathbf{t}$) for $n = 2$, and $n = 3$ cases.

Since $\mathbf{U}$ and $\mathbf{h(t)}$ are all unit length vectors, their scalar product can be expressed

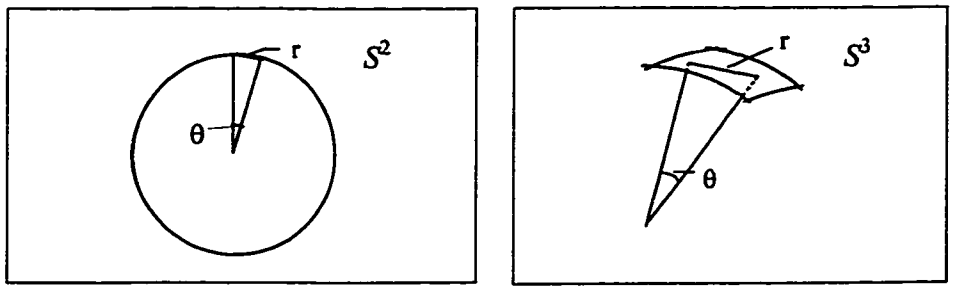

Figure 3.1: Relationships between θ and r for the $n = 2$ and $n = 3$ Cases

in terms of θ as:

$$\langle \mathbf{U} \cdot \mathbf{h(t)} \rangle = |\mathbf{U}| \cdot |\mathbf{h(t)}| \cdot \cos\theta = \cos\theta \tag{3.16}$$

3.2.3 Geometry of Maxima of Random Fields

By introducing the above geometric representation of a random field $Z(\mathbf{t})$, the extreme value distribution can be rewritten as:

$$\begin{aligned} P(\beta) &= P\left(\max_{\mathbf{T}} \langle \mathbf{U} \cdot \mathbf{h(t)} \rangle \geq \frac{\beta}{R_n \cdot |\mathbf{h}^*(\mathbf{t})|}\right) \\ &= P\left(\max_{\mathbf{T}} \cos\theta \geq \frac{\beta}{R_n \cdot |\mathbf{h}^*(\mathbf{t})|}\right) \\ &= P\left(\min_{\mathbf{T}} \theta \leq \arccos\left(\frac{\beta}{R_n \cdot |\mathbf{h}^*(\mathbf{t})|}\right)\right) \end{aligned} \tag{3.17}$$

Recall that R_n is a χ_n-random variable with the probability density function defined by equation (3.9), then $P(\beta)$ can be evaluated by the integration of the

conditional probability with respect to R_n:

$$P(\beta) = \int_{\frac{\beta}{|\mathbf{h}^*(\mathbf{t})|}}^{\infty} P\left(\min_{\mathbf{T}} \theta \leq \arccos(\frac{\beta}{r_n \cdot |\mathbf{h}^*(\mathbf{t})|})\right) f_{\chi_n}(r_n)\, dr_n \tag{3.18}$$

The integration area is obtained from the fact that,

$$\max_{\mathbf{T}} \cos\theta \geq \frac{\beta}{R_n \cdot |\mathbf{h}^*(\mathbf{t})|}, \quad \theta \to 0 \tag{3.19}$$

or,

$$0 < \frac{\beta}{R_n \cdot |\mathbf{h}^*(\mathbf{t})|} \leq 1 \tag{3.20}$$

hence we have:

$$\frac{\beta}{|\mathbf{h}^*(\mathbf{t})|} \leq R_n < \infty \tag{3.21}$$

Now, the conditional probability in (3.18) is related to a geometric probability. Recall that θ is the angle between $\mathbf{U}$ and $\mathbf{h}(\mathbf{t})$ while $\arccos(\frac{\beta}{r_n \cdot |\mathbf{h}^*(\mathbf{t})|})$ is a deterministic function dependent on $\mathbf{t}$, so $\min_{\mathbf{T}} \theta \leq \arccos(\frac{\beta}{r_n \cdot |\mathbf{h}^*(\mathbf{t})|})$ describes a set of realizations of $\mathbf{U}$, which have angles less than $\arccos(\frac{\beta}{r_n \cdot |\mathbf{h}^*(\mathbf{t})|})$ with $\mathbf{h}(\mathbf{t})$. According to the geometric meanings of $\mathbf{U}$, $\mathbf{h}(\mathbf{t})$ and the relationship between $r(\mathbf{t})$ and θ, it can also be explained as a set of points on the unit sphere surface with distances less than $r(\mathbf{t})$ from the manifold M, where $r(\mathbf{t})$ is a function of $\arccos(\frac{\beta}{r_n \cdot |\mathbf{h}^*(\mathbf{t})|})$ and therefore $r(\mathbf{t})$ becomes very small with $\beta \to \infty$ for the fixed r_n and $|\mathbf{h}^*(\mathbf{t})|$.

We can define the points on the unit sphere and satisfying the condition $\min_{\mathbf{T}} \theta \leq \arccos(\frac{\beta}{r_n \cdot |\mathbf{h}^*(\mathbf{t})|})$ as the neighborhood $N(M)$ of a manifold M, and assume that a

parametrization for it is given in the form:

$$N(M) = \left\{ \mathbf{U} : \mathbf{U} \in S^n,\ \max_{\mathbf{T}} \langle \mathbf{U} \cdot \mathbf{h(t)} \rangle \geq r(\mathbf{t}),\ \mathbf{t} \in \mathbf{T} \right\} \tag{3.22}$$

where $\mathbf{U}$ denotes the vector whose endpoint is the uniformly distributed point forming the surface of an n-dimensional unit sphere and $\mathbf{h(t)}$ is a function with domain $\mathbf{T} \subset R^k$ and values in $S^n \subset R^n$. To facilitate this interpretation, Figure 3.2 shows the neighborhoods of two 1- and one 2-dimensional manifolds M.

For the one-dimensional case, the sub-manifold M is a curve with interval $t \in (0, T)$ so that the neighborhood $N(M)$ looks like a tube with radius $r(t)$ around the curve. This explains the origin of the name of the tube method. In this thesis, we will refer to the neighborhood of the sub-manifold M as a 'tube', no matter what the dimension of the sub-manifold is.

Now it is clear that, of all the uniformly distributed points on the surface of an n-dimensional unit sphere, only those in the neighborhood $N(M)$ make a contribution to the extreme value distribution. Therefore, the conditional probability in equation (3.18) can be determined in terms of the ratio of points in the neighborhood $N(M)$, i.e. the volume $V_{n-1}(N)$ of $N(M)$, to all the points on the surface of the unit sphere, i.e. the volume ω_n of the surface area of the unit sphere:

$$P\left(\min_{\mathbf{T}} \theta \leq \arccos\left(\frac{\beta}{r_n \cdot |\mathbf{h}^*(\mathbf{t})|} \right) \right) = \frac{V_{n-1}(N)}{\omega_n} \tag{3.23}$$

The denominator, ω_n, can easily be evaluated by the widely used equation for

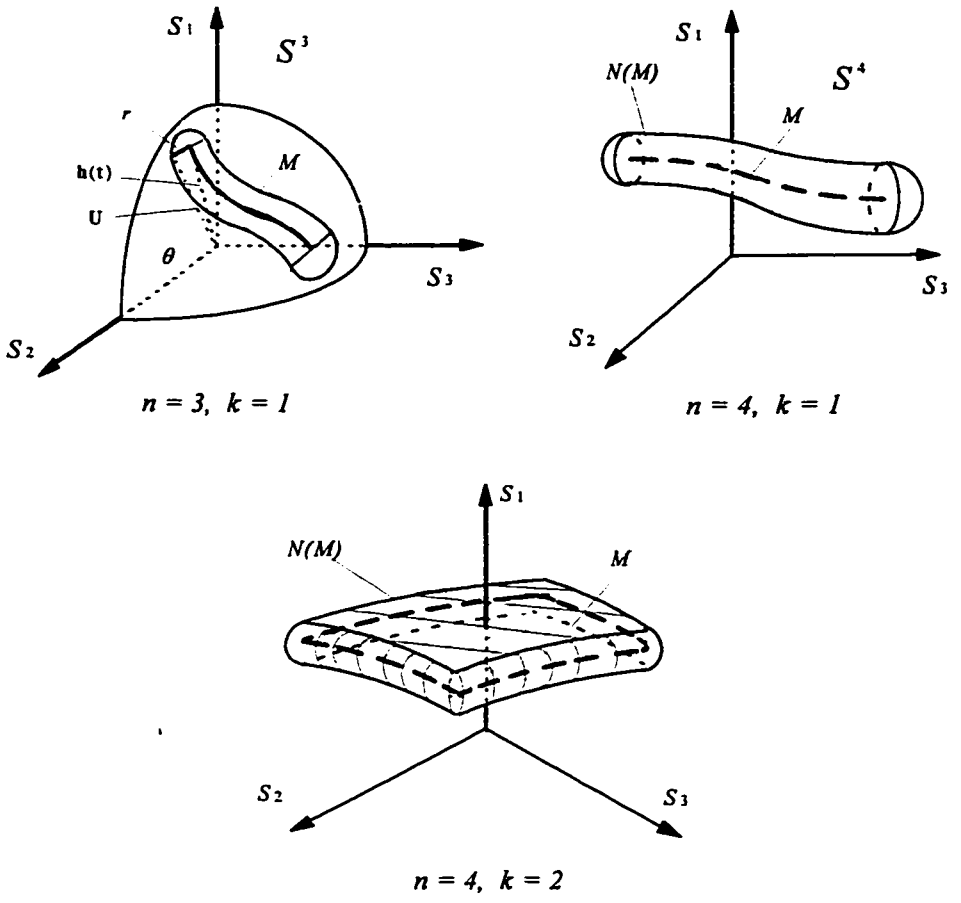

Figure 3.2: Neighborhoods of 1D and 2D Manifolds

the surface area of a sphere with radius one (Kendall, 1961):

$$\omega_n = \frac{2 \cdot \pi^{\frac{n}{2}}}{\Gamma\left(\frac{n}{2}\right)} \tag{3.24}$$

where $\Gamma(\cdot)$ is the Gamma function (Abramowitz and Stegun, 1972).

Now the only thing left is the calculation of the volume of an $(n-1)$-dimensional neighborhood (tube) of a k-dimensional sub-manifold embedded on the surface of an n-dimensional unit sphere. Once the volume of the tube is obtained, the calculation of the extreme value distribution is straightforward.

The above discussion represents the basic idea of the tube method. It is seen that the problem of maxima becomes more intuitive by introducing geometrical principles. There is no need to verify the assumptions regarding the Poisson process and it does not matter whether the random field is homogeneous or not. The key problem in the tube method is how to obtain the tube volume; this will be discussed in the following section.

3.3 Volume of the Tube

In this section, the calculation of the volume of a tube is studied. First, Weyl's formula (1939) for the volume of a tube is introduced and its limitation is pointed out. Then the volume of an $(n-1)$-dimensional manifold is outlined. Finally, a formula for the volume of the tube of a 2D sub-manifold is developed by means of Breitung's projection method (1997).

3.3.1 Weyl's Formula

As early as 1930s, the calculation of the volume of a tube had been studied by Hotelling (1939) and Weyl (1939). Hotelling studied the one-dimensional case ($k = 1$), while Weyl proposed a more general volume formula which is given below.

Assume that M is a k-dimensional manifold (without boundary) embedded in the hypersphere S^n for a finite n, where M and S^n are defined by equations (3.13) and (3.10) respectively. As in the preceding section, $\mathbf{h(t)}$ denotes a deterministic n-dimensional vector with unit length in the n-dimensional space R^n at a given $\mathbf{t}$, $\mathbf{t} = (t_1, t_2, ..., t_k) \in \mathbf{T}$; the endpoint of $\mathbf{h(t)}$ forms the manifold M; $\mathbf{U}$ denotes a vector with endpoint forming the surface of the unit sphere S^n; let θ be the angle between $\mathbf{U}$ and $\mathbf{h(t)}$ and $r(\mathbf{t})$ the distance between the endpoints of them. The relationship between θ and $r(\mathbf{t})$ is shown in equations (3.14), (3.15) and Figure 3.1. Then according to Weyl (1939), the volume V_{n-1} of the tube N defined by equation (3.22) is equal to:

$$V_{n-1}(N) = \omega_m \cdot \sum_{e=0,2,4\cdots}^{k} \kappa_e J_e(\theta) \tag{3.25}$$

where N means neighborhoods, $m = n - 1 - k$, ω_m is the surface volume of an m-dimensional unit sphere and given by equation (3.24). $J_e(\theta)'s$ are the incomplete beta functions:

$$J_0(\theta) = \int_0^\theta \sin^{k-1}(x) \cdot \cos^k(x) dx \tag{3.26}$$

$$J_e(\theta) = \frac{1}{k(k+2)\cdots(k+e-2)} \int_0^\theta \sin^{k+e-1}(x) \cdot \cos^{k-e}(x) dx \tag{3.27}$$

where $e = 2, 4, ..., \leq k$.

The coefficients κ_e in equation (3.25) are geometric constants related to a k-dimensional differentiable manifold M which is defined by the metric tensor matrix $\mathbf{M}$ (Weyl, 1939; Sun, 1993). The components of the metric tensor matrix $\mathbf{M}$ are given by the following inner product (Kreyszig, 1968, page 310):

$$m_{ij}(\mathbf{t}) = \left\langle \frac{\partial \mathbf{h}(\mathbf{t})}{\partial t_i}, \frac{\partial \mathbf{h}(\mathbf{t})}{\partial t_j} \right\rangle = \sum_{l=1}^{n} \frac{\partial h_l(\mathbf{t})}{\partial t_i} \cdot \frac{\partial h_l(\mathbf{t})}{\partial t_j} \quad (i, j = 1, 2, ..., k) \tag{3.28}$$

in which $\mathbf{t} = (t_1, t_2, ..., t_k) \in \mathbf{T}$. Note that $\mathbf{M}$ is symmetric.

κ_0 is the volume of the sub-manifold M and it is defined by:

$$\kappa_0 = \int_{\mathbf{T}} |\det \mathbf{M}|^{1/2} \, d\mathbf{t} \tag{3.29}$$

It can relatively easily be calculated in comparison with other geometric terms.

Weyl did not explain the explicit geometric meaning of the second coefficient κ_2 which is defined by:

$$\kappa_2 = \int_{\mathbf{T}} [-S/2 - k(k-1)/2] \cdot |\det \mathbf{M}|^{1/2} \, d\mathbf{t} \tag{3.30}$$

where S is the so-called intrinsic scalar curvature of the sub-manifold M and it is a function of the partial differentials of $m_{ij}(\mathbf{t})$ (3.28) with respect to t_l, $(i, j, l = 1, 2, ..., k)$.

The calculation of S involves the computation of the Riemannian curvature tensor, the Ricci curvature tensor and the Christoffel symbols (Kreyszig, 1968), which is very tedious and not really suitable for practical engineering problems. Directly applying Weyl's formula to equation (3.23) can result in a formula for the extreme

value distribution (Sun, 1993). Obviously, such a formula also includes the scalar curvature tensor which is very difficult to calculate. In an application (Sun, 1991) of it, a simulation method is used by Sun to estimate S in the special case that the corresponding metric tensor matrix is diagonal. But this is not applicable to the general case in which the metric tensor matrixes are not always diagonal. Therefore, a more practical formula for the tube volume should be developed. In the following sections, Breitung's projection method (1997) is used to derive an accurate formula for the tube volume in 2D cases.

3.3.2 Volume of an $(n-1)$-Dimensional Manifold

The volume of an $(n-1)$-dimensional manifold M^* embedded on an n-dimensional unit sphere, (that is, the M^* is part of the surface of the unit sphere), is well known (Thorpe, 1979) and is used to derive the formula for a tube volume. Note that the present section is restricted to the case that the manifold has a dimension equal to one less than that of the unit sphere. The more general case of a k-dimensional manifold is discussed in section 3.3.3.

Assume that an $(n-1)$-dimensional manifold M^* is given in the form:

$$M^* = \{\mathbf{h}(\mathbf{t}) : \mathbf{t} \in \mathbf{T}, \mathbf{h}(\mathbf{t}) = (h_1(\mathbf{t}), h_2(\mathbf{t}), ..., h_n(\mathbf{t}))\} \tag{3.31}$$

where $\mathbf{h}(\mathbf{t})$ is a unit length vector with domain $\mathbf{T}$, $\mathbf{t} = (t_1, t_2, ..., t_{n-1}) \in \mathbf{T}$, and values in $S^n \subset R^n$. Note that the difference between the two manifolds defined by the equations (3.13) and (3.31) is that the former is k-dimensional and the latter is $(n-1)$-dimensional with $k \leq n-2$. Assuming $\mathbf{h}(\mathbf{t})$ is one-to-one, then the volume

of M^* is determined by the integral (Thorpe, 1979):

$$V_{n-1}(M^*) = \int_{\mathbf{T}} \left|\det\left(\mathbf{E}_1^*(\mathbf{t}), \mathbf{E}_2^*(\mathbf{t}), ..., \mathbf{E}_{n-1}^*(\mathbf{t}), \mathbf{h}(\mathbf{t})\right)\right| d\mathbf{t} \tag{3.32}$$

Where $\mathbf{E}_i^*$ $(i = 1, 2, ..., n-1)$ are the unit coordinate vectors in the direction of t_i, which are defined by:

$$\mathbf{E}_i^* = \frac{\partial \mathbf{h}(\mathbf{t})}{\partial t_i} = \left(\frac{\partial h_1(\mathbf{t})}{\partial t_i}, \frac{\partial h_2(\mathbf{t})}{\partial t_i}, ..., \frac{\partial h_n(\mathbf{t})}{\partial t_i}\right) \tag{3.33}$$

They denote the velocities of the manifold M^* in the direction of t_i so that the coordinate vector fields along the surface, $\mathbf{E}_1^*(\mathbf{t}), \mathbf{E}_2^*(\mathbf{t}), ..., \mathbf{E}_{n-1}^*(\mathbf{t})$, form the tangential space of the surface at the point $\mathbf{u} = \mathbf{h}(\mathbf{t})$. Therefore, we have:

$$\mathbf{E}_i^*(\mathbf{t}) \cdot \mathbf{h}(\mathbf{t}) = 0 \qquad (i = 1, 2, ..., n-1) \tag{3.34}$$

This means that the injective vector function $\mathbf{h}(\mathbf{t})$ is normal to the tangential space at each point $\mathbf{u}$. Then equation (3.32) can be rewritten as:

$$\begin{aligned} & V_{n-1}(M^*) \\ = & \int_{\mathbf{T}} \left| \det \begin{pmatrix} \mathbf{E}_1^*(\mathbf{t}) \cdot \mathbf{E}_1^*(\mathbf{t}) & \cdots & \mathbf{E}_1^*(\mathbf{t}) \cdot \mathbf{E}_{n-1}^*(\mathbf{t}) & \mathbf{E}_1^*(\mathbf{t}) \cdot \mathbf{h}(\mathbf{t}) \\ \vdots & \cdots & \vdots & \vdots \\ \mathbf{E}_{n-1}^*(\mathbf{t}) \cdot \mathbf{E}_1^*(\mathbf{t}) & \cdots & \mathbf{E}_{n-1}^*(\mathbf{t}) \cdot \mathbf{E}_{n-1}^*(\mathbf{t}) & \mathbf{E}_{n-1}^*(\mathbf{t}) \cdot \mathbf{h}(\mathbf{t}) \\ \mathbf{h}(\mathbf{t}) \cdot \mathbf{E}_1^*(\mathbf{t}) & \cdots & \mathbf{h}(\mathbf{t}) \cdot \mathbf{E}_{n-1}^*(\mathbf{t}) & \mathbf{h}(\mathbf{t}) \cdot \mathbf{h}(\mathbf{t}) \end{pmatrix} \right|^{\frac{1}{2}} d\mathbf{t} \\ = & \int_{\mathbf{T}} \left|\det\left(\mathbf{E}_i^*(\mathbf{t}) \cdot \mathbf{E}_j^*(\mathbf{t})\right)\right|^{1/2} d\mathbf{t} \end{aligned} \tag{3.35}$$

$$= \int_{\mathbf{T}} |\det(\mathbf{M})|^{1/2} d\mathbf{t} \tag{3.36}$$

where $\mathbf{M}$ is the metric tensor matrix defined by equation (3.28).

An intuitive explanation why the coordinate vectors can be used to measure the volume of a manifold is shown in Figure 3.3.

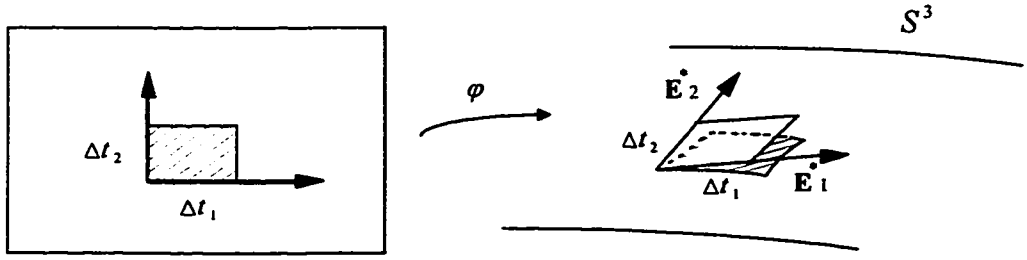

Figure 3.3: Area Magnification along the Parametrized 2D Surface of a 3D Unit Sphere

It is shown that the small shaded rectangle is mapped by the transformation φ to the surface of a unit sphere S^3. When $\Delta t_i \rightarrow 0$, the mapped area on the surface of the unit sphere is closely approximated by the rectangular area above it.

For our problem, M is a k-dimensional sub-manifold defined by equation (3.13). Of our interest is the volume of the neighborhood (tube), which is expressed by equation (3.22) and consisting of the points on the surface of the unit sphere with distance less than $r(\mathbf{t})$ from M. In order to evaluate the tube volume by using equation (3.23), the neighborhood $N(M)$ should first be expressed explicitly.

3.3.3 Neighborhood of a Manifold

The volume of the tube (3.22) depends on the k-dimensional sub-manifold M (3.13) and the distance $r(\mathbf{t})$ (3.15). M is defined by its own metric tensor matrix with the components defined by equation (3.28). To evaluate these components, we should first find the corresponding coordinate vector fields of M .

Let

$$\mathbf{E}_i = \frac{\partial \mathbf{h}(\mathbf{t})}{\partial t_i} = (\frac{\partial h_1(\mathbf{t})}{\partial t_i}, \frac{\partial h_2(\mathbf{t})}{\partial t_i}, ..., \frac{\partial h_n(\mathbf{t})}{\partial t_i}), \quad (i = 1, 2, ..., k) \tag{3.37}$$

be the coordinate vectors of the sub-manifold M at the endpoint $\mathbf{y} = \mathbf{h}(\mathbf{t})$ $(\mathbf{y} \in M)$, where k is the dimension of M. Similar to those coordinate vectors defined by equation (3.33), $\mathbf{E}_i$ denote the velocities of the sub-manifold M in the direction of t_i and $\mathbf{E}_1(\mathbf{t}), \mathbf{E}_2(\mathbf{t}), ..., \mathbf{E}_k(\mathbf{t})$ are the coordinate vectors along the surface of the unit sphere at the endpoint $\mathbf{y} = \mathbf{h}(\mathbf{t})$ $(\mathbf{y} \in M)$. Therefore, we have:

$$\mathbf{E}_i(\mathbf{t}) \cdot \mathbf{h}(\mathbf{t}) = 0, \quad (i = 1, 2, ..., k) \tag{3.38}$$

As defined by equation (3.28), the components of the metric tensor matrix $\mathbf{M}$ of the sub-manifold M are equal to:

$$m_{ij}(\mathbf{t}) = \mathbf{E}_i(\mathbf{t}) \cdot \mathbf{E}_j(\mathbf{t}), \quad (i, j = 1, 2, ..., k) \tag{3.39}$$

So far, the sub-manifold M is determined as long as the injective vector $\mathbf{h}(\mathbf{t})$ is known. But the volume of the tube cannot be obtained only by using the characteristics of M with the k-dimensional coordinates t_i, and the corresponding coordinate vectors $\mathbf{E}_i$ $(i = 1, 2, ..., k)$ since the tube itself is $(n-1)$-dimensional. The orthogo-

nal complement of the space spanned by $\mathbf{E}_i$ $(i = 1, 2, ..., k)$ should be determined in order to describe the neighborhood of M.

Assume that the coordinates for a point $\mathbf{z}$ in the $(n-1)$-dimensional neighborhood of M are $(t_1, t_2, ..., t_k, u_1, u_2, ..., u_m)$, $(m = n - 1 - k)$. At each endpoint of $\mathbf{y} = \mathbf{h}(\mathbf{t})$, a point in M, we can determine the unit vectors $\mathbf{n}_j$ along the surface in the direction of u_j $(j = 1, 2, ..., m)$ by:

$$\mathbf{E}_i \cdot \mathbf{n}_j = 0 \tag{3.40}$$

$$\mathbf{n}_j \cdot \mathbf{n}_l = 0 \tag{3.41}$$

$$\mathbf{y} \cdot \mathbf{n}_j = 0 \tag{3.42}$$

where $(i = 1, 2, ..., k)$, $(j, l = 1, 2, ..., m)$, $(j \neq l)$. It is seen that $\mathbf{n}_j$ $(j = 1, 2, ..., m)$ span an m-dimensional orthogonal system which is normal to the k-dimensional space spanned by the $\mathbf{E}_i$ $(i = 1, 2, ..., k)$.

Now we can construct a parametrization function for the points in the neighborhood of M by using the $(n-1)$-dimensional coordinate system $(t_1, t_2, ..., t_k, u_1, u_2, ..., u_m)$. As mentioned in section 3.2, we are interested in the probability of maxima when the threshold β is large, that is, the distance $r(\mathbf{t})$ is very small, so that each point $\mathbf{z}$ satisfying equation (3.22) can be expressed as:

$$\mathbf{z} = (1 + |\mathbf{u}|^2)^{-1/2}(\mathbf{y} + \sum_{i=1}^{m} u_i \mathbf{n}_i) \qquad |\mathbf{u}| \to 0 \tag{3.43}$$

where $\mathbf{u} = (u_1, u_2, ..., u_m)$, $(m = n - 1 - k)$ and $(\mathbf{y} \in M)$. It can easily be verified

that

$$\begin{aligned} |\mathbf{z}| &= \sqrt{|\mathbf{y}|^2 + \left|\sum_{i=1}^{m} u_i \mathbf{n}_i\right|^2} \cdot (1 + |\mathbf{u}|^2)^{-1/2} \\ &= \sqrt{1 + |\mathbf{u}|^2} \cdot (1 + |\mathbf{u}|^2)^{-1/2} \\ &= 1 \end{aligned} \tag{3.44}$$

which means that $\mathbf{z}$ is a unit vector.

It should be noted that the equation (3.43) does not include all the points in the neighborhood which satisfying equation (3.22). Actually, it considers only the points in the space spanned by $\mathbf{n}_1$, $\mathbf{n}_2, ..., \mathbf{n}_m$, that is, the space normal to the space of $\mathbf{E}_1$, $\mathbf{E}_2, ..., \mathbf{E}_k$ as shown in Figure 3.4 for the special cases $k = 1$ and $k = 2$ respectively.

As shown in Figure 3.5, other points close to the boundaries and endpoints of the sub-manifold M and satisfying equation (3.22) also contribute to the extreme value distribution and therefore should also be included as well for general cases. It is difficult to consider these points directly in equation (3.43) and to get the corresponding volume formula. For the lower dimensional cases, $k = 1$ and $k = 2$, the extreme value distribution associated with these endpoints and boundaries will be evaluated separately, which is discussed in detail in section 3.5. For convenience, we refer to the area of a random field corresponding to the points involved in equation (3.43) as the main area of the random field or a random field without boundary.

The maximum variance of the random field in the domain $\mathbf{T}$, to which the extreme value distribution is very sensitive, often occurs within the main area of the random field. Therefore, the exceedance probabilities contributed by the main area are often much larger than those by boundaries and endpoints. However, as indicated in

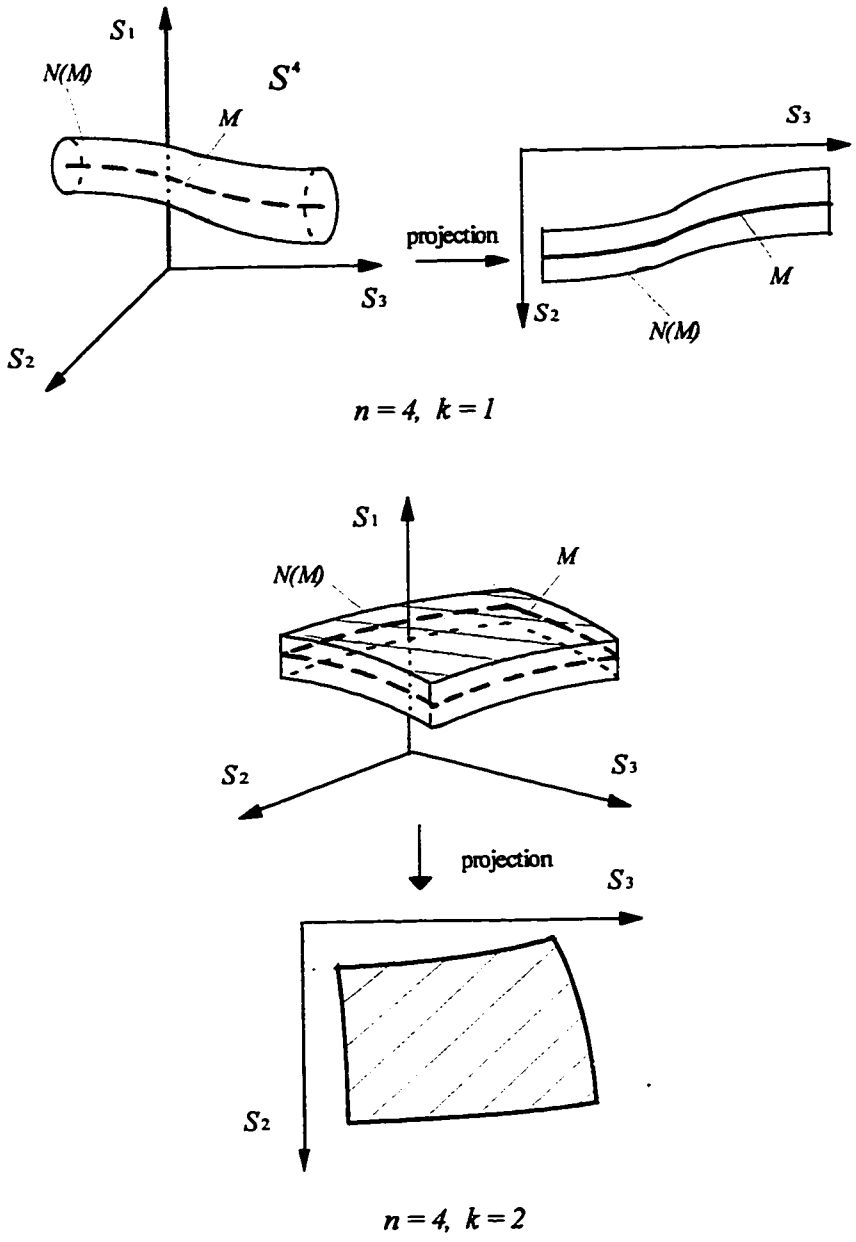

Figure 3.4: Points on the Unit Sphere Surface Considered by Equation (3.43) for $k = 1$ and $k = 2$ cases

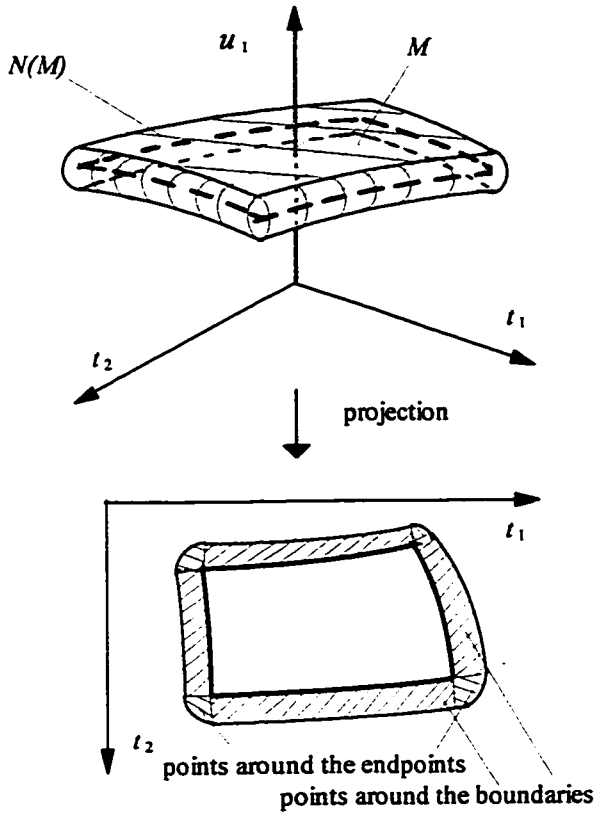

Figure 3.5: Points Close to the Boundaries and Endpoints, which are not Included by Equation (3.43) but Make Contributions to the Extreme Value Distribution in a 2D case.

Chapter 4, contributions by boundaries and endpoints cannot be neglected in general cases.

3.3.4 Volume of the Tube

Denoting the coordinate vectors of the tube by $\tilde{\mathbf{E}}_i$ $(i = 1, 2, ..., n-1)$, we can obtain the primary representation of $V_{n-1}(N)$, the volume of the $(n-1)$-dimensional tube, according to equation (3.32):

$$V_{n-1}(N) = \int_{\mathbf{T}} \int_{|\mathbf{u}| \leq r(\mathbf{t})} \left| \det \left(\tilde{\mathbf{E}}_1, \tilde{\mathbf{E}}_2, ..., \tilde{\mathbf{E}}_{n-1}, \mathbf{z} \right) \right| d\mathbf{u}d\mathbf{t} \tag{3.45}$$

The coordinate vectors $\tilde{\mathbf{E}}_i$ $(i = 1, 2, ..., n-1)$ are the changes of the unit vector $\mathbf{z}$ given by (3.43) with respect to the coordinates $(t_1, t_2, ..., t_k, u_1, u_2, ..., u_m)$:

$$\tilde{\mathbf{E}}_j = \frac{\partial \mathbf{z}}{\partial t_j}, \quad (j = 1, 2, ..., k) \tag{3.46}$$

$$\tilde{\mathbf{E}}_{i+k} = \frac{\partial \mathbf{z}}{\partial u_i}, \quad (i = 1, 2, ..., m) \tag{3.47}$$

In order to evaluate the tube volume defined by equation (3.45), the above two equations should first be expressed explicitly.

Insertion of the equation (3.43) into equation (3.46) and (3.47) yields:

$$\begin{aligned} \frac{\partial \mathbf{z}}{\partial t_j} &= (1 + |\mathbf{u}|^2)^{-1/2} \left(\frac{\partial \mathbf{y}}{\partial t_j} + \sum_{i=1}^{m} u_i \frac{\partial \mathbf{n}_i}{\partial t_j} \right) \\ &= (1 + |\mathbf{u}|^2)^{-1/2} \left(\mathbf{E}_j + \sum_{i=1}^{m} u_i \frac{\partial \mathbf{n}_i}{\partial t_j} \right), \quad (j = 1, 2, ..., k) \end{aligned} \tag{3.48}$$

$$\frac{\partial \mathbf{z}}{\partial u_i} = (1+|\mathbf{u}|^2)^{-1/2}\mathbf{n}_i + \frac{\partial (1+|\mathbf{u}|^2)^{-1/2}}{\partial u_i}\mathbf{z}, \quad (i = 1, 2, ..., m) \tag{3.49}$$

Notice that the unit vectors $\mathbf{y}$ and $\mathbf{n}_i$ are all dependent on $\mathbf{t}$, not on $\mathbf{u}$.

The second term in equation (3.49) is a vector parallel to $\mathbf{z}$ so that it has no contribution to the value of the determinant in the volume formula (3.45) and it can be ignored.

Now the only unknown term in the equations of the coordinate vectors is $\frac{\partial \mathbf{n}_i}{\partial t_j}$. According to equations (3.40), (3.41) and (3.42), the choice of $\mathbf{n}_i$ depends on the manifold M and its derivatives. Therefore, the tube volume depends on M and its derivatives but not on $\mathbf{n}_i$.

First, from the property of being normal to the unit vector $\mathbf{y}$, we have,

$$\mathbf{n}_i \cdot \mathbf{y} = \mathbf{0} \tag{3.50}$$

by differentiating the above equation with respect to t_j, we have:

$$\frac{\partial \mathbf{n}_i}{\partial t_j} \cdot \mathbf{y} = -\mathbf{n}_i \cdot \frac{\partial \mathbf{y}}{\partial t_j} = -\mathbf{n}_i \cdot \mathbf{E}_j = 0 \tag{3.51}$$

with $(i = 1, 2, ..., m)$, $(j = 1, 2, ..., k)$. This means that the vectors $\frac{\partial \mathbf{n}_i}{\partial t_j}$ are also orthogonal to the unit vectors $\mathbf{y}$ so that they must lie in the tangential space of the sub-manifold M at the point of $\mathbf{y}$. Since the tangential space is spanned by the coordinate vectors $\{\mathbf{E}_1, \mathbf{E}_2, ..., \mathbf{E}_k, \mathbf{n}_1, \mathbf{n}_2, ..., \mathbf{n}_m\}$, $\frac{\partial \mathbf{n}_i}{\partial t_j}$ can be expressed in terms of

them. We assume the form to be as follows:

$$\frac{\partial \mathbf{n}_i}{\partial t_j} = \sum_{\mu=1}^{k} g_{j\mu}^{i} \mathbf{E}_\mu + \sum_{\nu=1}^{m} g_{j\nu}^{i} \mathbf{n}_\nu \tag{3.52}$$

where $g_{j\mu}^{i}$, $g_{j\nu}^{i}$ are unknown coefficients dependent on $\mathbf{n}_i$, t_j and $\mathbf{E}_\mu$ or $\mathbf{n}_\nu$. As $\mathbf{n}_1$, $\mathbf{n}_2, ..., \mathbf{n}_m$ span the space orthogonal to the space spanned by $\mathbf{E}_1$, $\mathbf{E}_2, ..., \mathbf{E}_k$, they do not influence the value of the determinant in the tube volume formula (3.45). Therefore, the second term in equation (3.52) can also be ignored and there is only a need to find the coefficients $g_{j\mu}^{i}$.

By using the relationship between $\mathbf{E}_l$ $(l = 1, 2, ..., k)$ and $\mathbf{n}_i$ $(i = 1, 2, ..., m)$, we have,

$$\mathbf{E}_l \cdot \mathbf{n}_i = 0 \tag{3.53}$$

The differentiation of the above equation with respect to t_j results in:

$$\mathbf{E}_l \cdot \frac{\partial \mathbf{n}_i}{\partial t_j} + \frac{\partial \mathbf{E}_l}{\partial t_j} \cdot \mathbf{n}_i = 0 \tag{3.54}$$

Now it is necessary to introduce the second derivative of sub-manifold M. Let it be defined by:

$$\mathbf{h}_{lj} = \frac{\partial^2 \mathbf{h}(\mathbf{t})}{\partial t_l \partial t_j} = \left(\frac{\partial^2 h_1(\mathbf{t})}{\partial t_l \partial t_j}, \frac{\partial^2 h_2(\mathbf{t})}{\partial t_l \partial t_j}, ..., \frac{\partial^2 h_n(\mathbf{t})}{\partial t_l \partial t_j} \right)^T = \mathbf{h}_{jl} \tag{3.55}$$

with $(l, j = 1, 2, ..., k)$. It is obvious that $\mathbf{h}_{lj}$ is the curvature of the manifold M. And

let $\mathbf{H}$ denote the vector matrix of $\mathbf{h}_{lj}$:

$$\mathbf{H} = [\mathbf{h}_{lj}]_{l,j=1,2,...,k} \tag{3.56}$$

Notice that $\mathbf{H}$ is symmetric.

Making a substitution of equation (3.55) into (3.54), we obtain:

$$\mathbf{E}_l \cdot \frac{\partial \mathbf{n}_i}{\partial t_j} = -\mathbf{h}_{lj} \cdot \mathbf{n}_i \tag{3.57}$$

Multiplying both sides of equation (3.52) by $\mathbf{E}_l$ and then inserting the above equation into it, we get the following equation:

$$\mathbf{E}_l \cdot \frac{\partial \mathbf{n}_i}{\partial t_j} = \sum_{\mu=1}^{k} g_{j\mu}^{i} \mathbf{E}_l \cdot \mathbf{E}_\mu + \sum_{\nu=1}^{m} g_{j\nu}^{i} \mathbf{E}_l \cdot \mathbf{n}_\nu = -\mathbf{h}_{lj} \cdot \mathbf{n}_i \tag{3.58}$$

Recall that $\mathbf{E}_l \cdot \mathbf{n}_\nu = 0$ and $\mathbf{E}_l \cdot \mathbf{E}_\mu = m_{l\mu}$, we have:

$$\sum_{\mu=1}^{k} g_{j\mu}^{i} m_{l\mu} = -\mathbf{h}_{lj} \cdot \mathbf{n}_i, \quad (j, l, \mu = 1, 2, ..., k), \; (i = 1, 2, ..., m) \tag{3.59}$$

i.e.,

$$(m_{l1}, m_{l2}, ..., m_{lk}) \begin{pmatrix} g_{j1}^{i} \\ g_{j2}^{i} \\ \vdots \\ g_{jk}^{i} \end{pmatrix} = -\mathbf{h}_{lj} \cdot \mathbf{n}_i \tag{3.60}$$

As defined by equation (3.28), $\mathbf{M}$ is a metric tensor matrix so that it is always

positive and non-singular. Therefore, we can define its inverse matrix as follows:

$$\mathbf{M}^{-1} = (m_{l\mu}^{-1})_{l,\mu=1,2,...,k} \tag{3.61}$$

Also, let be defined m $k \times k$ matrices $\mathbf{G}_i$ by:

$$\mathbf{G}_i = \left[g_{j\mu}^i\right]_{j,\mu=1,2,...,k} \tag{3.62}$$

in which $(i = 1, 2, ..., m)$.

Then equation (3.60) can be rewritten in the following form:

$$\mathbf{G}_i = -\mathbf{M}^{-1} \cdot \mathbf{H} \cdot \mathbf{n}_i \tag{3.63}$$

This finally gives the expression of $g_{j\mu}^i$. Furthermore, by introducing,

$$\widetilde{\mathbf{H}} = -\mathbf{M}^{-1} \cdot \mathbf{H} \tag{3.64}$$

$g_{j\mu}^i$ can be simplified as,

$$\mathbf{G}_i = \widetilde{\mathbf{H}} \cdot \mathbf{n}_i \tag{3.65}$$

which is more explicit. Note that $\widetilde{\mathbf{H}}$ is also a $k \times k$ symmetric matrix with components:

$$\tilde{\mathbf{h}}_{lj} = \sum_{\mu=1}^{k} m_{l\mu} \cdot \mathbf{h}_{\mu j} \tag{3.66}$$

Now that the representation of $\frac{\partial \mathbf{n}_i}{\partial t_j}$ is explicit, the same can be applied to $\frac{\partial \mathbf{z}}{\partial t_j}$. However, it is necessary to simplify the representation of $\frac{\partial \mathbf{z}}{\partial t_j}$ before inserting it into

(3.45) for the tube volume. As discussed before, the second term in the parametrization function of $\frac{\partial \mathbf{n}_i}{\partial t_j}$ can be ignored so that we can express $\frac{\partial \mathbf{z}}{\partial t_j}$ in the form:

$$\frac{\partial \mathbf{z}}{\partial t_j} = (1+|\mathbf{u}|^2)^{-1/2}(\mathbf{E}_j + \sum_{i=1}^{m} u_i \sum_{\mu=1}^{k} g_{j\mu}^i \mathbf{E}_\mu) + \cdots \qquad (j = 1, 2, ..., k) \tag{3.67}$$

where $\cdots$ denotes the terms ignored.

By introducing the Kronecker delta $\delta_{j\mu}$,

$$\delta_{j\mu} = \begin{cases} 1, & j = \mu \\ 0, & j \neq \mu \end{cases} \quad (j, \mu = 1, 2, ..., k)$$

and extracting $\mathbf{E}_\mu$, we can rewrite (3.67) as follows:

$$\frac{\partial \mathbf{z}}{\partial t_j} = (1+|\mathbf{u}|^2)^{-1/2}(\delta_{j\mu} + \sum_{i=1}^{m} u_i \sum_{\mu=1}^{k} g_{j\mu}^i)\mathbf{E}_\mu + \cdots \tag{3.68}$$

This can be rewritten in a matrix form:

$$\begin{aligned} & \frac{\partial \mathbf{z}}{\partial t_j} \\ = \; & (1+|\mathbf{u}|^2)^{-\frac{1}{2}} \begin{bmatrix} \delta_{11} + \sum_{i=1}^m u_i g_{11}^i & \cdots & \delta_{1k} + \sum_{i=1}^m u_i g_{1k}^i \\ \vdots & \vdots & \vdots \\ \delta_{k1} + \sum_{i=1}^m u_i g_{k1}^i & \cdots & \delta_{kk} + \sum_{i=1}^m u_i g_{kk}^i \end{bmatrix} \begin{pmatrix} \mathbf{E}_1 \\ \vdots \\ \mathbf{E}_k \end{pmatrix} + \cdots \\ = \; & (1+|\mathbf{u}|^2)^{-\frac{1}{2}} \left[\mathbf{I}_k + \sum_{i=1}^{m} u_i \mathbf{G}_i \right] \begin{pmatrix} \mathbf{E}_1 \\ \vdots \\ \mathbf{E}_k \end{pmatrix} + \cdots \end{aligned}$$

$$= (1+|\mathbf{u}|^2)^{-\frac{1}{2}} \cdot \mathbf{A} \cdot \begin{pmatrix} \mathbf{E}_1 \\ \vdots \\ \mathbf{E}_k \end{pmatrix} + \cdots \tag{3.69}$$

where $\mathbf{I}_k$ is the $k \times k$ unit matrix, $\mathbf{G}_i$ is defined by equation (3.63) and $\mathbf{A}$ is equal to:

$$\mathbf{A} = \mathbf{I}_k + \sum_{i=1}^{m} u_i \mathbf{G}_i \tag{3.70}$$

Having the explicit expressions (3.49) of $\frac{\partial \mathbf{z}}{\partial u_i}$ and (3.69) of $\frac{\partial \mathbf{z}}{\partial t_j}$, we can obtain an alternative format for the volume of the neighborhood by inserting (3.49), (3.69) and the expression of $\mathbf{z}$ (3.43) into (3.45),

$$\begin{aligned} V_{n-1}(N) &= \int_{\mathbf{T}} \int_{|\mathbf{u}| \le r(\mathbf{t})} \left| \det\left(\tilde{\mathbf{E}}_1, \tilde{\mathbf{E}}_2, \ldots, \tilde{\mathbf{E}}_{n-1}, \mathbf{z}\right) \right| d\mathbf{u} d\mathbf{t} \\ &= \int_{\mathbf{T}} \int_{|\mathbf{u}| \le r(\mathbf{t})} (1+|\mathbf{u}|^2)^{-n/2} \left| \det \begin{pmatrix} \mathbf{A} \cdot \begin{pmatrix} \mathbf{E}_1 \\ \vdots \\ \mathbf{E}_k \end{pmatrix} \\ \mathbf{n}_1 \\ \vdots \\ \mathbf{n}_m \\ \mathbf{y} \end{pmatrix} \right| d\mathbf{u} d\mathbf{t} \\ &= \int_{\mathbf{T}} \int_{|\mathbf{u}| \le r(\mathbf{t})} (1+|\mathbf{u}|^2)^{-n/2} \left| \det \left(\mathbf{A} \cdot \begin{pmatrix} \mathbf{E}_1 \\ \vdots \\ \mathbf{E}_k \end{pmatrix} \right) \right| d\mathbf{u} d\mathbf{t} \end{aligned} \tag{3.71}$$

where $\mathbf{y} \in M$ and it originates from the expression of $\mathbf{z}$ (3.43).

Similar to those discussed before, all the terms with $\mathbf{n}_i$ are neglected because they are normal to the space spanned by $\mathbf{E}_1, \mathbf{E}_2, ..., \mathbf{E}_k$ and therefore they do not influence the value of the determinant. The last transformation is similar to that of equation (3.35).

The determinant in the integral in equation (3.71) can be rewritten as:

$$\begin{aligned}\left|\det\left(\mathbf{A}\cdot\begin{pmatrix}\mathbf{E}_1\\ \vdots\\ \mathbf{E}_k\end{pmatrix}\right)\right| &= \left|\det\mathbf{A}\cdot\det\begin{pmatrix}\mathbf{E}_1\\ \vdots\\ \mathbf{E}_k\end{pmatrix}\right| \\ &= |\det\mathbf{A}|\cdot\left|\det\left(\mathbf{E}_l(\mathbf{t})\cdot\mathbf{E}_j(\mathbf{t})\right)\right|^{1/2}_{l,j=1,...,k} \\ &= |\det\mathbf{A}|\cdot|\det(\mathbf{M})|^{1/2} \qquad (3.72)\end{aligned}$$

where $\mathbf{M}$ is the metric tensor matrix defined by equation (3.28). This gives the following tube volume formula:

$$V_{n-1}(N) = \int_{\mathbf{T}}\int_{|\mathbf{u}|\le r(\mathbf{t})}(1+|\mathbf{u}|^2)^{-n/2}\left|\det\left[\mathbf{I}_k+\sum_{i=1}^{m}u_i\mathbf{G}_i\right]\right|\cdot|\det(\mathbf{M})|^{1/2}\,d\mathbf{u}d\mathbf{t} \qquad (3.73)$$

Recall that $|\mathbf{u}|$ is the distance between the points in the neighborhood and those in the sub-manifold M, that is $|\mathbf{u}| = r(\mathbf{t})$. Assume that $r = r(\mathbf{t})$ at a fixed $\mathbf{t}$, then we have,

$$\mathbf{u} = |\mathbf{u}|\cdot\frac{\mathbf{u}}{|\mathbf{u}|} = r\cdot\mathbf{V} \qquad (3.74)$$

so that,

$$u_i = r\cdot V_i, \quad (i = 1, 2, ..., m) \qquad (3.75)$$

$$|\mathbf{V}| = 1 \qquad (3.76)$$

Using polar coordinates, we have:

$$d\mathbf{u} = r^{m-1} dr \cdot d\mathbf{V} \tag{3.77}$$

Then $V_{n-1}(N)$ can be rewritten in the form:

$$\begin{aligned} V_{n-1}(N) &= \int_{\mathbf{T}} \int_{r \leq r(\mathbf{t})} \frac{r^{m-1}}{(1+r^2)^{\frac{n}{2}}} \int_{|\mathbf{V}|=1} \det \left[\mathbf{I}_k + r \sum_{i=1}^{m} V_i \mathbf{G}_i \right] d\mathbf{V} \, |\det(\mathbf{M})|^{\frac{1}{2}} \, dr d\mathbf{t} \\ &= \int_{\mathbf{T}} \int_{r \leq r(\mathbf{t})} \frac{r^{m-1}}{(1+r^2)^{\frac{n}{2}}} \int_{|\mathbf{V}|=1} \det \mathbf{A} d\mathbf{V} \, |\det(\mathbf{M})|^{\frac{1}{2}} \, dr d\mathbf{t} \end{aligned} \tag{3.78}$$

Note that the integration area of $\mathbf{V}$ is the surface area of the m-dimensional unit sphere.

3.3.5 Evaluation of an Integral

So far, the preceding derivation is similar to Weyl (1939). The next step is to evaluate the integral involved in equation (3.78),

$$\int_{|\mathbf{V}|=1} \det \mathbf{A} d\mathbf{V} \tag{3.79}$$

in which the $k \times k$ matrix $\mathbf{A}$ is defined by equation (3.70) and $\mathbf{V} = (V_1, V_2, ..., V_m)$. Different evaluations of the integral result in different formulas for the tube volume, each of which will be discussed in turn.

a. Weyl's Method

Weyl (1939) decomposes the determinant in (3.79) as follows:

$$\det \mathbf{A} = \det \left[\mathbf{I}_k + r \sum_{i=1}^{m} V_i \mathbf{G}_i \right] = 1 + r\psi_1 + r^2\psi_2 + \cdots \tag{3.80}$$

Then he gets the expansion of the integral:

$$\int_{|\mathbf{V}|=1} \det \mathbf{A} d\mathbf{V} = \omega_m \cdot \left\{ 1 + \frac{r}{m} \left[-S/2 - k(k-1)/2) \right] \right\} + o(r^2) \tag{3.81}$$

where ω_m, the surface area of an m-dimensional unit sphere, is defined by equation (3.24). As mentioned in section 3.3.1, S is the intrinsic scalar curvature of the sub-manifold M which is a function of the partial differentials of $m_{ij}(\mathbf{t})$ defined by equation (3.28) with respect to t_l $(l = 1, 2, ..., k)$. S is difficult to evaluate in a practical problem. Therefore another evaluation of the integral, involving no S, should be developed in order to avoid calculating the intrinsic scalar curvature.

Breitung (1997) made a successful effort in this direction. By means of a 'projection method', an approximation formula for the integral (3.79) is proposed which is much easier to evaluate. Although it will be shown that Breitung's formula is incorrect, the projection method is really an effective idea and it will be used in this thesis to develop an accurate formula for the tube volume in 2D cases.

b. Breitung's Projection Method

Based on the assumption that $\mathbf{G}_i$ $(i = 1, 2, ..., m)$ are symmetric matrices and the condition $r \to 0$, Breitung (1997) expands the determinant in the integral (3.79) as

follows:

$$\begin{aligned} \det \mathbf{A} &= \det\left[I_k + r\sum_{i=1}^{m} V_i \mathbf{G}_i\right] \\ &= \det\left[I_k + r\mathbf{B}\right] \\ &= 1 + r \cdot tr(\mathbf{B}) + \frac{r^2}{2} \cdot \left[tr(\mathbf{B}\otimes\mathbf{B}) - tr(\mathbf{B}^2)\right] + o(r^2) \end{aligned} \tag{3.82}$$

in which $tr(\mathbf{B})$ is the trace of $\mathbf{B}$ and $\otimes$ denotes the Kronecker product of two matrices. This formula is derived by the facts that any symmetric matrix can be rewritten in a diagonal form by a suitable rotation and the trace of a matrix is invariant under rotation.

By substituting equation (3.82) into (3.79) and revising it, Breitung obtains:

$$\int_{|\mathbf{V}|=1} \det A d\mathbf{V} = \sum_{i,j=1}^{m} \int_{|\mathbf{V}|=1} V_i V_j \mathbf{n}_i \cdot \tilde{\mathbf{h}}_{ii} \cdot \tilde{\mathbf{h}}_{jj} \cdot \mathbf{n}_j d\mathbf{V} + o(r^2) \tag{3.83}$$

with $(i = 1, 2, ..., m)$ and $(l, j = 1, 2, ..., k)$.

To evaluate the above equation, Breitung introduced the projection method.

It is seen that the term $\mathbf{n}_i \cdot \tilde{\mathbf{h}}_{lj}$ are the projections of the vectors $\tilde{\mathbf{h}}_{lj}$ onto the subspace spanned by the vectors $\mathbf{n}_i$ $(i = 1, 2, ..., m)$, that is,

$$\mathbf{h}_{lj}^{+} = \mathbf{P} \cdot \tilde{\mathbf{h}}_{lj} \tag{3.84}$$

in which $\mathbf{h}_{lj}^{+}$ are the projections and $\mathbf{P}$ is the projection matrix onto the space spanned by the normal vectors $\mathbf{n}_1$, $\mathbf{n}_2, ..., \mathbf{n}_m$. Since $\mathbf{n}_1$, $\mathbf{n}_2, ..., \mathbf{n}_m$ are dependent on $\mathbf{E}_1$, $\mathbf{E}_2, ..., \mathbf{E}_k$ and $\mathbf{y}$, the projection matrix $\mathbf{P}$ is difficult to obtain directly. However,

by noting that the orthogonal system $\mathbf{n}_1, \mathbf{n}_2, ..., \mathbf{n}_m$ is normal to the space spanned by $\mathbf{E}_1, \mathbf{E}_2, ..., \mathbf{E}_k, \mathbf{y}$, and all of them together form the space R^n, one can determine $\mathbf{P}$ by the fact that the projection matrix onto a space is equal to the unity matrix minus the projection matrix onto the space that is normal and complementary to this subspace (Breitung, 1994). Therefore, to evaluate the matrix $\mathbf{P}$, the projection matrix $\mathbf{P}^*$ onto the subspace spanned by $\mathbf{E}_1, \mathbf{E}_2, ..., \mathbf{E}_k$ and $\mathbf{y}$ should first be found. Using the facts that $\mathbf{y}$ is a unit vector and normal to the coordinate vectors $\mathbf{E}_1, \mathbf{E}_2, ..., \mathbf{E}_k$, one obtains,

$$\mathbf{P}^* = \mathbf{E}\mathbf{M}^{-1}\mathbf{E}^T + \mathbf{y}\mathbf{y}^T \tag{3.85}$$

with $\mathbf{E}$ defined by,

$$\mathbf{E} = (\mathbf{E}_1, \mathbf{E}_2, ..., \mathbf{E}_k) \tag{3.86}$$

Notice that $\mathbf{P}^*$ is an $n \times n$ symmetric matrix. Then the projection matrix $\mathbf{P}$ can be determined by:

$$\mathbf{P} = \mathbf{I}_n - \mathbf{P}^* = \mathbf{I}_n - \mathbf{E}\mathbf{M}^{-1}\mathbf{E}^T - \mathbf{y}\mathbf{y}^T \tag{3.87}$$

in which $\mathbf{I}_n$ is the $n \times n$ unit matrix.

By applying the projection method introduced above, Breitung obtained:

$$\int_{|\mathbf{V}|=1} \det A d\mathbf{V} = \omega_m \left[1 + \frac{r^2}{2m} \cdot \sum_{\mu,\nu=1,\mu\neq\nu}^{k} \left\langle \mathbf{h}_{\mu\mu}^+, \mathbf{h}_{\nu\nu}^+ \right\rangle \right] + o(r^2) \tag{3.88}$$

where ω_m is the surface volume of an m-dimensional unit sphere and it is defined by equation (3.24).

However, it is easy to find that the assumption on which the above equation is based is incorrect. That is, the matrixes $\mathbf{G}_i$ may not be symmetric. According to

the definition in equation (3.63),

$$\mathbf{G}_i = -\mathbf{M}^{-1}\cdot\mathbf{H}\cdot\mathbf{n}_i \tag{3.89}$$

it is clear that although $\mathbf{M}^{-1}$ and $\mathbf{H}$ are symmetric, their products $\mathbf{G}_i$ are not necessarily symmetric,

$$\left(-\mathbf{M}^{-1}\cdot\mathbf{H}\right)^T = -\mathbf{H}^T\cdot\left(\mathbf{M}^{-1}\right)^T = -\mathbf{H}\cdot\mathbf{M}^{-1} \neq -\mathbf{M}^{-1}\cdot\mathbf{H} \tag{3.90}$$

So, Breitung's formula for $\int_{|\mathbf{V}|=1}\det\mathbf{A}d\mathbf{V}$ is incorrect.

Even so, the projection method is a useful tool for the following section.

c. Evaluation of $2D$ Cases by Projection Method

According to the previous discussion, it is clear that the key aspect of evaluating the volume of the tube is how to determine the integral $\int_{|\mathbf{V}|=1}\det\mathbf{A}d\mathbf{V}$.

Considering that the random fields in practical engineering problems are always 1D or 2D, we will focus on the lower dimensional cases in this thesis, especially $k=2$.

Actually, the value of the determinant of $\mathbf{A}$ can be obtained exactly for the lower dimensional cases. When $k=2$, $\mathbf{G}_i$ $(i=1,2,...,m)$ are 2×2 matrixes, we have,

$$\det\mathbf{A} = \det\left[\mathbf{I}_k + r\sum_{i=1}^{m}V_i\mathbf{G}_i\right] \tag{3.91}$$

$$= \det\left[\mathbf{I}_2 + \begin{pmatrix} r\sum_{i=1}^{m}V_i g_{11}^i & r\sum_{i=1}^{m}V_i g_{12}^i \\ r\sum_{i=1}^{m}V_i g_{21}^i & r\sum_{i=1}^{m}V_i g_{22}^i \end{pmatrix}\right] \tag{3.92}$$

since the matrix $\mathbf{A}$ is also a 2×2 matrix, it follows that,

$$\begin{aligned} \det \mathbf{A} &= 1 + r\sum_{i=1}^{m} V_i g_{11}^i + r\sum_{i=1}^{m} V_i g_{22}^i \\ &\quad + r^2 \sum_{i,j=1}^{m} V_i V_j g_{11}^i g_{22}^j - r^2 \sum_{i,j=1}^{m} V_i V_j g_{12}^i g_{21}^j \end{aligned} \tag{3.93}$$

For the 1D and 3D cases, similar results can easily be obtained as well.

Now we expand the integral for $k = 2$ in the following form,

$$\begin{aligned} \int_{|\mathbf{V}|=1} \det \mathbf{A} d\mathbf{V} &= \int_{|\mathbf{V}|=1} 1 d\mathbf{V} + r\sum_{i=1}^{m} \int_{|\mathbf{V}|=1} V_i g_{11}^i d\mathbf{V} \\ &\quad + r\sum_{i=1}^{m} \int_{|\mathbf{V}|=1} V_i g_{22}^i d\mathbf{V} + r^2 \sum_{i,j=1}^{m} \int_{|\mathbf{V}|=1} V_i V_j g_{11}^i g_{22}^j d\mathbf{V} \\ &\quad - r^2 \sum_{i,j=1}^{m} \int_{|\mathbf{V}|=1} V_i V_j g_{12}^i g_{21}^j d\mathbf{V} \end{aligned} \tag{3.94}$$

Recall that $\mathbf{V} = (V_1, V_2, ..., V_m)^T$ is a vector with unit length and that its endpoint is a uniformly distributed random variable. Therefore, the domain of the endpoint of V is the surface area of the m-dimensional unit sphere. This gives,

$$\int_{|\mathbf{V}|=1} 1 d\mathbf{V} = \omega_m \tag{3.95}$$

where ω_m is the surface area (or volume) of an m-dimensional unit sphere and it is defined by equation (3.24).

Due to symmetry, we also have,

$$\int_{|\mathbf{V}|=1} V_i d\mathbf{V} = 0 \tag{3.96}$$

$$\int_{|\mathbf{V}|=1} V_i V_j d\mathbf{V} = 0, \quad (i \neq j) \tag{3.97}$$

For the evaluation of $\int_{|\mathbf{V}|=1} V_i^2 d\mathbf{V}$, we begin with the fact that $|\mathbf{V}| = 1$,i.e.,

$$\sum_{i=1}^{m} V_i^2 = 1 \tag{3.98}$$

Since the endpoint of $\mathbf{V}$ is a uniformly distributed random variable and $(V_1, V_2, ..., V_m)$ form an orthogonal system, it results,

$$\mathbb{E}\left\{\sum_{i=1}^{m} V_i^2\right\} = 1 \Rightarrow \sum_{i=1}^{m} \mathbb{E}\left\{V_i^2\right\} = 1 \tag{3.99}$$

where $\mathbb{E}\{\cdot\}$ is the expected value operator, defined by (2.6).

Due to symmetry, it gives,

$$\mathbb{E}\left(V_i^2\right) = \frac{1}{m} \tag{3.100}$$

Because of symmetry, we have once more:

$$\begin{aligned} \int_{|\mathbf{V}|=1} V_i^2 d\mathbf{V} &= \mathbb{E}\left\{\int_{|\mathbf{V}|=1} V_i^2 d\mathbf{V}\right\} \\ &= \int_{|\mathbf{V}|=1} \mathbb{E}\left\{V_i^2\right\} d\mathbf{V} \end{aligned} \tag{3.101}$$

Insertion of equations (3.95) and (3.100) into the above equation results in,

$$\int_{|\mathbf{V}|=1} V_i^2 d\mathbf{V} = \frac{\omega_m}{m} \tag{3.102}$$

Then the integral $\int_{|\mathbf{V}|=1} \det \mathbf{A} dV$ can be rewritten in the form,

$$\int_{|\mathbf{V}|=1} \det \mathbf{A} d\mathbf{V} = \omega_m \left\{ 1 + \frac{r^2}{m} \left[\sum_{i=1}^{m} g_{11}^i g_{22}^i - \sum_{i=1}^{m} g_{12}^i g_{21}^i \right] \right\} \tag{3.103}$$

Substituting the representation of g_{ij}^i by its definition in equation (3.63), we get,

$$\begin{aligned} & \int_{|\mathbf{V}|=1} \det \mathbf{A} d\mathbf{V} \\ = \; & \omega_m \left\{ 1 + \frac{r^2}{m} \left[\sum_{i=1}^{m} \tilde{\mathbf{h}}_{11} \cdot \mathbf{n}_i \cdot \tilde{\mathbf{h}}_{22} \cdot \mathbf{n}_i - \sum_{i=1}^{m} \tilde{\mathbf{h}}_{12} \cdot \mathbf{n}_i \cdot \tilde{\mathbf{h}}_{21} \cdot \mathbf{n}_i \right] \right\} \\ = \; & \omega_m \left\{ 1 + \frac{r^2}{m} \left[\tilde{\mathbf{h}}_{11} \cdot \left(\sum_{i=1}^{m} \mathbf{n}_i \cdot \mathbf{n}_i \right) \cdot \tilde{\mathbf{h}}_{22} - \tilde{\mathbf{h}}_{12} \cdot \left(\sum_{i=1}^{m} \mathbf{n}_i \cdot \mathbf{n}_i \right) \cdot \tilde{\mathbf{h}}_{21} \right] \right\} \end{aligned} \tag{3.104}$$

Taking into account that $\mathbf{n}_1$, $\mathbf{n}_2, ..., \mathbf{n}_m$ form an orthogonal system, we can conclude that $\sum_{i=1}^{m} \mathbf{n}_i \cdot \mathbf{n}_i$ is the projection matrix onto the space spanned by $\mathbf{n}_1$, $\mathbf{n}_2, ..., \mathbf{n}_m$, i.e.,

$$\sum_{i=1}^{m} \mathbf{n}_i \cdot \mathbf{n}_i = \mathbf{P} \tag{3.105}$$

where $\mathbf{P}$ is the projection matrix onto the space spanned by the normal vectors $\mathbf{n}_1$, $\mathbf{n}_2, ..., \mathbf{n}_m$ and can easily be determined based on equation (3.87). Therefore, the evaluations of the integral formula (3.104) and the tube volume become manageable.

For simplification purpose, the term $[\cdot]$ in the integral (3.104) can be rewritten in the following form by introducing equation (3.105),

$$\begin{aligned} & \left[\tilde{\mathbf{h}}_{11} \cdot \left(\sum_{i=1}^{m} \mathbf{n}_i \cdot \mathbf{n}_i \right) \cdot \tilde{\mathbf{h}}_{22} - \tilde{\mathbf{h}}_{12} \cdot \left(\sum_{i=1}^{m} \mathbf{n}_i \cdot \mathbf{n}_i \right) \cdot \tilde{\mathbf{h}}_{21} \right] \\ = \; & \left[\tilde{\mathbf{h}}_{11} \cdot \mathbf{P} \cdot \tilde{\mathbf{h}}_{22} - \tilde{\mathbf{h}}_{12} \cdot \mathbf{P} \cdot \tilde{\mathbf{h}}_{21} \right] \end{aligned} \tag{3.106}$$

According to the derivation in Appendix B,

$$\mathbf{P} = \mathbf{P}^T \cdot \mathbf{P} \tag{3.107}$$

This gives,

$$\begin{aligned} \left[\tilde{\mathbf{h}}_{11} \cdot \mathbf{P} \cdot \tilde{\mathbf{h}}_{22} - \tilde{\mathbf{h}}_{12} \cdot \mathbf{P} \cdot \tilde{\mathbf{h}}_{21}\right] &= \left[\tilde{\mathbf{h}}_{11} \cdot \mathbf{P}^T \cdot \mathbf{P} \cdot \tilde{\mathbf{h}}_{22} - \tilde{\mathbf{h}}_{12} \cdot \mathbf{P}^T \cdot \mathbf{P} \cdot \tilde{\mathbf{h}}_{21}\right] \\ &= \left\langle \mathbf{h}_{11}^+, \mathbf{h}_{22}^+ \right\rangle - \left\langle \mathbf{h}_{12}^+, \mathbf{h}_{21}^+ \right\rangle \end{aligned} \tag{3.108}$$

The latest transformation is performed by introducing equation (3.84),

$$\mathbf{h}_{ij}^+ = \mathbf{P} \cdot \tilde{\mathbf{h}}_{ij} \tag{3.109}$$

At last, we obtain the simplified form of the integral,

$$\int_{|\mathbf{V}|=1} \det \mathbf{A} d\mathbf{V} = \omega_m \left\{ 1 + \frac{r^2}{m} \left(\left\langle \mathbf{h}_{11}^+, \mathbf{h}_{22}^+ \right\rangle - \left\langle \mathbf{h}_{12}^+, \mathbf{h}_{21}^+ \right\rangle \right) \right\} \tag{3.110}$$

d. Comparison Between Breitung's and Weyl's Methods

Considering Breitung's formula (3.88) for 2D ($k = 2$) cases, we have,

$$\int_{|\mathbf{V}|=1} \det A d\mathbf{V} = \omega_m \left[1 + \frac{r^2}{m} \cdot \left\langle \mathbf{h}_{11}^+, \mathbf{h}_{22}^+ \right\rangle \right] + o(r^2) \tag{3.111}$$

In comparison to our proposed formula (3.110), it can be seen that Breitung's formula only considers the diagonal elements of $\mathbf{G}_i$ while it neglects others. This will result in a larger tube volume and therefore a larger maxima probability.

Notice that the formats of the three formulas for the integral are very similar. Based on this, although we are mainly dealing with the case $k = 2$, it is better to choose the following format for the integral in the advance derivation for the maxima probability for general purpose,

$$\int_{|\mathbf{V}|=1} \det A d\mathbf{V} = \omega_m \left(1 + \frac{r^2}{m} \cdot c_2\right) \tag{3.112}$$

with,

$$c_2 = \left\langle \mathbf{h}_{11}^+, \mathbf{h}_{22}^+ \right\rangle - \left\langle \mathbf{h}_{12}^+, \mathbf{h}_{21}^+ \right\rangle, \quad \text{for} \quad k = 2 \tag{3.113}$$

It is clear that only the expressions of c_2 are different in the three formulas for the integral. Since c_2 only depends on the manifold M, the following derivation for the maxima probability is applicable to general cases and there is only a need to change c_2 when considering different random fields. According to the definition of $\mathbf{h}_{ij}^+$ (3.84), it is obvious that c_2 is related to the curvature of the manifold M.

3.3.6 Proposed Formula

Insertion of equation (3.112) into (3.78) results in the explicit representation of the tube volume,

$$V_{n-1}(N) = \int_{\mathbf{T}} \int_{r \le r(\mathbf{t})} \frac{r^{m-1}}{(1+r^2)^{n/2}} \omega_m \left(1 + \frac{r^2}{m} \cdot c_2\right) \cdot c_1 dr d\mathbf{t} \tag{3.114}$$

in which

$$c_1 = |\det(\mathbf{M})|^{1/2} \tag{3.115}$$

which is a function of $\mathbf{t}$ and c_2 is given by (3.113) for $k = 2$.

According to equation (3.15), with $r \to 0$, r is approximately equal to $\tan\theta$. This gives an alternative form for the tube volume,

$$\begin{aligned} V_{n-1}(N) &= \int_{\mathbf{T}} \int_{\theta} \frac{\sin^{m-1}\theta}{\cos^{m-1}\theta} \cos^{n}\theta \cdot \omega_m \left(1 + \frac{\sin^2\theta}{\cos^2\theta} \cdot \frac{c_2}{m}\right) c_1 \sec^2\theta d\theta d\mathbf{t} \\ &= \int_{\mathbf{T}} \left(\omega_m \int_{\theta} \sin^{m-1}\theta \cos^{k}\theta d\theta + \omega_m \int_{\theta} \frac{1}{m} \sin^{m+1}\theta \cos^{k-2}\theta d\theta \cdot c_2\right) c_1 d\mathbf{t} \\ &= \int_{\mathbf{T}} \left(\omega_m J_0(\theta) + \omega_m J_2(\theta) c_2\right) c_1 d\mathbf{t} \end{aligned} \tag{3.116}$$

where $J_0(\theta)$, $J_2(\theta)$ are the same as those defined by equation (3.26) and (3.27).

Since the above equation is derived using equation (3.43) directly, as discussed in section 3.3.3, it is not the total volume of the tube but the volume of the tube corresponding to the main area of the random field.

By comparing with Weyl's formula (3.25) for the tube volume, we can see that the first two terms of Weyl's formula are almost the same as our proposed formula except that the expression of c_2 is different. Our formula is accurate for 2D cases and successfully avoids the calculation of the scalar curvature in Weyl's equation (3.25).

3.4 Maxima of Random Fields

In previous sections, the basic idea of the tube method is outlined and the relationship between geometric concepts and the maxima of random fields is given by equations (3.18) and (3.23). In fact, the probability distribution of maxima of a random field is related to the ratio of the volume of a tube and the surface volume of a unit sphere.

Since the tube volume has been given by equation (3.116), the derivation of the maxima of random fields is manageable. By using Weyl's (1939) formula for the tube

volume (3.25), Sun (1993) proposed a two-term formula for the extreme value distribution without listing the derivation process. Farasyn (1997) derived a corresponding formula for the one-dimensional cases by means of Hotelling's (1939) equation and also developed the formula for the probability associated with endpoints. Before presenting our own derivation, Sun's and Farasyn's results will be introduced briefly.

3.4.1 Existing Results

a. Sun (1993)

Suppose $Z(\mathbf{t})$ is a differentiable non-homogeneous Gaussian random field with unit variance, domain $\mathbf{T}$ and without boundary (see the discussion in section 3.3.3). Then as the threshold $\beta \rightarrow \infty$, the extreme value distribution of the random field is equal to,

$$P(\beta) = P(\max_{\mathbf{T}} Z(\mathbf{t}) \geq \beta) = \kappa_0 \psi_0^*(\beta) + \kappa_2 \psi_2^*(\beta) + o\left(\psi_2^*(\beta)\right) \tag{3.117}$$

where κ_0, κ_2 are the same parameters as those in Weyl's formula (3.25) for the tube volume and $\psi_e^*(\beta)$ $(e = 0, 2)$ are defined by,

$$\psi_e^*(\beta) = \frac{1}{2^{1+e/2}\pi^{(k+1)/2}} \int_{\beta^2/2}^{\infty} u^{(k+1-e)/2-1} \exp(-u) du \tag{3.118}$$

Note that Sun's formula is applicable to the k-dimensional random field (k is finite) with unit variance. Furthermore, the direct use of Weyl's formula is the cause that Sun's formula does not include the contributions by boundaries and endpoints but is based on the scalar curvature S which is difficult to calculate.

b. Farasyn (1997)

Considering a differentiable non-homogenous 1D Gaussian random field $Z(\mathbf{t})$ with domain $T = (0, T)$, Farasyn (1997) found,

$$\begin{aligned} P(\beta) &= P(\max_{T} Z(t) \geq \beta) \\ &= \frac{1}{2\pi}\int_0^T \exp\left(-\frac{\beta^2}{2\left|\mathbf{h}^*(t)\right|^2}\right) c(t)\, dt + \frac{1}{2}\Phi\left(-\frac{\beta}{\left|\mathbf{h}^*(0)\right|}\right) \\ &\quad + \frac{1}{2}\Phi\left(-\frac{\beta}{\left|\mathbf{h}^*(T)\right|}\right) + \sum_{j=1}^{M}\Phi\left(-\frac{\beta}{\left|\mathbf{h}^*(t_j)\right|}\right) \end{aligned} \tag{3.119}$$

in which $\beta \to \infty$ and $\Phi(\cdot)$ is the standard normal distribution function. The second and third terms are the contributions by endpoints and the last term represents the probability associated with discontinuous jumps, with M the number of discontinuous points. Farasyn defined $c(t)$ by,

$$c(t) = \sqrt{\sum_{i=1}^{N}\left(\frac{d}{dt}\left(\frac{h_i^*(t)}{\left|\mathbf{h}^*(t)\right|}\right)\right)^2} \tag{3.120}$$

Recalling that $\frac{h_i^*(t)}{|\mathbf{h}^*(t)|} = h_i(t)$, this gives,

$$\begin{aligned} c(t) &= \sqrt{\sum_{i=1}^{N}\left(\frac{dh_i(t)}{dt}\right)^2} \\ &= \sqrt{\frac{d\mathbf{h}(t)}{dt}\cdot\frac{d\mathbf{h}(t)}{dt}} \\ &= \left[\det(\mathbf{E}_1\cdot\mathbf{E}_1)\right]^{1/2} \end{aligned} \tag{3.121}$$

This means that $c(t)$ is actually equal to c_1 as defined by (3.115) for the one dimensional case.

3.4.2 Proposed Formula

As discussed in section 3.2.3, for a k-dimensional differentiable Gaussian random field $Z(\mathbf{t})$ with zero mean, domain $\mathbf{T}$ and the discrete format (3.2), the maxima of the random field is related to the volume of a tube, $V_{n-1}(N)$. According to equations (3.18) and (3.23) in section 3.2.3, we have,

$$\begin{aligned} P(\beta) &= P(\max_{\mathbf{T}} Z(\mathbf{t}) \geq \beta) \\ &= \int_{\frac{\beta}{|\mathbf{h}^*(\mathbf{t})|}}^{\infty} P\left(\min_{\mathbf{T}} \theta \leq \arccos(\frac{\beta}{r_n \cdot |\mathbf{h}^*(\mathbf{t})|})\right) f_{\chi_n}(r_n)\, dr_n \\ &= \int_{\frac{\beta}{|\mathbf{h}^*(\mathbf{t})|}}^{\infty} \frac{V_{n-1}(N)}{\omega_n} f_{\chi_n}(r_n)\, dr_n \end{aligned} \tag{3.122}$$

where β is the threshold; $|\mathbf{h}^*(\mathbf{t})|$ is the standard deviation of the random field, the components of $\mathbf{h}^*(\mathbf{t})$, $h_i^*(\mathbf{t})$ $(i = 1, 2, ..., n)$, are a set of twice continuously differentially deterministic functions; $f_{\chi_n}(r_n)$ is the probability density function of χ_n-random variables, which is defined by equation (3.9); ω_m is the surface volume of an m-dimensional unit sphere and it is defined by equation (3.24).

The tube volume $V_{n-1}(N)$ has been given in equation (3.116). Introducing it, we get,

$$P(\beta) = \int_{\mathbf{T}} \left[\frac{\omega_m}{\omega_n} \int_{\frac{\beta}{|\mathbf{h}^*(\mathbf{t})|}}^{\infty} J_0(\theta) f_{\chi_n}(r_n)\, dr_n + \frac{\omega_m}{\omega_n} \int_{\frac{\beta}{|\mathbf{h}^*(\mathbf{t})|}}^{\infty} J_2(\theta) f_{\chi_n}(r_n)\, dr_n \cdot c_2\right] c_1 d\mathbf{t} \tag{3.123}$$

where c_1 is given by (3.115); c_2 is given by (3.113) for $k = 2$, and $J_0(\theta)$, $J_2(\theta)$ are defined by (3.26) and (3.27) respectively.

By defining,

$$\psi_0(\beta) = \frac{\omega_m}{\omega_n}\int_{\frac{\beta}{|\mathbf{h}^*(\mathbf{t})|}}^{\infty} J_0(\theta) f_{\chi_n}(r_n)\, dr_n \tag{3.124}$$

$$\psi_2(\beta) = \frac{\omega_m}{\omega_n}\int_{\frac{\beta}{|\mathbf{h}^*(\mathbf{t})|}}^{\infty} J_2(\theta) f_{\chi_n}(r_n)\, dr_n \tag{3.125}$$

we finally obtain,

$$\begin{aligned} P(\beta) &= \int_{\mathbf{T}} \psi_0(\beta)\cdot c_1 d\mathbf{t} + \int_{\mathbf{T}} \psi_2(\beta)\cdot c_2 \cdot c_1 d\mathbf{t} \\ &= P_{m1}(\beta) + P_{m2}(\beta) \end{aligned} \tag{3.126}$$

As discussed before, c_2 is related to the curvature of the manifold M (3.13). Therefore, the second term of the final result of the maxima of the random field is related to the curvature of M as well.

The process of the simplifications of equations (3.124) and (3.125) are given in Appendix A. The results are:

$$\psi_0(\beta) = \frac{1}{2\pi^{\frac{k+1}{2}}}\Gamma\left(\frac{k+1}{2}, \frac{\beta^2}{2\,|\mathbf{h}^*(\mathbf{t})|^2}\right) \tag{3.127}$$

$$\psi_2(\beta) = \frac{1}{4\pi^{\frac{k+1}{2}}}\Gamma\left(\frac{k-1}{2}, \frac{\beta^2}{2\,|\mathbf{h}^*(\mathbf{t})|^2}\right) \tag{3.128}$$

where $\Gamma(\cdot)$ is the incomplete gamma function (Abramowitz and Stegun, 1972) defined by,

$$\Gamma(a,z) = \int_z^{\infty} u^{a-1} e^{-u} du \tag{3.129}$$

As mentioned in section 3.3.6, the tube volume $V_{n-1}(N)$ given by (3.116) rep-

resents only the volume of the tube corresponding to the main area of the random field. Therefore, it only includes the probability associated with main (central) area of the random field. The probability associated with boundaries and endpoints, is discussed in section 3.5.

3.4.3 Comparison

By comparing the proposed formula (3.126) with Sun's (3.117), we can find that the differences between them are: first, $\psi_0(\beta)$, $\psi_2(\beta)$ in the proposed formula are functions of t since they are for random fields with time dependent variances; second, κ_2 in Sun's formula involves the scalar curvature S.

In order to compare with Farasyn's formula (3.119), we go back to the derivation for the tube volume in section 3.3.5 and consider the $k = 1$ case.

According to equation (3.91), we have for $k = 1$,

$$\det \mathbf{A} = 1 + r \sum_{i=1}^{m} V_i g_{11}^i \tag{3.130}$$

Using equations (3.95) and (3.96), we get the simplified integral,

$$\int_{|\mathbf{V}|=1} \det \mathbf{A} d\mathbf{V} = \omega_m \tag{3.131}$$

It follows that for $k = 1$:

$$P(\beta) = \int_T \psi_0(\beta) \cdot c_1 dt \tag{3.132}$$

This means that the second term in equation (3.126) vanishes when $k = 1$.

Actually, we can get the same result by analyzing equation (3.126) directly. Since,

$$c_2 = \left\langle \mathbf{h}_{11}^{+}, \mathbf{h}_{22}^{+} \right\rangle - \left\langle \mathbf{h}_{12}^{+}, \mathbf{h}_{21}^{+} \right\rangle \tag{3.133}$$

$\mathbf{h}_{22}^{+}, \mathbf{h}_{12}^{+}, \mathbf{h}_{21}^{+}$ are all equal to zero when $k = 1$ according to the definition (3.84). This gives $c_2 = 0$ and equation (3.132).

From equation (3.127), we have $\psi_0(\beta)$ for $k = 1$,

$$\psi_0(\beta) = \frac{1}{2\pi} \exp\left(-\frac{\beta^2}{2\left|\mathbf{h}^*(t)\right|^2} \right) \tag{3.134}$$

Combining with the fact that $c(t) = c_1$ for $k = 1$, one can conclude that the first term of Farasyn's formula (3.119) is a special case of our proposed formula (3.126).

3.4.4 Simplification for Homogeneous cases

The proposed formula (3.126) is valid for the general non-homogeneous case. Obviously, it can also be applied to the homogeneous case.

According to section 2.2, for a homogeneous random field $Z(\mathbf{t})$, the variance σ_Z^2 and the correlation function $R_{ZZ}\left(\mathbf{t}, \mathbf{t}'\right)$are not dependent on $\mathbf{t}$. This means that the functions $\psi_0(\beta)$, $\psi_2(\beta)$ in the proposed formula are not functions of $\mathbf{t}$ in the homogeneous case. For the elements of the metric tensor matrix $\mathbf{M}$ (3.28),

$$\begin{aligned} m_{ij}(\mathbf{t}) &= \mathbf{E}_i(\mathbf{t}) \cdot \mathbf{E}_j(\mathbf{t}) \\ &= \frac{\partial \mathbf{h}(\mathbf{t})}{\partial t_i} \cdot \frac{\partial \mathbf{h}(\mathbf{t})}{\partial t_j} \\ &= \frac{\partial \mathbf{h}^*(\mathbf{t})}{\partial t_i} \cdot \frac{\partial \mathbf{h}^*(\mathbf{t})}{\partial t_j} \cdot \frac{1}{\sigma_Z^2} \end{aligned}$$

$$= \frac{\partial R_{ZZ}(\mathbf{s},\mathbf{t})}{\partial s_i \partial t_j}\Big|_{\mathbf{s}=\mathbf{t}} \cdot \frac{1}{\sigma_Z^2} \tag{3.135}$$

It is clear that $m_{ij}(\mathbf{t})$ is also not dependent on $\mathbf{t}$, since $R_{ZZ}(\mathbf{s},\mathbf{t})$ is time invariant. Therefore, the proposed formula (3.126) can be rewritten as,

$$P(\beta) = \psi_0(\beta) \cdot c_1 \int_{\mathbf{T}} d\mathbf{t} + \psi_2(\beta) \cdot c_1 \int_{\mathbf{T}} c_2 d\mathbf{t} \tag{3.136}$$

In Sun's formula (3.117) (Sun, 1993),

$$c_2 = \kappa_2 = -\frac{S}{2} - \frac{k(k-1)}{2} \tag{3.137}$$

According to the definition (Kreyszig, 1968), the scalar curvature S is a function of the partial differentials of $m_{ij}(\mathbf{t})$ with respect to $\mathbf{t}$. Since $m_{ij}(\mathbf{t})$ does not depend on $\mathbf{t}$ for the homogeneous case, S is equal to zero. This gives for $k = 2$,

$$c_2 = \kappa_2 = -1 \tag{3.138}$$

in Sun's formula, which can be rewritten as,

$$P(\beta) = [\psi_0^*(\beta) - \psi_2^*(\beta)] \cdot c_1 \int_{\mathbf{T}} d\mathbf{t} \tag{3.139}$$

In our proposed formula, for $k = 2$, we have:

$$c_2 = \left\langle \mathbf{h}_{11}^+, \mathbf{h}_{22}^+ \right\rangle - \left\langle \mathbf{h}_{12}^+, \mathbf{h}_{21}^+ \right\rangle \tag{3.140}$$

But as shown in Appendix B,

$$c_2 = \left\langle \mathbf{h}_{11}^{+}, \mathbf{h}_{22}^{+} \right\rangle - \left\langle \mathbf{h}_{12}^{+}, \mathbf{h}_{21}^{+} \right\rangle = -1 \tag{3.141}$$

which coincidences with $c_2 = \kappa_2 = -1$ in Sun's formula for the 2D homogenous case.

This gives an alternative format for the proposed formula for the 2D homogenous case,

$$P(\beta) = [\psi_0(\beta) - \psi_2(\beta)] \cdot c_1 \int_{\mathbf{T}} d\mathbf{t} \tag{3.142}$$

The above equation is exactly the same as (3.139), since $\psi_e(\beta)$ is equal to $\psi_e^*(\beta)$ in the homogenous case.

In general, we may express the proposed formula (3.126) in the following format:

$$\begin{aligned} P(\beta) &= \int_{\mathbf{T}} [\psi_0(\beta) + \psi_2(\beta) \cdot c_2] \cdot c_1 d\mathbf{t} \\ &= \int_{\mathbf{T}} [\psi_0(\beta) - \psi_2(\beta)] \cdot c_1 d\mathbf{t} + \int_{\mathbf{T}} \psi_2(\beta) \cdot c_3 \cdot c_1 d\mathbf{t} \end{aligned} \tag{3.143}$$

in which $c_3 = c_2 + 1$, the first term and the second term represent the probability associated with the homogeneous component and the non-homogeneous component of the random field, respectively.

3.5 Probability Associated with Boundaries and Endpoints

As mentioned in section 3.3.3 and shown by Figures 3.4 and 3.5, equation (3.43) only considers the points in the space spanned by $\mathbf{n}_1$, $\mathbf{n}_2$, ..., $\mathbf{n}_m$, the space normal to the

space spanned by $\mathbf{E}_1$, $\mathbf{E}_2$, ..., $\mathbf{E}_k$. Therefore, the proposed formula (3.126), which is derived using equation (3.43), is only suitable for the random field without boundary. The probability associated with boundaries and endpoints themselves needs to be considered separately.

3.5.1 Boundaries

For the two-dimensional case, the probability associated with boundaries can easily be obtained by applying Farasyn's (1997) one-dimensional formula. We have,

$$P_b(\beta) = \frac{1}{2}\sum_{i=1}^{n_b}\frac{1}{2\pi}\int_{\mathbf{T}_i}\exp\left(-\frac{\beta^2}{2\left|\mathbf{h}^*\left(\mathbf{t}_i\right)\right|^2}\right)c_1 d\mathbf{t}_i \tag{3.144}$$

where n_b is the number of the boundaries, c_1 is defined by equation (3.115). Since half of the tubes around the boundaries have been considered by the proposed formula (3.126) for the main area of the random field, the factor $\frac{1}{2}$ must be put in front of the right hand side of the above equation.

3.5.2 Endpoints

The formula for the probability associated with endpoints in 2D case can be obtained by slightly revising Farasyn's (1997) endpoint formula. Note that part of the points around the endpoints and making contributions to the maxima probability have been involved in the formulas for main area and boundaries so that we only need to consider the remainder.

At each endpoint i, we define α_i as the angle between the two boundaries. It can

be determined by,

$$\alpha_i = \arccos \frac{\mathbf{E}_a \cdot \mathbf{E}_b}{|\mathbf{E}_a| \cdot |\mathbf{E}_b|} \tag{3.145}$$

in which $\mathbf{E}_a, \mathbf{E}_b$ are the tangential vectors of the two boundaries at the corresponding endpoint and are defined by equation (3.37).

As indicated in Figure 3.6, the shaded area has been considered by the main area and the boundary formulas, while the ratio of the neighborhood points left around the endpoint divided by the total is,

$$\frac{\pi - \alpha_i}{2\pi} \tag{3.146}$$

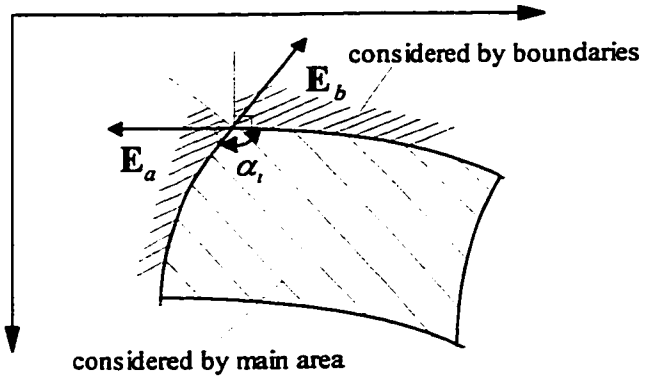

Figure 3.6: Points around Endpoint Contributing to the Maxima Probability in a $2D$ case

By applying Farasyn's (1997) endpoint formula involved in equation (3.119), we

get the equation for the probability associated with endpoints for the 2D case,

$$P_e(\beta) = \sum_{i=1}^{n_e} \frac{\pi - \alpha_i}{2\pi} \cdot \Phi\left(-\frac{\beta}{|\mathbf{h}^*(\mathbf{t}_i)|}\right) \tag{3.147}$$

where n_e is the number of the endpoints; $\mathbf{t}_i$ is the fixed location of the endpoint i in the random field; $\Phi(\cdot)$ is the standard normal distribution function.

3.6 Summary (2D Random Fields)

By adding the probabilities contributed by the main area (3.126), the boundaries (3.144) and the endpoints (3.147) together, the following global formula for the extreme value distribution in a two-dimensional case is obtained,

$$\begin{aligned} P(\beta) &= \int_{\mathbf{T}} \psi_0(\beta) \cdot c_1 d\mathbf{t} + \int_{\mathbf{T}} \psi_2(\beta) \cdot c_2 \cdot c_1 d\mathbf{t} \\ &\quad + \frac{1}{2} \sum_{i=1}^{n_b} \frac{1}{2\pi} \int_{\mathbf{T}_i} \exp\left(-\frac{\beta^2}{2|\mathbf{h}^*(\mathbf{t}_i)|^2}\right) c_1 d\mathbf{t}_i \\ &\quad + \sum_{i=1}^{n_e} \frac{\pi - \alpha_i}{2\pi} \cdot \Phi\left(-\frac{\beta}{|\mathbf{h}^*(\mathbf{t}_i)|}\right) \end{aligned} \tag{3.148}$$

in which,

$$c_2 = \left\langle \mathbf{h}_{11}^+, \mathbf{h}_{22}^+ \right\rangle - \left\langle \mathbf{h}_{12}^+, \mathbf{h}_{21}^+ \right\rangle \tag{3.149}$$

and $c_1, \psi_0(\beta), \psi_2(\beta)$ are defined by equations (3.115), (3.127) and (3.128) respectively. Note that c_1 is a function of the first derivatives of the manifold M, c_2 is a function of the second derivatives of M and it is equal to -1 when the random field is homogeneous. Since the maximum variance of the random field usually occurs

within the domain of the random field, the first term of equation (3.148) is usually dominant, unless the maximum variance occurs in the boundaries of the random field.

3.7 Random Fields with Non-zero Mean

The tube method discussed in the previous sections is based on the assumption that the random field $Z(\mathbf{t})$ has zero mean. Actually, it can easily be applied to random fields with non-zero mean.

Any random field $Z^*(\mathbf{t})$ with non-zero mean can be expressed as the summation of its mean value function $m(\mathbf{t})$ and a random field $Z(\mathbf{t})$ with zero mean:

$$Z^*(\mathbf{t}) = m(\mathbf{t}) + Z(\mathbf{t}) \tag{3.150}$$

Of interest is the extreme value distribution of the random field $Z^*(\mathbf{t})$, that is,

$$P(\beta^*) = P\left(\max_{\mathbf{T}} Z^*(\mathbf{t}) \geq \beta^*\right) \tag{3.151}$$

where β^* is the threshold.

By using the equation (3.150), the above equation can be rewritten as,

$$\begin{aligned} P(\beta^*) &= P\left(\max_{\mathbf{T}} Z(\mathbf{t}) \geq \beta^* - m(\mathbf{t})\right) \\ &= P\left(\max_{\mathbf{T}} Z(\mathbf{t}) \geq \beta(\mathbf{t})\right) \end{aligned} \tag{3.152}$$

Therefore, the original problem is transformed to that for the extreme value

distribution of a random field with zero-mean and time dependent threshold $\beta(\mathbf{t}) = \beta^* - m(\mathbf{t})$. Since the tube method is not limited to the constant threshold problem, the above equation can easily be evaluated by applying the tube method.

It can be concluded that the assumption of the zero-mean random field in the derivation of the tube method does not affect the generality of the method. But in the application of the tube method to a non-zero mean random field, we should keep in mind that a strongly fluctuating mean value function will affect the quality of the tube method, similar to the effect of the fluctuation of the variance function, which will be discussed in detail in the following chapter.

Chapter 4

Verification and Application

4.1 Introduction

In the preceding chapter, the new tube method for the extreme value distribution of a two-dimensional differentiable Gaussian random field is explained. In the following sections, the calculation procedure for the proposed formula is first outlined. Then it is compared with other existing methods for verification purposes; the properties of the tube method are discussed in detail. In section 4.4, the tube method is applied to other practical problems. The global procedure including data analysis, the application to the discretization of a random field and the practical application of the tube method are illustrated for a data set of air pollution measurements.

4.2 Analysis Procedure

A summary of the analysis procedure is given in the flowchart of Figure 4.1.

According to Chapter 3, the discretization format (3.2) of a random field should first be obtained. The expressions of the deterministic functions, $h_i^*(\mathbf{t})$ $(i = 1, 2, ..., n)$ in equation (3.2) have to be known, where n is the dimension of the unit sphere and $\mathbf{t} = (t_1, t_2, ..., t_k) \in \mathbf{T}$, k is the dimension of the random field (considered here, are the cases $k = 1$ or $k = 2$).

With reference to equations (3.115), (3.149) and (3.145), it can be seen that the

parameters c_1, c_2 and α_i in the proposed formula (3.148) are all functions of the derivatives of $h_i(\mathbf{t})$ $(i = 1, 2, ..., n)$, which are defined by equation (3.12):

$$h_i(\mathbf{t}) = \frac{h_i^*(\mathbf{t})}{|\mathbf{h}^*(\mathbf{t})|} = \frac{h_i^*(\mathbf{t})}{\sigma(\mathbf{t})}, \qquad (i = 1, 2, ..., n), \tag{4.1}$$

where $\sigma(\mathbf{t})$ is the standard deviation function of the discretized random field and it is determined by equation (3.4). The remaining parameters, $\psi_0(\beta)$ (3.127) and $\psi_2(\beta)$ (3.128), are time dependent functions of $\sigma(\mathbf{t})$. Therefore, in order to obtain the extreme value distribution, the standard deviation $\sigma(\mathbf{t})$ and the derivatives of $h_i(\mathbf{t})$ $(i = 1, 2, ..., n)$ should be evaluated at any time $\mathbf{t}$ in the domain $\mathbf{T}$, and the corresponding formulas should be expressed explicitly and put into the program directly. As shown in Appendix C, these formulas are quite involved.

Due to the complication of those functions involved in the time integration, a direct integration over the time domain is impossible and a numerical integration method must be used. By comparison, we found that Simpson's formula (Burden et al., 1978) for a 1D case is a comparatively accurate and efficient numerical method. That is,

$$\int_a^b f(t)dt = \Delta t \left[\frac{1}{6}f(a) + \frac{1}{6}f(b) + \frac{4}{6}\sum_{k=1}^{n} f(t_{2k-1}) + \frac{2}{6}\sum_{k=1}^{n-1} f(t_{2k})\right] \tag{4.2}$$

where $t \in [a, b]$, Δt is the time interval; n is the number of the nodal points and t_k are the nodal points within the domain, $t_k = a + k\frac{\Delta t}{2}$. Simpson's formula for a 2D case can be obtained by the extension of the 1D formula to a 2D case. Assuming

that the time domain is a square, we obtain,

$$\int_a^b \int_c^d f(\mathbf{t})d\mathbf{t} = \frac{\Delta t_1 \cdot \Delta t_2}{36} \cdot [\sum f(\mathbf{t}_e) + 2\sum f(\mathbf{t}_b^e) + 4\sum f(\mathbf{t}_b^o) + 4\sum f(\mathbf{t}_m^{e,e}) + 16\sum f(\mathbf{t}_m^{o,o}) + 8\sum f(\mathbf{t}_m^{o,e})] \quad (4.3)$$

in which $\mathbf{t} = (t_1, t_2)$, $t_1 \in [a, b]$, $t_2 \in [c, d]$; $\mathbf{t}_e$ are the endpoints of the time domain, $\mathbf{t}_b^o$ mean the time points on the boundaries and with odd numbers for t_1 or t_2; $\mathbf{t}_m^{e,e}$ are the time points within the domain with even numbers for both t_1 and t_2; other parameters, $\mathbf{t}_b^e$, $\mathbf{t}_m^{o,o}$ and $\mathbf{t}_m^{o,e}$ are time points defined similarly. By choosing the intervals small enough, Simpson's formula can give quite satisfactory accuracy (Burden et al, 1978).

For the calculation procedure, first, at any chosen time point $\mathbf{t}$, derivatives of $h_i(\mathbf{t})$ and the variance $\sigma^2(\mathbf{t})$ can be evaluated by substituting $\mathbf{t}$ in the corresponding formulas given in Appendix C. Second, the matrixes involved in the formulas (3.115), (3.149) and (3.145), $\mathbf{E}$, $\mathbf{H}$, $\mathbf{P}$, which are defined by (3.37), (3.56) and (3.87) respectively, can be calculated. Then the integrations in equation (3.148) can be evaluated by using (4.2) and (4.3). Finally, the summation of the integrations is the extreme value distribution. It should be noted that the probabilities associated with the endpoints, the boundaries and the main part of a random field have to be calculated separately.

The calculation procedure of the tube method is summarized in Figure 4.1.

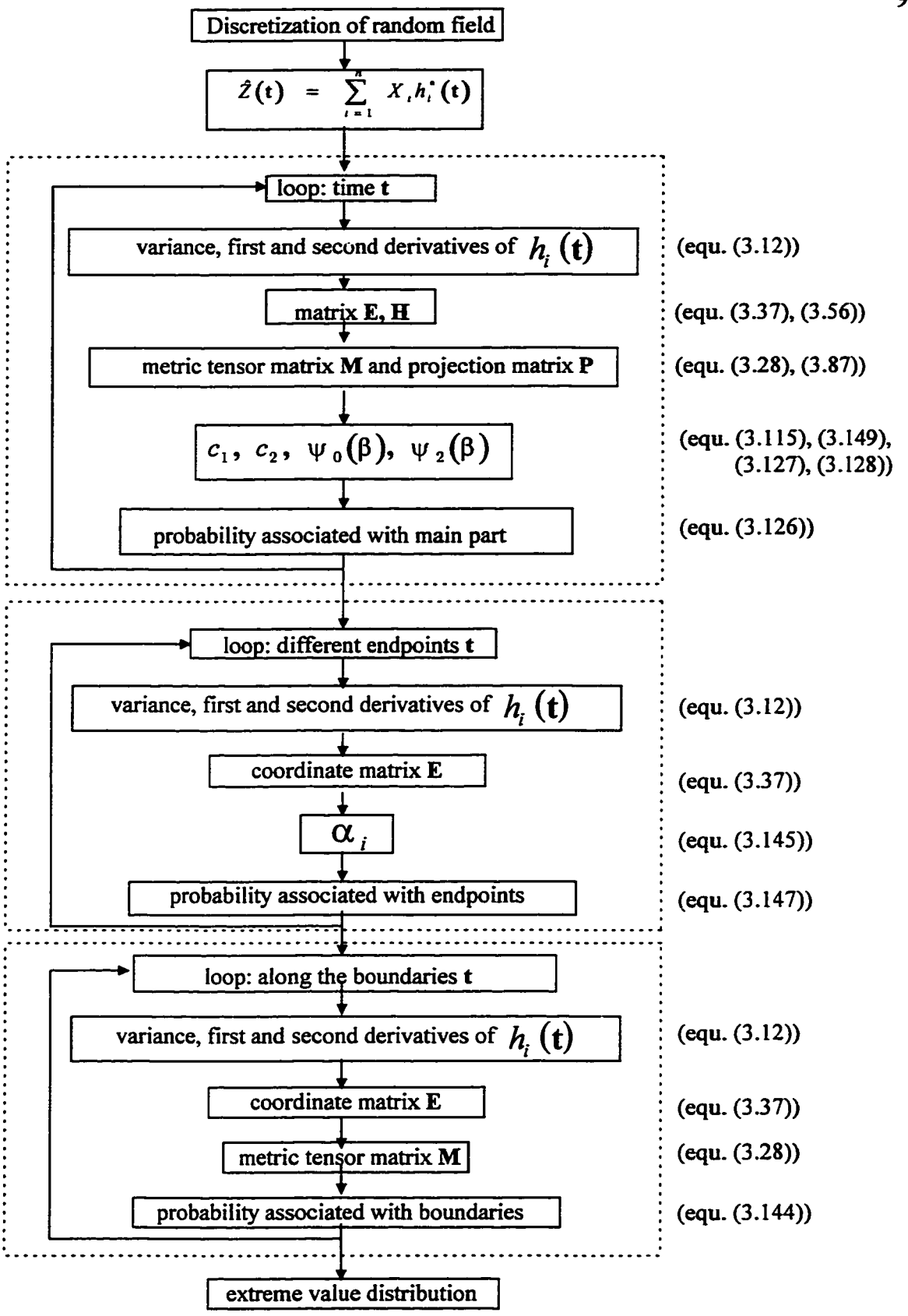

Figure 4.1 Analysis Procedure of the Tube Method

4.3 Verification

The objective of this section is to verify the accuracy of the tube method. Section 4.3.1 introduces a harmonic series model, on the basis of which, different kinds of random fields can easily be constructed. In section 4.3.2, by means of numerical examples, the simulation method is used to verify the accuracy of the tube method in different situations. Section 4.3.3 is devoted to the discussions about the overlap associated with the tube method, which affects the quality of the tube method. Comparisons between the tube method and other existing approaches, Vanmarcke's and Adler's methods, for the maxima of random fields are conducted in sections 4.3.4 and 4.3.5, respectively.

4.3.1 Harmonic Series Model

In order to verify the accuracy of the tube method by numerical examples, we first consider a harmonic series model consisting of cosine and sine terms. The format for a two-dimensional Gaussian random field $Z(\mathbf{t})$ is the following:

$$Z(\mathbf{t}) = \sum_{i=1}^{n} X_{2i-1} a_{2i-1} \cos(\omega_{2i-1} t_1) \sin(\omega_{2i-1} t_2) + X_{2i} a_{2i} \cos(\omega_{2i} t_1) \sin(\omega_{2i} t_2) \quad (4.4)$$

where X_i ($i = 1, 2, ..., n$) are independent Gaussian random variables; a_i, ω_i ($i = 1, 2, ..., n$) are deterministic parameters . It is clear that the harmonic series model has the required format (3.2) for the tube method. By choosing suitable parameters, different kinds of random fields can be obtained. They are very useful to illustrate the geometry properties of the tube method.

4.3.2 Verification by Simulation

a. Simulation Method

Consuming huge amount of computations, the Monte Carlo simulation method is still widely used as an 'exact' method to verify the accuracy of other approximative methods, especially in the area of reliability.

To simulate a Gaussian random field $Z(\mathbf{t})$, ($\mathbf{t} = (t_1, t_2, ..., t_k) \in \mathbf{T}$, generally $k = 1$ or $k = 2$), it is convenience to use the discretized version (3.2) of the random field:

$$\widehat{Z}(\mathbf{t}) = \sum_{i=1}^{n} X_i h_i^*(\mathbf{t}) \tag{4.5}$$

where X_i, $h_i^*(\mathbf{t})$ $(i = 1, 2, ..., n)$ are independent normally distributed random variables and deterministic functions respectively. First, independent normally distributed random numbers can be generated by the transformation from independent identically distributed random numbers, which are generated by a random number generator. Then a number n_z of samples $z(\mathbf{t})$ of the random field can be obtained by substituting the random numbers into the above equation. Assume that n_{ex} of the n samples satisfy the following equation,

$$\max_{\mathbf{T}} z(\mathbf{t}) \geq \beta \tag{4.6}$$

in which β is the threshold, the exceedance probability $P(\beta)$ of $Z(\mathbf{t})$ can be estimated by $\widehat{P}$:

$$P(\beta) \simeq \widehat{P} = \frac{n_{ex}}{n_z} \tag{4.7}$$

As n_z increases, the approximation $\widehat{P}$ becomes better. According to Rubenstein

(1981), for a given level of accuracy in terms of the coefficient of variation (COV) of $\widehat{P}$, the corresponding n_z can be determined by the following equation,

$$COV_{\widehat{P}} \approx \sqrt{\left[n_z \widehat{P}\left(1-\widehat{P}\right)\right]^{-1}} \tag{4.8}$$

Our interest is in the upper tail probability, which is always very small. Obviously, the required n_z must be very large. This means that the computational effort is very large. That is why the simulation method for random fields is a verification method, not a practical one.

b. Homogeneous Random Field

By using the harmonic series model, we can construct the following two-dimensional homogeneous random field,

$$\begin{aligned} Z(\mathbf{t}) &= 0.5\sum_{i=1}^{4}(X_{4i-3}\sin\omega_i t_1 \sin\omega_i t_2 + X_{4i-2}\cos\omega_i t_1 \sin\omega_i t_2 \\ &\quad + X_{4i-1}\sin\omega_i t_1 \cos\omega_i t_2 + X_{4i}\cos\omega_i t_1 \cos\omega_i t_2) \end{aligned} \tag{4.9}$$

in which $t_1,\ t_2 \in [0,1]$; $X_i\ (i=1,2,3,4)$ are independent Gaussian random variables; $\omega_i\ (i=1,2,3,4) = \frac{\pi}{4}, \frac{\pi}{2}, \pi, 2\pi$. Therefore, the dimensions of the unit sphere and the random field are $n = 16$ and $k = 2$ respectively. It can easily be verified that the variance is unity everywhere.

The results from both the tube method and the simulation method are shown in Figure 4.2. Both the simulation interval and the integration interval of the tube method are taken as $\Delta t_i = 0.05\ (i=1,2)$.

In Figure 4.2, TM means the tube method; the line labeled 'TM Without Bound-

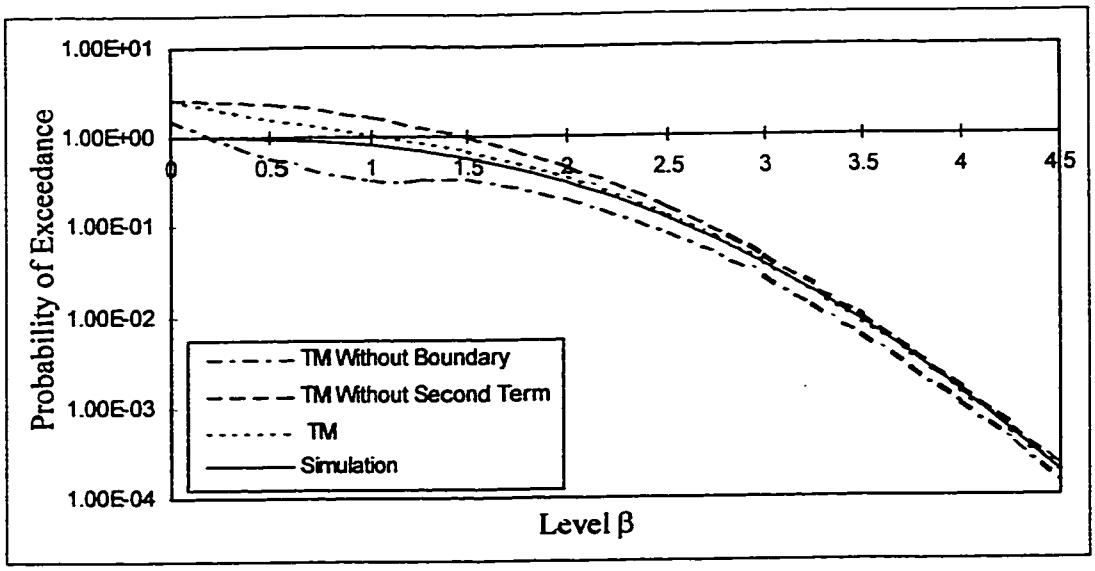

Figure 4.2: Extreme Value Distribution of the Homogeneous Example

ary' denotes the results which are obtained using the tube method, without considering the probability associated with the boundary; the second line in the legend means the results obtained using the tube method but without considering the second term in equation (3.148); the third and fourth lines mean the results obtained using the tube method equation (3.148) and using simulation respectively.

It can seen that, for the large threshold β, the results obtained using the tube method are in excellent agreement with those obtained with the simulation. Furthermore, neglecting the probability associated with boundaries underestimates the exceedance probability in this example. This is due to the large variance along the boundaries and the comparatively small time domain. This shows that, in a general case, the contribution of boundaries and endpoints cannot be ignored. The graph also shows that the second term in equation (3.148), which is related to the curvature

of the manifold M, plays an active role as well. The simulation results are based on 10^6 simulations, which take almost two days on a 80486 PC, in sharp contrast to the few minutes spent on the tube method, to obtain the final results.

c. Non-homogeneous Case

Similarly, a two-dimensional non-homogeneous random field can be constructed as follows,

$$Z(\mathbf{t}) = \sum_{i=1}^{4}(X_{2i-1}\sin\omega_i t_1 \sin\omega_i t_2 + X_{2i}\cos\omega_i t_1 \cos\omega_i t_2) \tag{4.10}$$

where $t_1, t_2 \in [0,1]$; the frequencies $\omega_i\,(i = 1,2,3,4) = \frac{\pi}{4}, \frac{\pi}{2}, \pi, 2\pi$. Then the dimension of the unit sphere is $n = 8$.

Five samples of the variance of $Z(\mathbf{t})$ are plotted in Figure 4.3, in which t_1 is a variable and t_2 are constants. Final results are plotted in Figure 4.4, in which, TM means the tube method; the solid line denotes the results obtained using the simulation; the dashed lines denote the results obtained using the tube method, whereas the second line in the legend means the results do not consider the contribution of the endpoints. It shows that the accuracy of the tube method is very good in this example, even though there is small difference of 18 % at $\beta = 3$ between the results obtained using the two methods. Furthermore, ignoring the probability associated with endpoints causes large errors. The variances shown in Figure 4.3 explain the reason for this. It can be seen that the maxima variance occurs at the endpoints.

Due to the fluctuation of the variance, both the simulation interval and the integration interval of the tube method are chosen as small as 0.02. Because of this, the 10^6 simulations, on which the simulation results are based, take around 10 days on a 80586 100Hz PC, while just a few minutes are needed for the tube method on

the same PC.

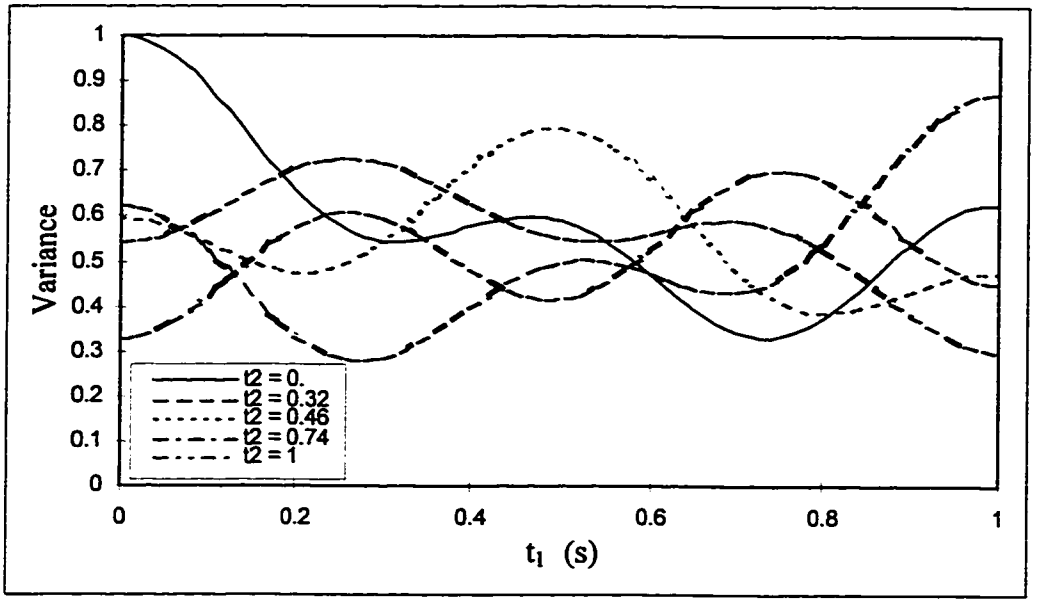

Figure 4.3: Samples of Variances of the Non-homogeneous Example

4.3.3 Effect of Overlap

Even though the tube method is seen to perform very well in the preceding examples, it can also be seen that the tube method slightly underestimates the extreme value distribution in some cases, especially when the threshold is small or the fluctuation of the variance is large. The direct cause for this can be attributed to the 'overlap' associated with the tube method, which has been discussed for the one-dimensional case by Farasyn (1997).

In order to explain the 'overlap' of the tube method, we have to go back to geometric principles. As discussed in section 3.2, for a random field defined by

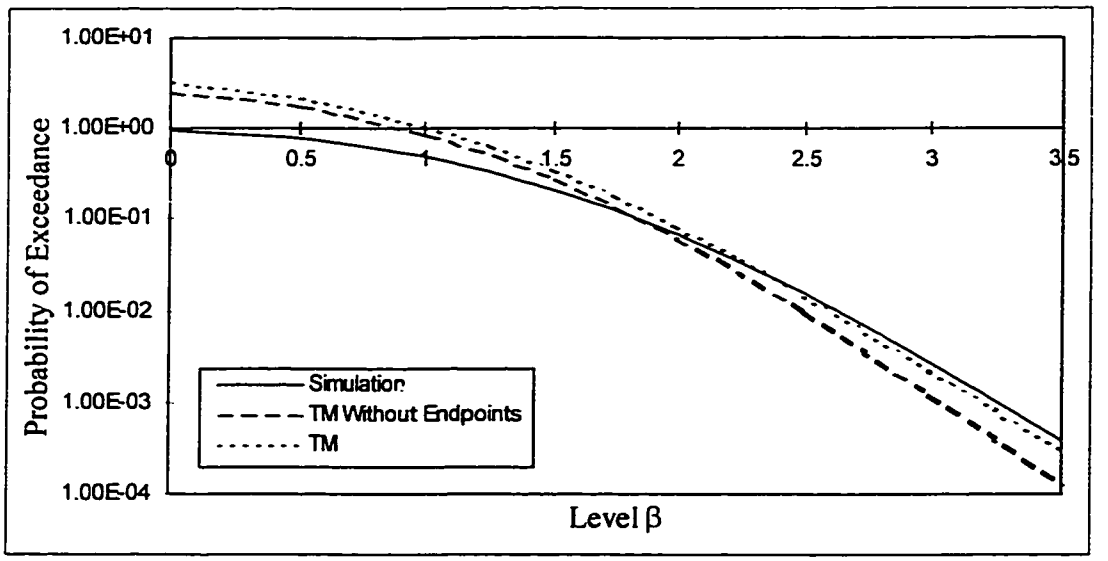

Figure 4.4: Extreme Value Distribution of the Non-homogeneous Example

equation (3.2),

$$\widehat{Z}(\mathbf{t}) = \sum_{i=1}^{n} X_i h_i^*(\mathbf{t}) \tag{4.11}$$

where X_i $(i = 1, 2, ..., n)$ are independent normally distributed random variables and $h_i^*(\mathbf{t})$ $(i = 1, 2, ..., n)$ are deterministic functions, the exceedance probability is related to the ratio of the volume of the neighborhoods $N(M)$ of the manifold M (defined by equation (3.13)) and the surface volume of an n-dimensional unit sphere. The neighborhood $N(M)$ is formed by the points on the surface of the unit sphere within a distance $r(\mathbf{t})$ from the manifold M. And $r(\mathbf{t})$ is determined by

$$r(\mathbf{t}) = \sqrt{2(1 - \frac{\beta}{r_n |\mathbf{h}^*(\mathbf{t})|})} \tag{4.12}$$

where β is the threshold and $|\mathbf{h}^*(\mathbf{t})|^2$ is the variance at a given point $\mathbf{t}$, r_n is a sample

of R_n which is defined by equation (3.6).

There are two kinds of 'overlap'. The first one is caused by too large an area of the manifold M on the surface of a unit sphere or too small a threshold. Obviously, a unit sphere has a certain surface area so that the manifold M on the surface of the unit sphere cannot be too large. Otherwise, the surface area may be double-counted when calculating the volume of the neighborhood $N(M)$. The higher dimensional cases are too complicate to be imagined. It is intuitive and helpful to consider the $n = 2$ or $n = 3$ case. Figure 4.5 depicts the overlap caused by the large area of the manifold M ($k = 2$) in the $n = 3$ case. According to equation (4.12), the distance $r(\mathbf{t})$ is proportional to the threshold β when r_n and $|\mathbf{h}^*(\mathbf{t})|$ are fixed. And the maximum of $r(\mathbf{t})$ is equal to$\sqrt{2}$ as $\beta \to 0$. As shown by the $n = 2$ case in Figure 4.6, even for a manifold M ($k = 1$) with an area that is not too large, an overlap may occur for a large distance $r(\mathbf{t})$ corresponding to a small threshold. However, it is clear that with an increase of the threshold, such an overlap will vanish if the manifold M itself has no overlap. Therefore, the case indicated in Figure 4.6 will usually not be a problem, since our interest lies in the upper tail probability.

Another kind of overlap is related to the radius of curvature of the manifold M. For simplification, we consider a one-dimensional random field ($k = 1$) defined by equation (4.11). The corresponding manifold M on the surface of the unit sphere is a curve, as shown in Figure 4.7. Figure 4.8 depicts an amplified local part of the manifold which has a constant radius of curvature r_c from point a to b. Recall that the area of the tube around the manifold curve on a unit sphere surface includes only the area perpendicular to the curve, which is calculated along the curve. In the case that the distance $r(t)$ along the curve from point a to b is constant and equal to the

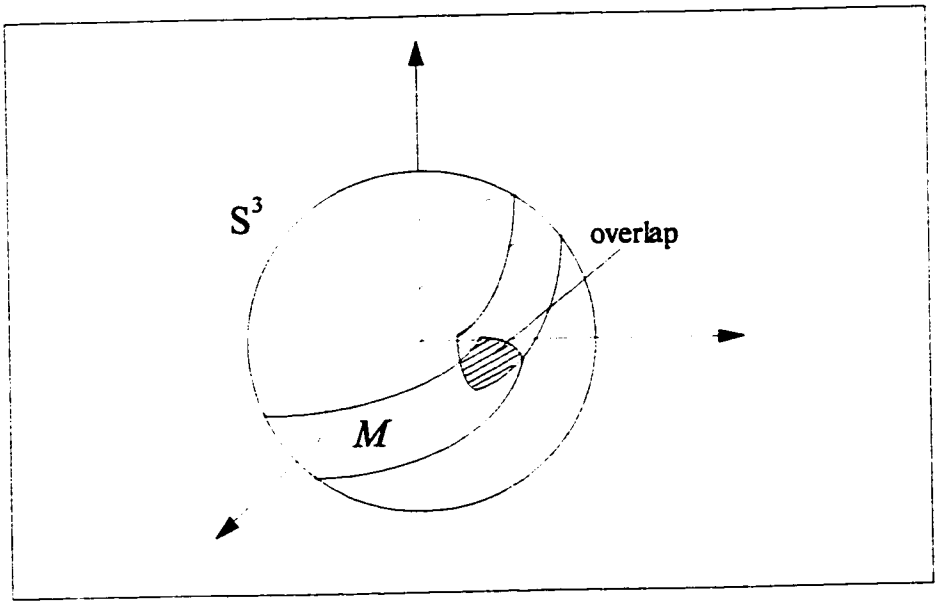

Figure 4.5: Overlap by Large Manifold

radius of curvature r_c, the tube area around the curve from a to b has no overlap as shown in Figure 4.8.

As illustrated in Figure 4.9, overlap does not occur either when $r(t)$ is less than the radius of curvature r_c. But for the case $r(t) > r_c$, which is indicated in Figure 4.10, it can be seen that the c area may be counted several times when calculating the tube area along different parts of the manifold curve. Clearly, r_c can be referred to as a critical radius which imposes a limitation on the overlap that can occur at a given time. Obviously, the threshold β and the radius of curvature of the manifold influence this kind of overlap, which will become more serious when β and the radius of curvature are small. Apart from the effect of β, the radius of curvature

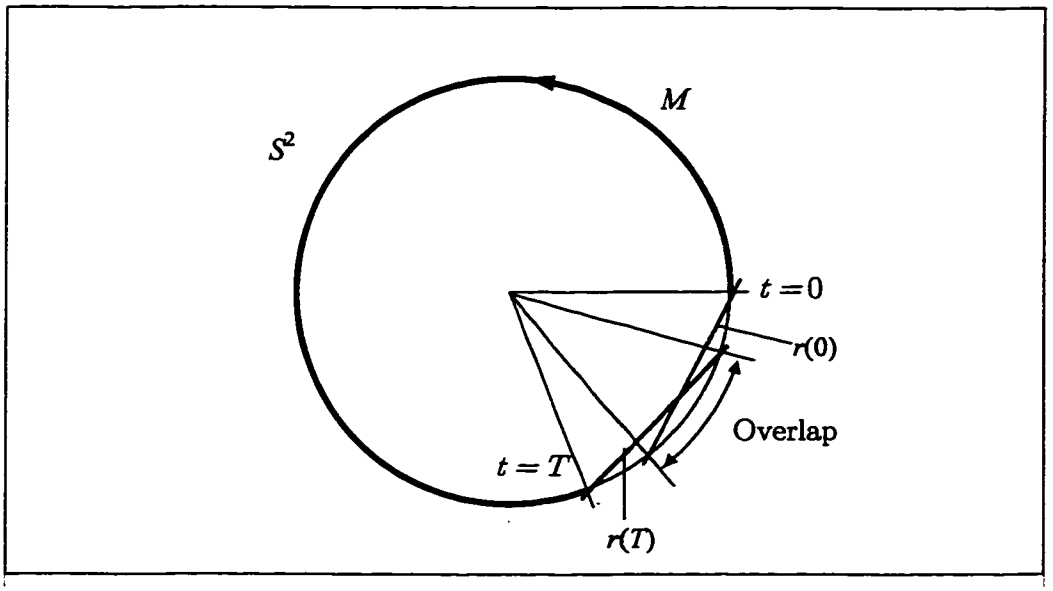

Figure 4.6: Overlap by Small β

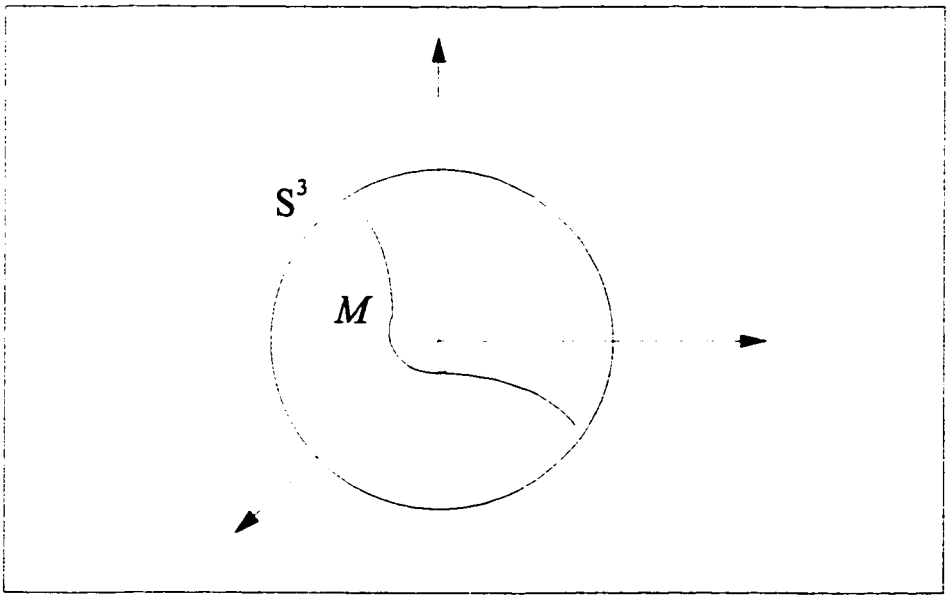

Figure 4.7: One-Dimensional Manifold M on the Surface of a Three-Dimensional Unit Sphere

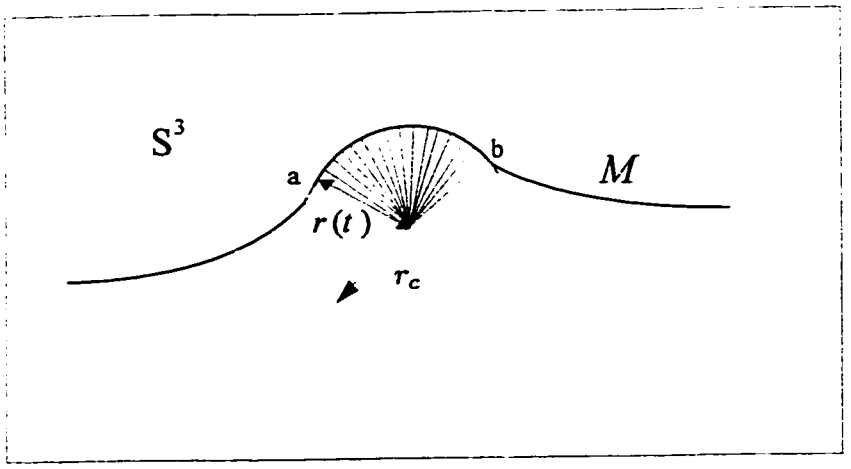

Figure 4.8: Part of Manifold M with Constant $r(t)$ Equal to the Radius of Curvature r_c

is determined by the vector $\mathbf{h^*(t)}$ and the variance $|\mathbf{h^*(t)}|^2$. Before normalization,

$$\mathbf{h(t)} = \frac{\mathbf{h^*(t)}}{|\mathbf{h^*(t)}|} \tag{4.13}$$

the manifold $M^* = \left\{x^*,\ x^* = (h_1^*(\mathbf{t}), h_2^*(\mathbf{t}), ..., h_n^*(\mathbf{t}))^T\right\}$ can be regarded as a path or an area with the length $|\mathbf{h^*(t)}|$in an n-dimensional Euclidean space. By normalization, M^* is projected onto the surface of a unit sphere. And the corresponding projection area is the manifold M. It is clear that if the fluctuation of the variance $|\mathbf{h^*(t)}|$ is large, the manifold M will be more curved than it is before normalization. That is why the tube method applied to a homogeneous random field is more accurate than when it is applied to a non-homogeneous one.

According to the above discussion, it is clear that the tube method has its own limitation. Special attention should be paid to the magnitude of the time domain and the fluctuation of the variance of a random field, in any practical application.

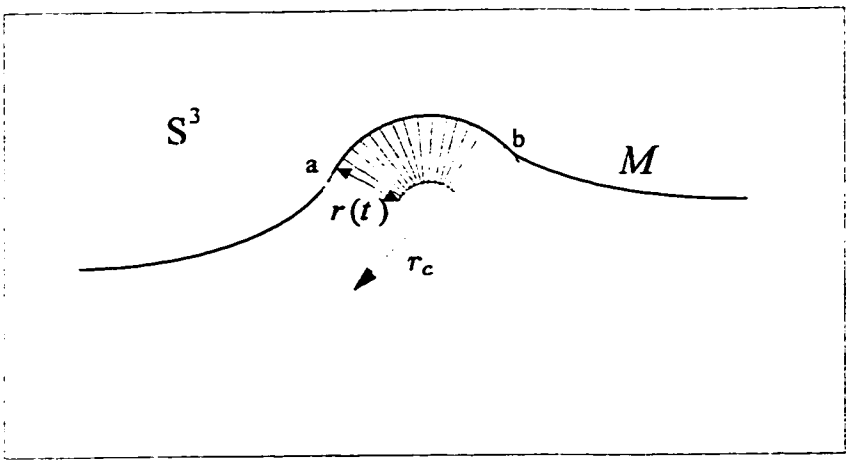

Figure 4.9: Part of the Manifold M with Constant $r(t)$ Less than the Radius of Curvature r_c

Nevertheless, considering that a large random field can be divided into smaller ones and the variance variation in most practical random fields is not too large, the tube method is generally accurate and efficient.

4.3.4 Comparison with Vanmarcke's Approach

Introduced in Chapter 2, Vanmarcke's 2D extreme value equations (Vanmarcke, 1983) is compared with the tube method in the following. Theoretical analysis is performed, followed by a numerical example.

a. Theoretical Analysis

In this section, we review Vanmarcke's asymptotic method applicable only to 2D homogeneous Gaussian random fields and compare it with the tube method.

For a homogeneous Gaussian random field $Z(t_1, t_2)$ with zero mean and standard

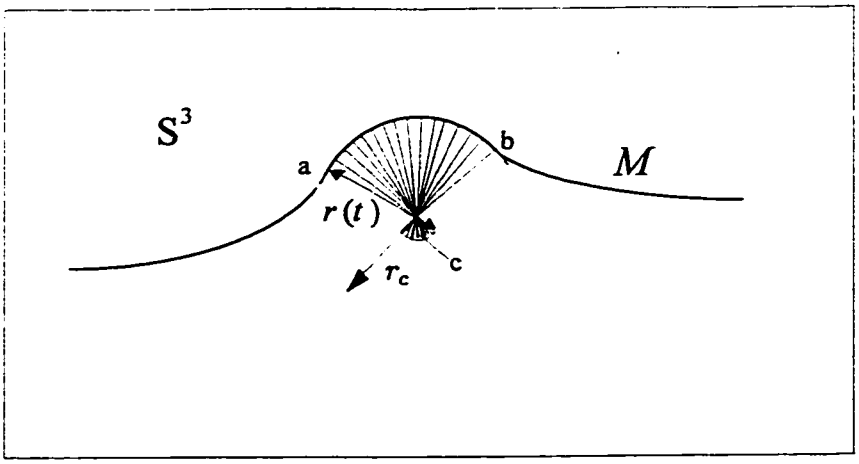

Figure 4.10: Overlap for Part of the Manifold M with Constant $r(t)$ Larger than the Radius of Curvature r_c

deviation σ, the probability density function $f_Z(z)$ of $Z(t_1, t_2)$ is given by

$$f_Z(z) = \frac{1}{\sqrt{2\pi}\sigma} \exp(-\frac{z^2}{2\sigma^2}) \tag{4.14}$$

An approximate series is given by Dwight (1961) for evaluating the cumulative distribution function $F_Z(z)$:

$$F_Z(z) = 1 - \frac{\sigma}{\sqrt{2\pi}z} \exp(-\frac{z^2}{2\sigma^2}) \cdot \Phi(z/\sigma) \quad \text{for large } z/\sigma \tag{4.15}$$

where

$$\Phi(u) \simeq 1 - \frac{1}{u^2} + \frac{3}{u^3} - \frac{1 \cdot 3 \cdot 5}{u^6} + \cdots \tag{4.16}$$

since $\Phi(\beta/\sigma)$ approaches unity when the threshold β is relatively large, $F_Z(\beta)$ can

be approximated by:

$$F_Z(\beta) \simeq 1 - \frac{\sigma}{\sqrt{2\pi}\beta} \exp(-\frac{\beta^2}{2\sigma^2}) \tag{4.17}$$

Then Vanmarcke's basic formula (2.28) can be rewritten as,

$$P_{vm1}(\beta) \sim \frac{1}{2\pi^{3/2}} \left(\frac{\beta^2}{2}\right)^{1/2} \cdot \exp\left(-\frac{\beta^2}{2\sigma}\right) \cdot a_0 \cdot |\mathbf{\Lambda}_{11}|^{1/2} \cdot \sigma^{-3} \tag{4.18}$$

where $P_{vm1}(\beta)$ denotes the extreme value distribution of the random field, β is the threshold, a_0 is the area of the rectangular time domain and $\mathbf{\Lambda}_{11}$ is defined by equation (2.30).

According to equations (2.31) and (3.135), one component λ_{20} of $\mathbf{\Lambda}_{11}$, the spectral moment of $Z(t_1, t_2)$, can be rewritten as,

$$\begin{aligned} \lambda_{20} &= \int \omega_1^2 S_{Z_1 Z_1}(\omega_1)\, d\omega_1 \\ &= \int S_{Z_1' Z_1'}(\omega_1)\, d\omega_1 \\ &= \frac{\partial R_{z_1 z_1}(\mathbf{s}, \mathbf{t})}{\partial s_1 \partial t_1} \Big|_{\mathbf{s}=\mathbf{t}} \\ &= \mathbf{E}_1 \cdot \mathbf{E}_1 \cdot \sigma^2 \end{aligned} \tag{4.19}$$

where Z_1 denotes $Z(t_1, t_2)$ with only t_1 a variable; $R_{Z_1 Z_1}(\cdot)$ is the autocorrelation function defined by equation (2.5) and $\mathbf{E}_1$ is a coordinate vector defined by equation (3.37). Similarly, we can obtain,

$$\lambda_{11} = \mathbf{E}_1 \cdot \mathbf{E}_2 \cdot \sigma^2 \tag{4.20}$$

$$\lambda_{02} = \mathbf{E}_2 \cdot \mathbf{E}_2 \cdot \sigma^2 \tag{4.21}$$

$$\lambda_{40} = \mathbf{h}_{11} \cdot \mathbf{h}_{11} \cdot \sigma^2 \tag{4.22}$$

$$\lambda_{04} = \mathbf{h}_{22} \cdot \mathbf{h}_{22} \cdot \sigma^2 \tag{4.23}$$

$$\lambda_{22} = \mathbf{h}_{11} \cdot \mathbf{h}_{22} \cdot \sigma^2 \tag{4.24}$$

where $\mathbf{h}_{ii}$ $(i = 1, 2)$ are defined by equation (3.55). It can be seen that these parameters involved in the tube method are related to the spectral moments of $Z(t_1, t_2)$. Now $|\mathbf{\Lambda}_{11}|^{1/2}$ can be rewritten as,

$$|\mathbf{\Lambda}_{11}|^{1/2} = \begin{vmatrix} \mathbf{E}_1 \cdot \mathbf{E}_1 & \mathbf{E}_1 \cdot \mathbf{E}_2 \\ \mathbf{E}_2 \cdot \mathbf{E}_1 & \mathbf{E}_2 \cdot \mathbf{E}_2 \end{vmatrix}^{1/2} \cdot \sigma^2 = (\det \mathbf{M})^{1/2} \cdot \sigma^2 \tag{4.25}$$

in which $\mathbf{M}$ is the metric tensor matrix defined by equation (3.28). Insertion of the above equation into (4.18) yields,

$$P_{vm1}(\beta) \sim \frac{1}{2\pi^{3/2}} \left(\frac{\beta^2}{2\sigma^2}\right)^{1/2} \cdot \exp\left(-\frac{\beta^2}{2\sigma^2}\right) \cdot a_0 \cdot (\det \mathbf{M})^{1/2} \tag{4.26}$$

On the other hand, by applying the tube method to the same random field $Z(t_1, t_2)$ with the domain $\mathbf{T}$, we repeat the first term in equation (3.136),

$$P_{m1}(\beta) = \psi_0(\beta) \cdot c_1 \int_{\mathbf{T}} d\mathbf{t} = \psi_0(\beta) \cdot a_0 \cdot (\det \mathbf{M})^{1/2} \tag{4.27}$$

since the area of the random field with rectangular domain $a_0 = \int_{\mathbf{T}} d\mathbf{t}$ and $c_1 = (\det \mathbf{M})^{1/2}$ which is defined by equation (3.115). $\psi_0(\beta)$ is given by equation (3.127),

$$\psi_0(\beta) = \frac{1}{2\pi^{\frac{k+1}{2}}} \Gamma\left(\frac{k+1}{2}, \frac{\beta^2}{2\,|\mathbf{h}^*(\mathbf{t})|^2}\right) \tag{4.28}$$

where $\Gamma(\cdot)$ is the incomplete gamma function defined by equation (3.129) and it has the following expansion formula (Abramowitz and Stegun, 1972):

$$\begin{aligned}
&\Gamma\left(a, \frac{\beta^2}{2\sigma^2}\right) \\
&= \left(\frac{\beta^2}{2\sigma^2}\right)^{a-1} \exp\left(-\frac{\beta^2}{2\sigma^2}\right) \left[1 + \frac{a-1}{\frac{\beta^2}{2\sigma^2}} + \frac{(a-1)(a-2)}{\left(\frac{\beta^2}{2\sigma^2}\right)^2} + \cdots\right] \\
&\overset{\beta\to\infty}{\approx} \left(\frac{\beta^2}{2\sigma^2}\right)^{a-1} \exp\left(-\frac{\beta^2}{2\sigma^2}\right)
\end{aligned} \tag{4.29}$$

Using the above equation, we have the approximation equation of $\psi_0(\beta)$ for the $k = 2$ case,

$$\psi_0(\beta) \overset{\beta\to\infty}{\approx} \frac{1}{2\pi^{3/2}} \left(\frac{\beta^2}{2\sigma^2}\right)^{1/2} \cdot \exp\left(-\frac{\beta^2}{2\sigma^2}\right) \qquad (k = 2) \tag{4.30}$$

Insertion of it into equation (4.27) yields,

$$P_{m1}(\beta) \sim \frac{1}{2\pi^{3/2}} \left(\frac{\beta^2}{2\sigma^2}\right)^{1/2} \cdot \exp\left(-\frac{\beta^2}{2\sigma^2}\right) \cdot a_0 \cdot \left(\det \mathbf{M}\right)^{1/2} \tag{4.31}$$

which is the same equation as (4.26).

It can be concluded that Vanmarcke's basic formula (2.28) is the same as the first term of our proposed formula (3.148) when the threshold is large and the random field is two-dimensional, homogeneous and Gaussian.

b. Comparison with a Numerical Example

For general purposes, we use Vanmarcke's improved formula (2.32) for the numerical comparison. Considering a 2D homogeneous Gaussian random field $Z(t_1, t_2)$ with zero mean and unit variance, the probability density function $f_R(r)$ and the cumu-

lative probability distribution function $F_R(r)$ of the envelope (Vanmarcke, 1983) of $Z(t_1, t_2)$, in Vanmarcke's improved formula, are given as follows (Vanmarcke, 1983),

$$f_R(r) = r\exp\left(-\frac{r^2}{2}\right), \qquad r \geq 0 \tag{4.32}$$

$$F_R(r) = 1-\exp\left(-\frac{r^2}{2}\right), \qquad r \geq 0 \tag{4.33}$$

The p.d.f. $f_Z(z)$ and the c.d.f. $F_Z(z)$ of $Z(t_1, t_2)$ are given in equations (4.14) and (4.15) respectively. As introduced in Chapter 2, other parameters $\Delta^{(ij)}$and $\varepsilon^{(i)}$ $(i, j = 1, 2)$, defined by equations (2.36), (2.37) and (2.38) respectively, are all related to the spectral moments. According to the foregoing discussion, they can easily be evaluated using $\mathbf{E}_i$ and $\mathbf{h}_{ij}$ $(i, j = 1, 2)$.

We use the example expressed by equation (4.9) once more. Figure 4.11 shows the results obtained using the tube method, Vanmarcke's improved formula and the simulation.

It is clear that the results obtained using Vanmarcke's improved formula coincide perfectly with those obtained using the first term of the proposed formula (3.148) when β is large enough.

Therefore, we can conclude that Vanmarcke's formulas are virtually the same as the first term of the proposed formula for 2D homogeneous Gaussian random fields when the threshold is large. This means that they do not consider the probability associated with endpoints and boundaries of the random field and also neglect the probability related to the curvature of the manifold M (3.13). As illustrated in the preceding sections, these probabilities cannot be ignored in general situations. Fur-

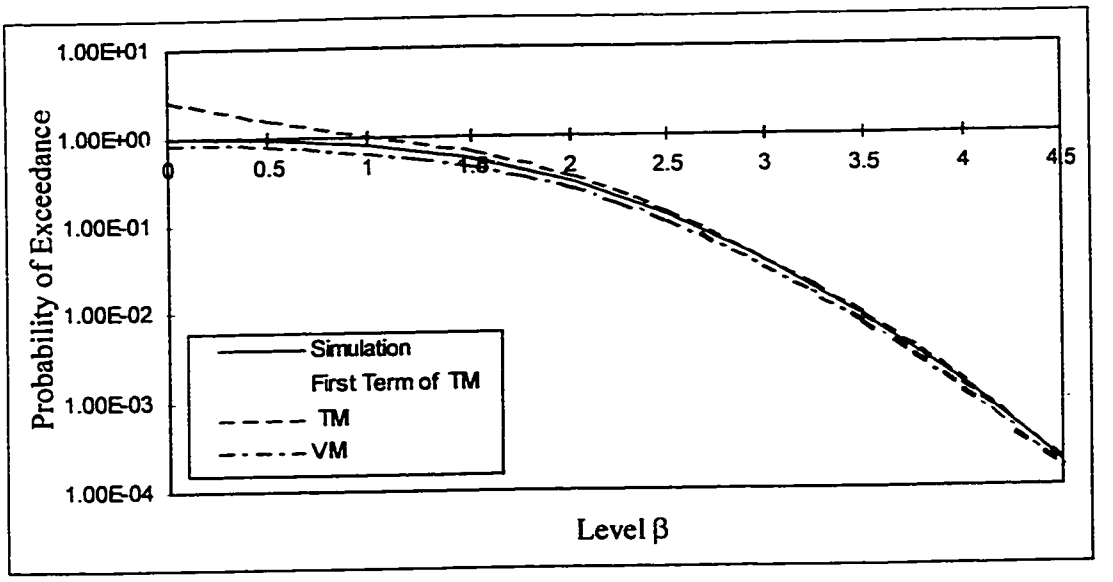

Figure 4.11: Example Results Obtained Using the Tube Method, Vanmarcke's Improved Formula and Simulation for a 2D Homogeneous Gaussian Random Field

thermore, Vanmarcke's approach is only applicable to homogeneous random fields.

4.3.5 Comparison with Adler's Formula

Let $Z(t_1, t_2)$ be a two-dimensional ($k = 2$) homogeneous Gaussian random field with zero mean and unit variance $\sigma^2 = 1$, according to Adler's formula (2.39), it can be seen that this formula is also an asymptotic one and can be rewritten as,

$$P_{ad}(\beta) = P\left(\max_{\mathbf{T}} Z(t_1, t_2) > \beta\right) \sim (2\pi)^{-k/2} \Psi(\beta) (\beta)^k |\mathbf{\Lambda}_{11}|^{1/2} a_0 \qquad (4.34)$$

where β, a_0 are the threshold and the area of the rectangular domain $\mathbf{T}$ of the random field respectively; $\Psi(\beta)$ is defined by equation (2.40) and $\mathbf{\Lambda}_{11}$ is defined by equation

(2.30), $|\mathbf{\Lambda}_{11}|^{1/2}$ is given by equation (4.25):

$$|\mathbf{\Lambda}_{11}|^{1/2} = (\det \mathbf{M})^{1/2} \cdot \sigma^2 = (\det \mathbf{M})^{1/2} \tag{4.35}$$

since the variance is unity.

Substituting the above equation and the expression of $\Psi(\beta)$ (2.40) into (4.34), we obtain for $k = 2$,

$$P_{ad}(\beta) \sim (2\pi)^{-\frac{3}{2}} \beta \exp(-\frac{\beta^2}{2}) \left(\det \mathbf{M}\right)^{1/2} a_0 \tag{4.36}$$

Obviously, it is the same as equation (4.31) for $\sigma = 1$.

This means that Adler's formula is also the same as the first term of our proposed formula (3.148) for two-dimensional homogenous Gaussian random fields with zero mean and unit variance when the threshold is relatively large.

4.4 Practical Application

4.4.1 Introduction

In this section, the tube method is applied to a practical problem involving air pollution. The entire procedure, from the analysis of 'crude' data, the discretization of the random field, to the calculation of the extreme value distribution, is discussed in detail. Difficulties that may occur are pointed out during the analysis. The comparisons between the results obtained using the tube method and those using traditional approaches are made at the end. They show that the tube method is feasible, accurate, efficient and it can easily be applied to practical problems.

4.4.2 Air Pollution Data

In the analysis and control of air qualities, the annual maximum concentration of an air pollutant at a particular location is of major concern. Due to random fluctuations in a variety of weather and emission variables, the maximum concentration at a fixed time is a random variable. For the extreme value distribution of the concentration of an air pollutant, Larsen's procedure (1977) is widely used. In practice, air pollutant concentrations are measured at different points in time. So, they form sequences of data. Larsen's procedure is based on extreme value theory for sequences outlined in section 2.3.2 and the assumption that these sequences are stationary.

Horowitz (1980) pointed out that the stationarity requirement presented a potential difficulty for Larsen's procedure, since air pollutant concentrations exhibit systematic seasonal, weekly, and diurnal periodicities so that non-stationarity should be considered. In a practical example, he developed a non-stationary representation for air pollutant concentration sequences and verified it by the χ^2 test, a periodogram analysis and simulation. Then by extending the extreme value traditional theory to non-stationary sequences, he obtained the corresponding extreme value distribution and indicated that the results obtained using Larsen's procedure were incorrect. In the following, Horowitz's approach is introduced using the air pollution data (Horowitz, 1980). Subsequently, the tube method is applied to this data set and the results are discussed and compared with those obtained by Horowitz's method.

The data set considered consists of air quality data obtained during the St. Louis, Missouri, Regional Air Pollution Study (RAPS). They are daily maximum one-hour average ozone concentrations measured at RAPS Station 109 during 1976. The data

are shown in Figure 4.12.

4.4.3 Horowitz's Approach

In analyzing the maxima of the ozone concentrations, Horowitz (1980) considered the mean value as a time dependent function. As shown in Figure 4.12, the air pollutant concentrations clearly need a time dependent model.

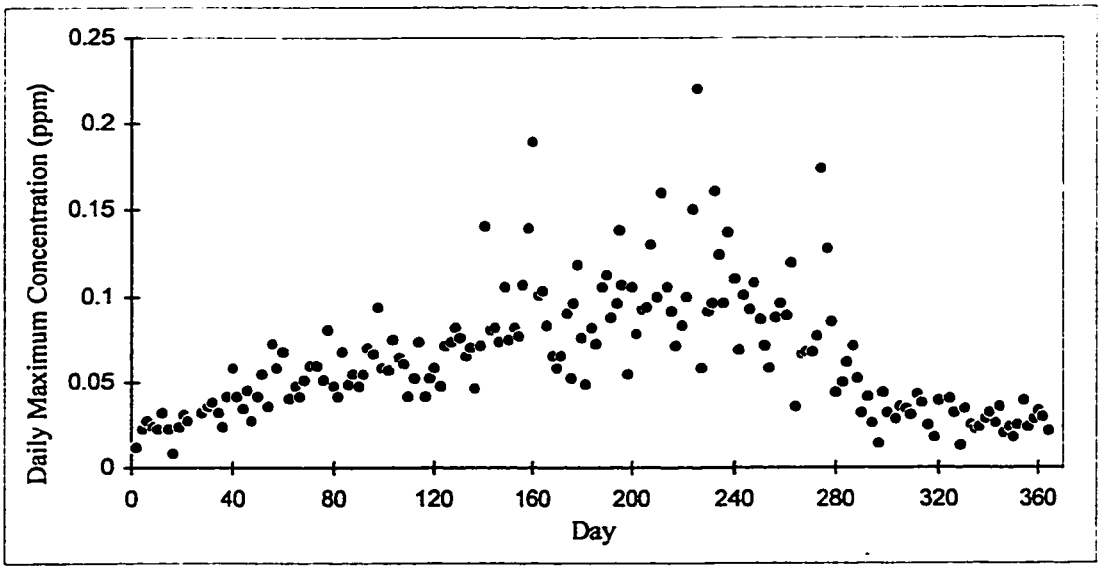

Figure 4.12: Daily Maximum 1-hour Average Ozone Concentrations at RAPS Station 109

Let $Z'(t)$ be the observed maximum 1-hour average ozone concentration (in ppm.) on day t $(1 \leq t \leq 366)$, Horowitz expressed $Z'(t)$ by the following equation:

$$\log Z'(t) = m(t) + X_t \tag{4.37}$$

in which $m(t)$ is a deterministic function of t that gives the mean value of the stochas-

tic process on day t; X_t is a stationary sequence of normally distributed, possibly auto-correlated random variables with zero mean, constant variance σ^2 satisfying equations (2.21) and (2.22), that is,

$$\mathbb{E}(X_t X_{t+k})/\sigma^2 = \rho_k \qquad \text{for all } t \text{ and } k \geq 1 \tag{4.38}$$

$$\sum_{k=1}^{\infty} \rho_k^2 < \infty \tag{4.39}$$

where ρ_k is the coefficient of correlation.

By applying the extreme value theory for sequences outlined in section 2.3.2, Horowitz derived the corresponding asymptotic approximation for the extreme value distribution of $Z'(t)$ for large n (the number of data, $n = 366$ for the set of air pollution data),

$$P\left(\max(Z_1', Z_2', ..., Z_n') \geq \beta\right) = 1 - \exp\{-\exp[-(\beta - b_n)/a_n]\} \tag{4.40}$$

where,

$$a_n = \sigma b_n/(2\log n)^{1/2} \tag{4.41}$$

$$b_n = \exp(\sigma c_n + f_n^*) \tag{4.42}$$

$$f_n^* = \sigma(2\log n)^{-1/2} \log\left\{n^{-1}\sum_{t=1}^{n} \exp\left[(2\log n)^{1/2} m(t)/\sigma\right]\right\} \tag{4.43}$$

and c_n is defined by equation (2.25).

When $m(t)$ is a constant, the above equations (4.40) through (4.43) are almost

the same as those in Larsen's procedure and they describe the Type I extreme value distribution (Leadbetter, et al., 1983).

For the data given in Figure 4.12, according to equation (4.37), Horowitz estimated the following quadratic-mean-value equation,

$$\log Z'(t) = -4.00 + 1.73 \times 10^{-2}t - 4.7 \times 10^{-5}t^2 + X_t \qquad (4.44)$$

in which X_t are normally distributed random variables with zero mean, standard deviation $\sigma = 0.32$ and coefficients of correlation $\rho_k = (0.38)^k$, $\sum \rho_k^2 = 0.17$.

Therefore, the above equation satisfies the equation (4.38) and (4.39), the extreme value distribution can be evaluated directly by equations (4.40) through (4.41). The results are compared with simulation based on equation (4.44) and those from Larsen's procedure by Horowitz (1980). The comparison shows that the asymptotic distribution function (4.40) approximates the simulated distribution well except in lower tails whereas Larsen's procedure overestimates the distribution greatly.

The improvement made by Horowitz is expected since air pollutant concentrations are clearly time dependent. However, this improvement is not enough to reflect the reality of air pollutant concentrations. First, the variance should also be regarded as time dependent, as illustrated in the following section of data analysis. Second, equations (4.40) through (4.41) do not consider the correlation structure between random variables. Horowitz verified that his approach was applicable to random sequences independent or not by neglecting the correlation structure, once the equations (4.38) and (4.39) are satisfied. However, the correlation structure of a stochastic process does affect the extreme value distribution. This is due to limitations of traditional

extreme value theory, but they do not arise in the case of the tube method as shown in the following sections.

4.4.4 Data Analysis

For any practical problem involving random media, it is a basic and important step to find the optimum representation of the actual random field. As illustrated by Horowitz (1980), an unsuitable representation can cause serious errors.

Air pollutant concentrations $Z'(t)$ are usually assumed to be lognormally distributed. By simple transformation, the corresponding normal stochastic process $Z(t)$ can easily be obtained:

$$Z(t) = \log\left[Z'(t)\right] \tag{4.45}$$

Therefore, there is only a need to estimate the first two moments and the correlation function, since they contain all the required probability properties of the normal stochastic process $Z(t)$.

a. Mean Value Function

The mean value function $\widehat{m}_k(t)$ (k : the order of the function) of $Z(t)$ can be estimated by the least square (LS) method, that is, by minimizing the square error between the estimated function $\widehat{m}_k(t)$ and the realizations of $Z(t)$

$$\text{minimize} \quad \sum_{t=1}^{n} [\widehat{m}_k(t) - Z(t)]^2 \tag{4.46}$$

Assume that $\widehat{m}_k(t)$ is a polynomial function,

$$\widehat{m}_k(t) = \sum_{i=0}^{k} a_i t^i \tag{4.47}$$

in which a_i are deterministic parameters; t is time and k is the order of the polynomial function. Differentiation of equation (4.46) with respect to a_i yields the following linear equations,

$$\begin{bmatrix} 1 & \sum_{t=1}^{n} t & \cdots & \sum_{t=1}^{n} t^k \\ \sum_{t=1}^{n} t & \sum_{t=1}^{n} t^2 & \cdots & \sum_{t=1}^{n} t^{k+1} \\ \vdots & \vdots & \ddots & \vdots \\ \sum_{t=1}^{n} t^k & \sum_{t=1}^{n} t^{k+1} & \cdots & \sum_{t=1}^{n} t^{2k} \end{bmatrix} \cdot \begin{Bmatrix} a_0 \\ a_1 \\ \vdots \\ a_k \end{Bmatrix} = \begin{Bmatrix} \sum_{t=1}^{n} Z(t) \\ \sum_{t=1}^{n} Z(t)t \\ \vdots \\ \sum_{t=1}^{n} Z(t)t^k \end{Bmatrix} \tag{4.48}$$

By solving the above equations, the expression of the mean value function can be obtained. Figure 4.13 depicts the log-transformed data $Z(t)$ $(1 \leq t \leq 366)$ and the mean value functions with orders $k = 2$ and $k = 10$. The $k = 2$ is the mean value function used by Horowitz (1980). It can be seen that the 10-th order mean value function fits the realizations $Z(t)$ better, especially for larger $Z(t)$ $(160 \leq t \leq 280)$ and $Z(t)$ around the two ends of the domain. Although Horowitz mentioned that functions with orders greater than 2 were found not to improve the fit obtained using equation (4.44), the comparison in section 4.4.6 will show that the effects of different order mean value functions are considerable.

In the application of the LS method, it is found that the LS method is not accurate at both the beginning and the end of a time domain. For the purpose of accuracy, it can be assumed without loss of generality that $Z(t+$ one year$) = Z(t)$,

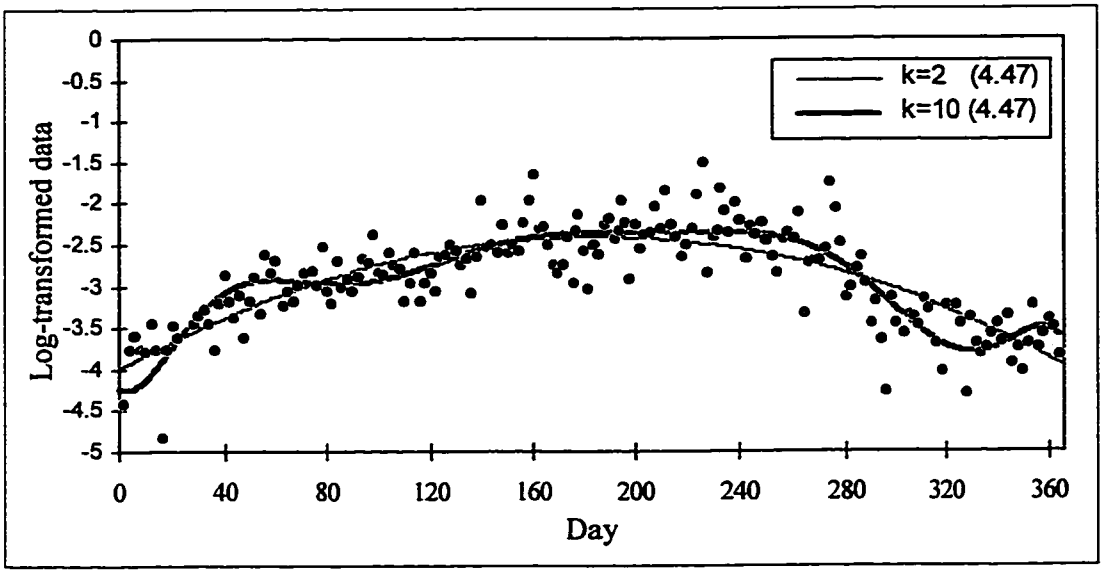

Figure 4.13: Log-transformed Ozone Concentraions and Mean Value Curves

thus we can extend the time domain by copying the data at both ends of the time domain, then the accuracy of the mean value function corresponding to the original time domain is improved.

b. Variance Function

Figure 4.14 shows the zero mean data obtained by :

$$Z(t) - \widehat{m}_{10}(t) \tag{4.49}$$

where $Z(t)$ are the log-transformed data plotted in Figure 4.13, $\widehat{m}_{10}(t)$ is the mean value function of order 10.

To estimate the variance function $\widehat{\sigma}_v(t)$ (v : the order of the function), it is reasonable to assume that variances are constants within short periods of time, for

instance 10 days. Then by using the moving average method (Chatfield, 1984), we obtain the variance shown in Figure 4.15. It is clear that the variance is time dependent as well.

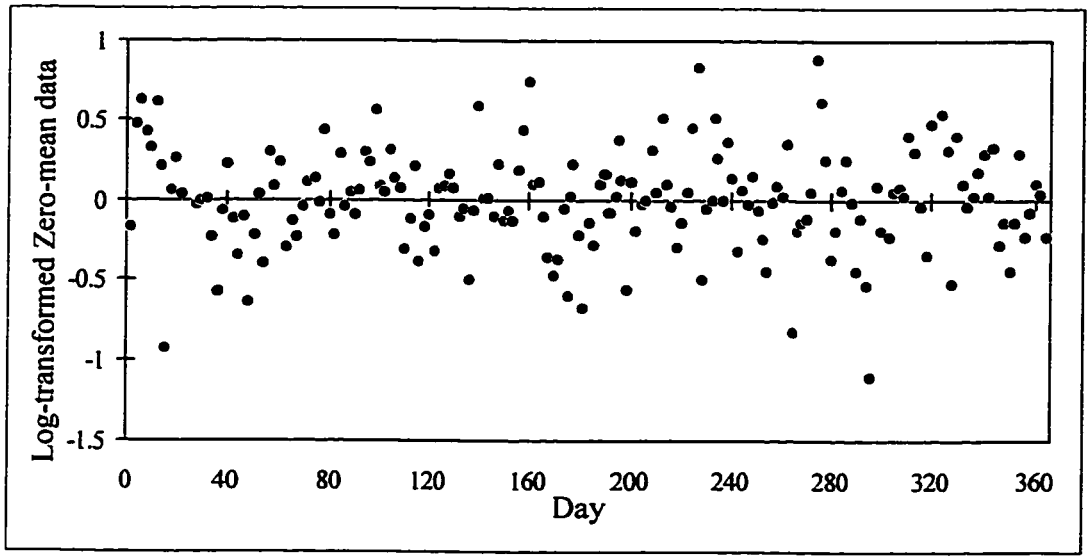

Figure 4.14: Log-transformed Zero Mean Ozone Concentrations

Now the LS method can be applied to obtain standard deviation functions. The 10-th order and 19-th order standard deviation functions are indicated in Figure 4.15. Generally speaking, the larger the number of the parameters used in the standard deviation function, the better the fit will be, but the statistical error on the larger number of estimated parameters will increase. Note that the uncertainties associated with these parameters are not included in the final statistical prediction. These uncertainties may be very large. The horizontal dashed line in Figure 4.15 is $\sigma = 0.32$, which is the standard deviation function used by Horowitz for the extreme value distribution. It will be shown in section 4.4.6 that extreme value distributions

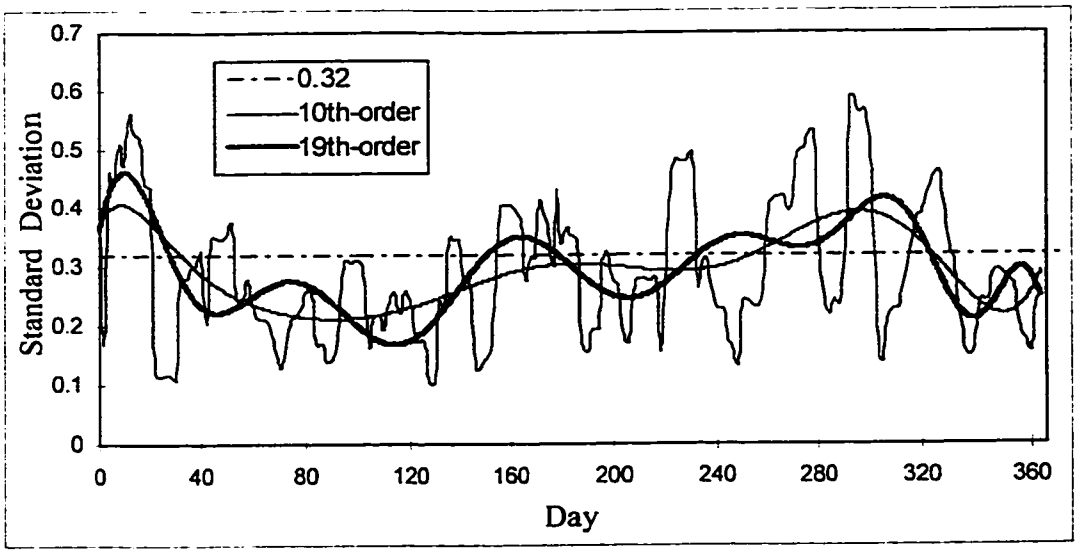

Figure 4.15: Standard Deviation of Transformed Ozone Concentrations and Best fits Curves

based on different standard deviation functions are different, particularly in the upper tail.

Having functions of the mean value and the variance, we can normalize the original process by

$$Y(t) = \frac{Z(t) - \widehat{m}_k(t)}{\widehat{\sigma}_v(t)} \qquad (1 \leq t \leq 366) \tag{4.50}$$

where $Y(t)$ is the normalized process. The statistics of the normalized data corresponding to the 10-th order mean value function and the 10-th order variance function are shown as follows,

$$\mathbb{E}(Y) = 0.0035 \tag{4.51}$$

$$\sigma_Y = 1.0667 \tag{4.52}$$

$$\gamma_1 = -0.128 \tag{4.53}$$

in which $\mathbb{E}(Y)$ and σ_Y are the expected value and the standard deviation of $Y(t)$ respectively; γ_1 is the coefficient of skewness determined by:

$$\gamma_1 = \frac{\sum_{i=1}^{n} (Y_i)^3}{n} \tag{4.54}$$

where Y_i $(i = (1, 2, ..., n),\ n = 366)$ are normalized sequences. These mean that the normalized data $Y(t)$ are almost standard normally distributed.

c. Autocorrelation Function

In practice, sequences of air pollutant concentrations tend to be highly correlated, rather than independent (Patel, 1973). Therefore, the autocorrelation function of air pollutant concentrations should be estimated and considered in extreme value applications.

According to Chatfield (1984), coefficients of correlation ρ_k can be approximated by,

$$\rho_k = \frac{c_k}{c_0} \tag{4.55}$$

with

$$c_k = \frac{1}{n-k} \sum_{i=1}^{n-k} (Y_i \cdot Y_{i+k}), \quad k \geq 0 \text{ and large } n \tag{4.56}$$

where Y_i are the normalized data.

The correlogram of the normalized data $Y(t)$ $(1 \leq t \leq 366)$ corresponding to the 10-th order mean value function and the 19-th order standard deviation function is plotted in Figure 4.16. It shows that concentrations within five days are strongly

correlated. Due to physical reasons, the autocorrelation should approach zero as k increases. But the correlogram becomes more and more irregular for large time interval k, which is due to the decreasing number of the data used for the calculation of the coefficients of correlation as k increases. The coefficients of correlation in equation (4.55) are discrete and therefore cannot be used directly in the tube method. The following function is chosen:

$$R(k) = (0.4436)^k \tag{4.57}$$

which is plotted in Figure 4.17 by a solid line. It can be seen that this equation approximates the correlogram well.

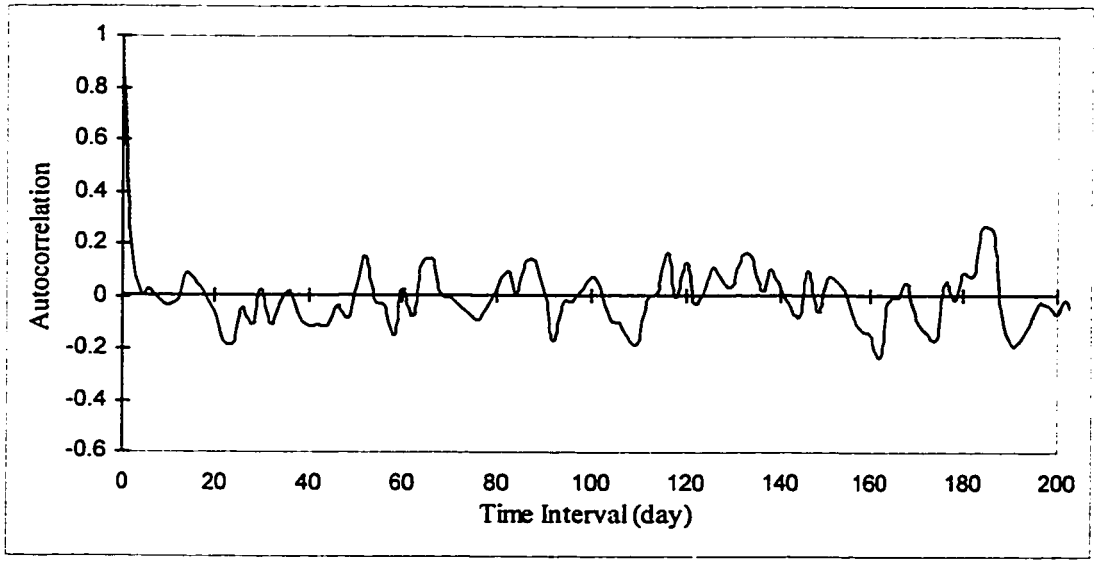

Figure 4.16: Correlogram of the Normalized and Transformed Ozone Concentrations

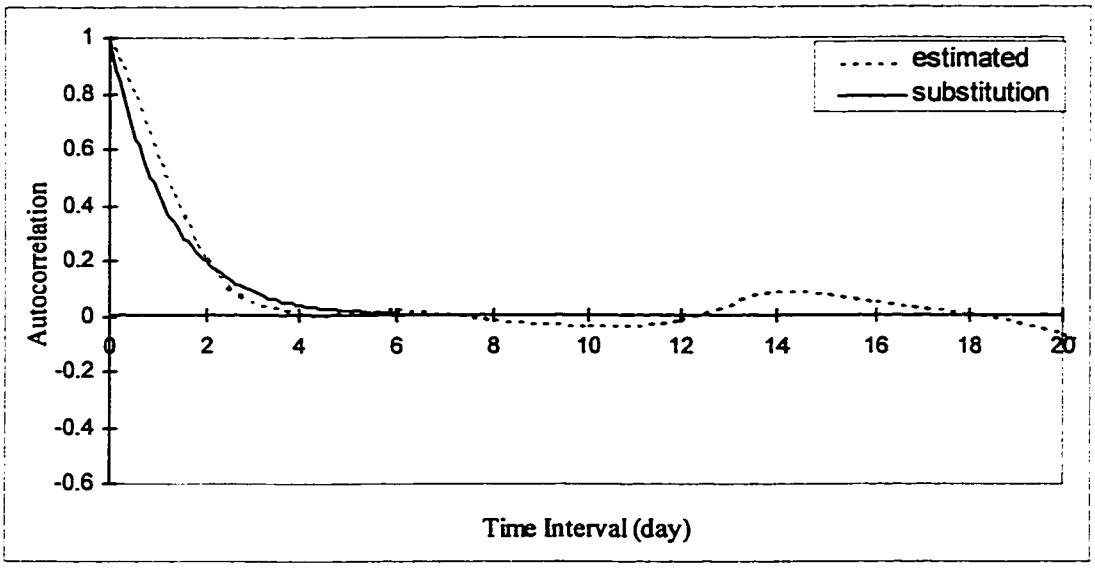

Figure 4.17: Part of the Correlogram and the Fitting Correlation Function

d. Spectral Analysis

The Analysis in the preceding sections is limited to the time domain. A spectral analysis is also necessary. By means of the Fast Fourier Transformation (IMSL, 1996), the spectra for the normalized data $Y(t)$ is calculated and plotted in Figure 4.18. The corresponding first three dominant frequencies ω_i are,

$$\omega_1 = 0.1396; \omega_2 = 0.3840; \omega_3 = 0.8552 \ \ units \tag{4.58}$$

The corresponding spectral power density function $S(\omega)$ can be determined by:

$$S(\omega) = 2 \cdot \sum_{k=0}^{n-1} \rho_k \cdot e^{-i\omega\Delta\tau k}\Delta\tau \tag{4.59}$$

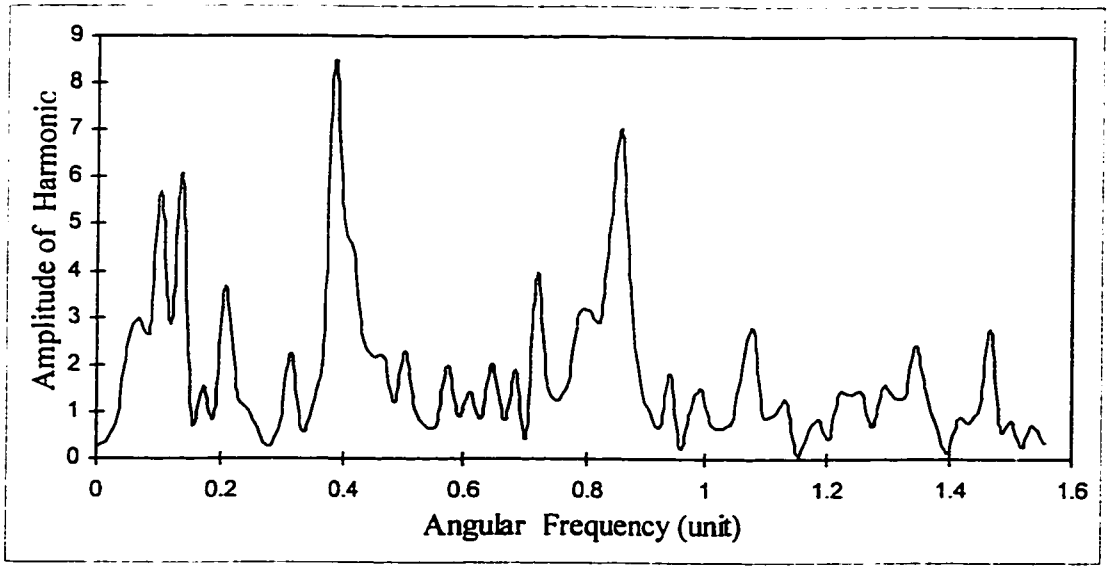

Figure 4.18: Estimated Spectrum for Normalized and Transformed Ozone Concentrations

where coefficients of correlation ρ_k are defined by equation (4.55), $\Delta\tau$ is the time interval, ω denotes the frequency and $i = \sqrt{-1}$. Figure 4.19 depicts the spectral power density function of $Y(t)$. Both of the two figures 4.18 and 4.19 show that basic frequencies of $Y(t)$ concentrate in the domain lower than 2 units.

4.4.5 Discretization of the Random Field

As discussed in section 2.4, the tube method requires the format (3.2) of a random field in terms of random variables. Of the all discretization methods, the Extension Optimal Linear Discretization method (EOLD) (Li and Der Kiureghian, 1993) and the Ground Motion Model method (GMM) (Der Kiureghian and Li, 1996) are the most accurate and efficient. Both these methods are used to discretize the stochastic process of air pollutant concentrations in this section.

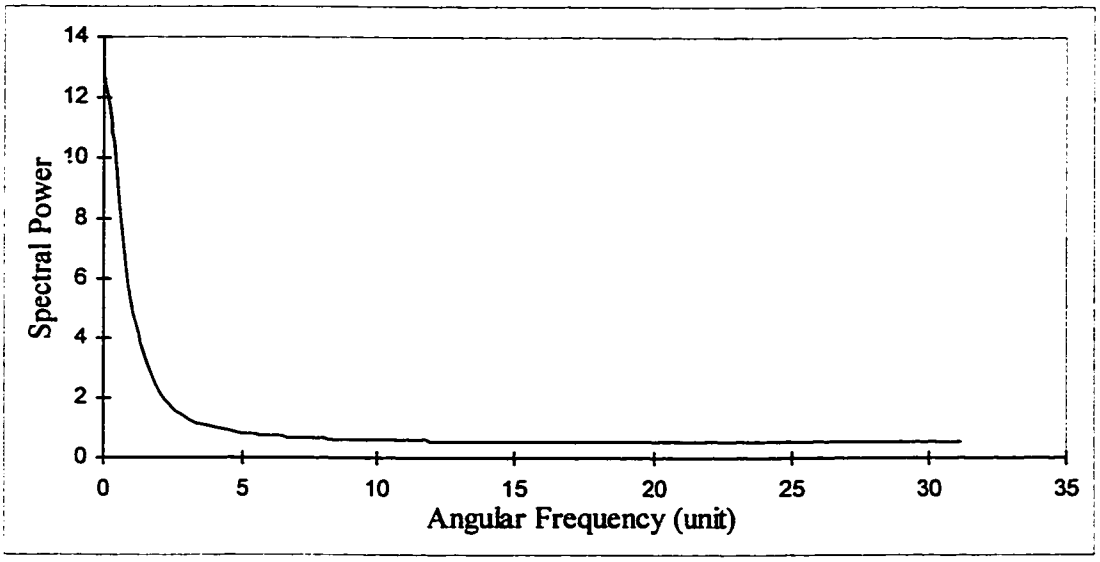

Figure 4.19: Spectral Density of Normalized and Transformed Ozone Concentrations

a. Extension Optimal Linear Discretization Method

Instead of discretizing the original stochastic process $Z(t)$, we can simply discretize the normalized process $Y(t)$ (4.50). First step, the appropriate element size of $Y(t)$ should be determined on the basis of the required level of accuracy and endurable CPU time. As illustrated in Figure 4.17, the correlation length a of $Y(t)$ is about 5 days. According to the discussion in Li (1993) and Wei (1995), a satisfactory accuracy usually is acquired when $\frac{l}{a} \leq 0.1$, where l is the size of each element. Therefore, we select l as either 0.5 day or 0.25 day.

Based on the introduction in section 2.4, $Y(t)$ can now be expressed as,

$$\widehat{Y}(t) = \sum_{i=1}^{n} V_i b_i(t) \tag{4.60}$$

where n is the nodal number and equal to $\frac{366}{l} + 1$, V_i are random variables of nodal

values, and $b_i(t)$ are defined by equation (2.45), in which the components of the covariance matrix $\mathbf{C}$ (2.47) and the vector $\mathbf{d}(t)$ (2.46) are defined by equation (4.57). It is clear that the matrix $\mathbf{C}$ is known at specified nodal points. According to the spectral decomposition method (see section 2.4.2), V_i can be represented in terms of the eigenvalues and eigenvectors of $\mathbf{C}$,

$$\mathbf{V} = \sum_{i=1}^{r} \sqrt{\lambda_i} X_i \mathbf{\Phi}_i \tag{4.61}$$

in which, $r \leq n$, λ_i,$\mathbf{\Phi}_i$ are the eigenvalues and eigenvectors of the covariance matrix $\mathbf{C}$ respectively and they can easily be calculated. While X_i are independently standard normal variables. By inserting the above equation into (4.60), we have the discretization format of $Y(t)$ in terms of X_i,

$$\widehat{Y}(t) = \sum_{i=1}^{r} \frac{X_i}{\sqrt{\lambda_i}} \mathbf{\Phi}_i^T \mathbf{d}(t) \tag{4.62}$$

where the vector $\mathbf{d}(t)$ is defined by equation (2.46).

To make a quantitative assessment of the accuracy of a discretization, the most commonly used measure is to compare the error in variance. Such a comparison is made in Figure 4.20, which shows that the choices of element size $l = 0.25$ day and $l = 0.5$ day both result in sufficient accuracy by noting that the original variance of $Y(t)$ is unity. Furthermore, examples will show that the change from $l = 0.5$ to $l = 0.25$ almost does not affect the extreme value distribution. This means that $l = 0.5$ is enough for a high level of accuracy. Since increasing the number of elements may greatly enhance the computational effort, especially in the spectral

decomposition, a larger element size is preferred if the accuracy is satisfactory.

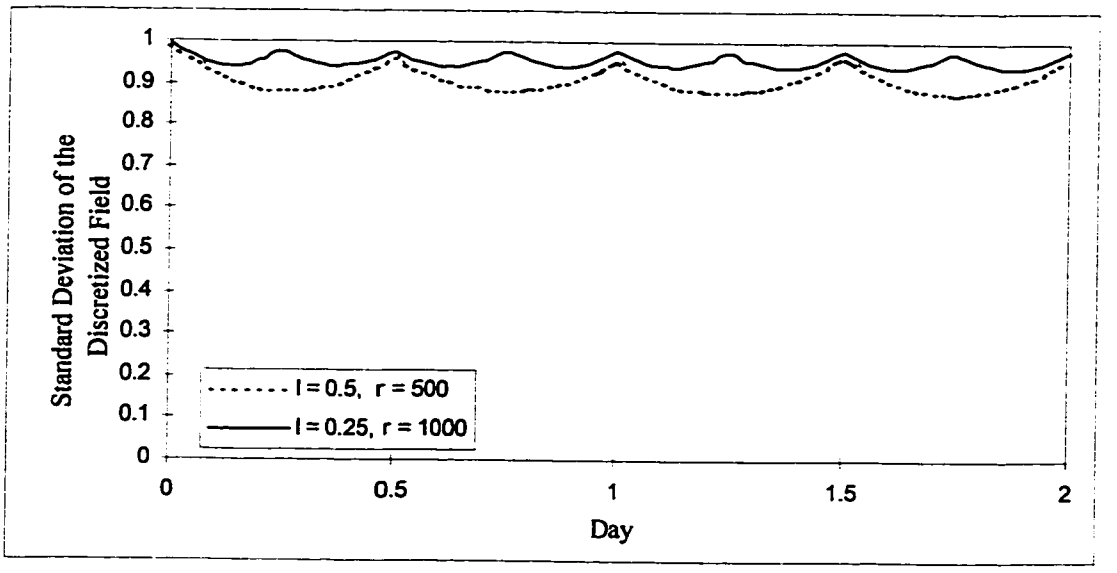

Figure 4.20: The Change of the Standard Deviation of the Random Field After Discretization

Finally, the required discretization format of the original stochastic process is obtained by using equation (4.50),

$$\widehat{Z}(t) = \widehat{m}_k(t) + \widehat{\sigma}_v(t) \sum_{i=1}^{r} \frac{X_i}{\sqrt{\lambda_i}} \mathbf{\Phi}_i^T \mathbf{d}(t) \tag{4.63}$$

Notice that, in the above equation, $\widehat{m}_k(t)$ and $\widehat{\sigma}_v(t)$ are obtained before the discretization, while $\lambda_i, \mathbf{\Phi}_i$and $\mathbf{d}(t)$ are all related to the autocorrelation function (4.57) and they can easily be evaluated by applying (4.57).

According to the discussion, it is clear that the key thing in the discretization of a random field is how to model the correlation structure of the random field.

To apply equation (4.63) to the tube method, we rewrite it as follows using

equation (4.57),

$$\begin{aligned}\widehat{Z}(t) &= \widehat{m}_k(t) + \sum_{i=1}^{r} \frac{X_i}{\sqrt{\lambda_i}} \widehat{\sigma}_v(t)\, \mathbf{\Phi}_i^T \mathbf{d}(t) \\ &= \widehat{m}_k(t) + \sum_{i=1}^{r} \frac{X_i}{\sqrt{\lambda_i}} \widehat{\sigma}_v(t) \sum_{j=1}^{n} \Phi_{ij} R(t - t_j) \qquad (4.64) \\ &= \widehat{m}_k(t) + \sum_{i=1}^{r} x_i h_i^*(t) \qquad (4.65)\end{aligned}$$

where $\Phi_{ij} (i = 1, 2, ..., r;\ j = 1, 2, ..., n)$ are components of $\mathbf{\Phi}_i$.

Then we get,

$$h_i^*(t) = \frac{\widehat{\sigma}_v(t)}{\sqrt{\lambda_i}} \sum_{j=1}^{n} \Phi_{ij} R(t - t_j) \qquad (4.66)$$

$$\begin{aligned}|\mathbf{h}^*(t)| &= \sqrt{\sum_{i=1}^{n} \left(h_i^*(t)\right)^2} \\ &= \widehat{\sigma}_v(t) \left\{ \sum_{i=1}^{r} \frac{1}{\lambda_i} \left[\sum_{j=1}^{n} \Phi_{ij} R(t - t_j) \right]^2 \right\}^{1/2} \qquad (4.67) \\ &= \widehat{\sigma}_v(t) \qquad (4.68)\end{aligned}$$

$$h_i(t) = \frac{h_i^*(t)}{|\mathbf{h}^*(t)|} = \frac{1}{\sqrt{\lambda_i}} \sum_{j=1}^{n} \Phi_{ij} R(t - t_j) \qquad (4.69)$$

Insertion of (4.57) yields,

$$\begin{aligned}\frac{\partial h_i^*(t)}{\partial t} &= \frac{\partial \widehat{\sigma}_v(t)/\partial t}{\sqrt{\lambda_i}} \sum_{j=1}^{n} \Phi_{ij} R(t - t_j) + \frac{\widehat{\sigma}_v(t)}{\sqrt{\lambda_i}} \sum_{j=1}^{n} \Phi_{ij} \frac{\partial R(t - t_j)}{\partial t} \\ &= \frac{1}{\sqrt{\lambda_i}} \sum_{j=1}^{n} \Phi_{ij} R(t - t_j) \left[\frac{\partial \widehat{\sigma}_v(t)}{\partial t} + \widehat{\sigma}_v(t) \ln 0.4436 \right] \qquad (4.70)\end{aligned}$$

$$\frac{\partial h_i(t)}{\partial t} = \frac{1}{\sqrt{\lambda_i}} \sum_{j=1}^{n} \Phi_{ij} R(t - t_j) \ln 0.4436 \tag{4.71}$$

The equations (4.66) through (4.71) can now easily be inserted into the required tube procedure.

b. Ground Motion Model Method

Since this method was originally developed to model earthquake ground motions, it is only applicable to stochastic processes with zero mean. Therefore, we apply it to the discretization of the process:

$$Y(t) = Z(t) - \widehat{m}_k(t) \tag{4.72}$$

For the ground motion model method, the discretization format is given by equation (2.73). To find the discretization format of a stochastic process, it is appropriate to estimate filter properties and modulation functions required for this format, by trying to keep as much information of the probability structure as possible.

Recall that, in the ground motion model method (see section 2.4.3), the output of a filter subject to a white noise input is an acceleration process. Therefore, in the literature, the problem of estimating the parameters of filters is linked to the so called dynamic system identification problem since both the output and the input of the filter are known. As a comparatively accurate and efficient method, the Extended Kalman Filter method (Hoshiya et al., 1984) was originally used to estimate those parameters. Although this method works well for constructed processes, it fails to converge for the air pollutant concentration data. The reason may be due to the strong fluctuation of the air pollutant data and the strict condition for convergence

of the Extended Kalman Filter method.

Another commonly used method for parameter estimations is to minimize the square error between the data $Y(t)$ ($1 \leq t \leq 366$) and the approximations $\widehat{Y}(t)$,

$$\text{minimize} \quad \sum_{t}\sum_{t'}\left\{\mathbb{E}\left[\widehat{Y}(t)\widehat{Y}(t')\right] - Y(t)Y(t')\right\}^2 \qquad (1 \leq t,\, t' \leq 366) \tag{4.73}$$

Obviously, the more time points t, the more accurate the estimations will be. For the ground motion model method, $\widehat{Y}(t)$ is expressed by equation (2.74), therefore (4.73) can be written as,

$$\begin{aligned}
&\sum_{t}\sum_{t'}\left\{\mathbb{E}\left[\sum_{l=1}^{n} Y_l h_l^*(t) \cdot \sum_{k=1}^{n} Y_k h_k^*\left(t'\right)\right] - Y(t)Y(t')\right\}^2 \\
= &\sum_{t}\sum_{t'}\left\{\left[\sum_{l=1}^{n}\sum_{k=1}^{n}\mathbb{E}\left(Y_l \cdot Y_k\right) h_l^*(t)\, h_k^*\left(t'\right)\right] - Y(t)Y(t')\right\}^2 \\
= &\sum_{t}\sum_{t'}\left\{\left[\sum_{l=1}^{n} h_l^*(t)\, h_l^*\left(t'\right)\right] - Y(t)Y(t')\right\}^2
\end{aligned} \tag{4.74}$$

where $1 \leq t,\, t' \leq 366$ and n is the number of the specified nodal points.

By choosing appropriate time points, numerical approaches (such as the Newton method) can be applied to search for the lowest point. But the efficiency is very low due to the fluctuation of the 'crude' data, the large number of unknown parameters and the three summations in the above equation.

In order to improve the efficiency, we can choose the variance function as the modulation function. Thus the number of unknown parameters is reduced. According to equation (2.73), the stochastic process of air pollutant concentrations can be

rewritten as,

$$\begin{aligned}\widehat{Z}(t) &= \widehat{m}_k(t) + \widehat{\sigma}_v(t) \sum_{i=1}^{n} X_i \sum_{j=1}^{k} a_{ij}(t) \\ &= \widehat{m}_k(t) + \widehat{\sigma}_v(t) \sum_{i=1}^{n} X_i h_i^*(t) \\ &= \widehat{m}_k(t) + \widehat{\sigma}_v(t) \widehat{Y}(t) \end{aligned} \tag{4.75}$$

in which k is the number of filters, X_i is a independently standard normal variable, $a_{ij}(t)$ is the shape function corresponding to the i-th random variable and j-th filter, $n = 366$, $h_i^*(t) = \sum_{j=1}^{k} a_{ij}(t)$, and $\widehat{Y}(t) = \sum_{i=1}^{n} X_i h_i^*(t)$.

Now $\widehat{Y}(t)$ is a stochastic process with zero mean and unit variance.

Then the 'crude' data are smoothed. According to equation (4.73), we can see that the essence of this method is to estimate parameters by minimizing the error of correlation structures, while the error is caused by the discretization. Therefore, we can substitute $Y(t)Y(t')$ by a smoothed correlation function defined by equation (4.57). Then we get the alternative format of equation (4.74),

$$\sum_{t} \sum_{t'} \left\{ \left[\sum_{l=1}^{n} h_l^*(t)\, h_l^*\left(t'\right) \right] - R(t-t') \right\}^2 \qquad (t,\, t' = 1, 2, ..., 366) \tag{4.76}$$

Now, the efficiency of searching for the absolute minimum is improved greatly. The parameters corresponding to the minimum of (4.76) are given in table 4.1.

Substituting these parameters into equation (2.68), we get the deterministic approximation of $a_{ij}(t)$ $(i = 1, 2, ..., 366;\ j = 1, 2, ..., k;\ k$: number of filters). Hence, the discretization format (2.74) is obtained and it is ready for the application of the tube method for the extreme value distribution.

Table 4.1: Estimated Parameters of Filter Properties in Ground Motion Model

i	1	2	3
ω_i (frequencies)	0.1384	0.4846	0.8458
ξ_i (damping ratioes)	0.9650	0.7320	0.9400

In comparison with the EOLD, it can be seen that the focus of both methods is to find the optimal approximations of stochastic processes, which contain enough correlation information. The EOLD uses the spectral decomposition method which consumes a lot of computational effort when the element number is large, but it uses the correlation function directly so that it is more accurate. The ground motion model method uses the minimization approach to approximate correlation structures. This approach is much simpler but the accuracy is lower since it is an approximation method. However, if the absolute minimum point in the ground motion model method can be found, this method should have the same accuracy as the EOLD but a higher efficiency.

4.4.6 Results of the Tube Method

With the discretized random fields (4.64) and (4.75), the tube method can be applied to the extreme value distribution of air pollutant concentrations by following the procedure outlined in section 4.2 and the flowchart Figure 4.1.

The final results of the extreme value distributions using different methods are plotted in Figure 4.21:

Curve 1: Horowitz's method (see section 4.4.3), 2-nd order mean value function

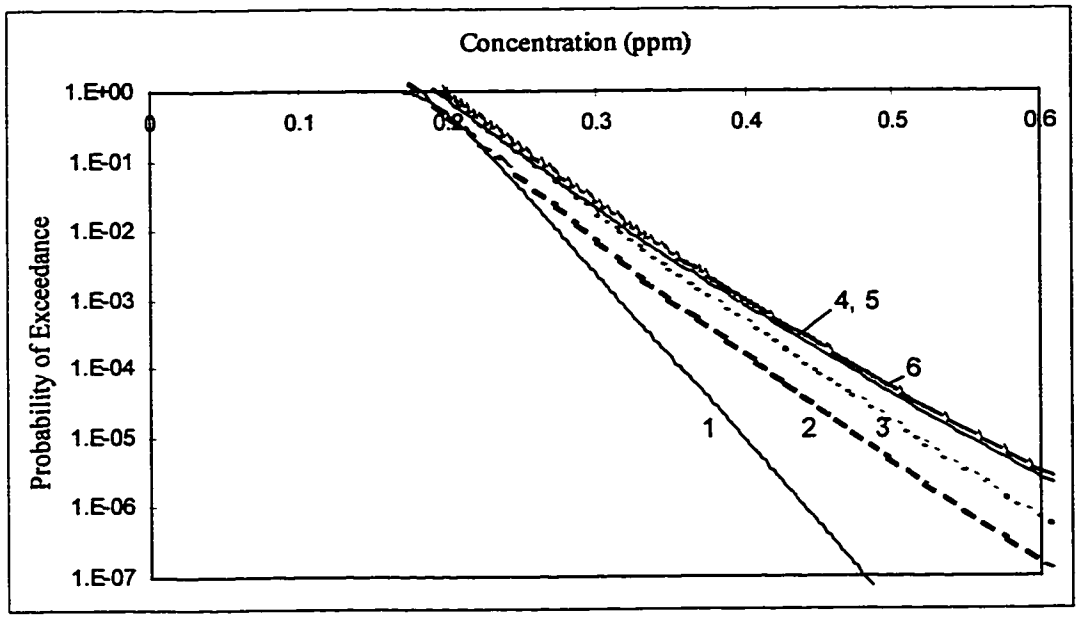

Figure 4.21: Comparison of Extreme Value Distributions of Annual Maximum Ozone Concentrations at RAPS Station 109

(Figure 4.13), constant $\sigma = 0.32$;

Curve 2: the tube method, 2-nd order mean value function (Figure 4.13), constant $\sigma = 0.32$, using the correlation function (4.57) and EOLD;

Curve 3: the tube method, 10-th order mean value function (Figure 4.13), constant $\sigma = 0.32$, using the correlation function (4.57) and EOLD;

Curve 4: the tube method, 10-th order mean value function, 19-th order standard deviation function (Figure 4.15), using the correlation function (4.57) and EOLD;

Curve 5: the tube method, 10-th order mean value function, 19-th order standard deviation function, using the correlation function (4.57) and the ground motion model method, in which the frequencies are given by equation (4.58) and the damping ratios are all assumed to be 0.6;

Curve 6: the tube method, 10-th order mean value function, 19-th order standard deviation function, using the correlation function (4.57) and the ground motion model method, in which the parameters are obtained by equation (4.76) and given in table 4.1.

It is clear that the results from different methods and assumptions are quite different.

Curve 1 and curve 2 are obtained using the same mean value and standard deviation functions. It can be seen that the difference between the two results is large for lower probability levels. Due to limitations of traditional extreme value theory, Horowitz's method does not consider the correlation structure of the random field and the fluctuation of the variance. The effects of the correlation structure of a random field on the exceedance probabilities depend on different situations; on the other hand, according to the analysis in the previous sections, it is obvious that the variance of the air pollutant concentrations needs a time dependent model, similar to the mean value function. It is difficult to say that which one of the two results is more accurate since we have only one sample of the air pollutant concentrations. However, there is no doubt that the tube method is more flexible and feasible.

The distinction between curve 2 and curve 3 is due only to the mean value functions. Although Horowitz (1980) stated that any order of the mean value functions greater than 2 had been found not to improve the fit obtained between mean value functions, the large difference between curves 2 and 3 indicates that the accuracy of a mean value function has a great influence on the exceedance probabilities. The effect of the accuracy of the mean value function on large exceedance probability is almost the same as that on small one, since the two lines are virtually parallel.

The difference between curves 3 and 4 lies only in the variance functions used. It shows that the effect of the accuracy of the variance functions on larger exceedance probability is much smaller than that of the mean value functions. But it increases quickly with the decreasing of the probability. This is coincident with the fact that small exceedance probabilities are sensitive to the peak values of the variance of a random field. Therefore, it is important to use the time dependent model of the variance.

The comparisons among curves 4, 5 and 6 illustrate the accuracies of the two discretization methods, the EOLD and the GMM. The results given by curve 4 is more reliable than those by curve 6, because the former are obtained using directly the correlation function of the stochastic process, in contrast to approximating the correlation function in curve 6. Curve 5 denotes the results obtained by assuming that the spectral of the output in ground motion model is the same as that of filters. The coincidence between curves 4 and 5 indicates that the ground motion model may also be accurate, provided that precise parameters in filter properties can be obtained.

The most reliable results should be those shown by curve 4, the results obtained using the tube method, since they are obtained using a more precise mean value, variance and correlation structure. In addition, the tube method gives the extreme value distribution directly by avoiding making Poisson assumption.

In summary, the tube method is much more flexible to be combined with commonly used data analysis methods, discretization methods and it has no limitations to consider correlation structures and the fluctuation of the variance, therefore, the results obtained using the tube method is more reasonable. Data analysis, the pro-

cess to find the approximation of an original random field, is also important since it is the basis of the analysis.

Chapter 5

Conclusions and Recommendations

5.1 Summary and Conclusions

An important element in probabilistic structural analysis, the extreme value distribution of random fields is studied using the tube method in this thesis. In contrast to traditional extreme value theory based on point-process theory (See Section 2.3), the tube method can directly approximate the extreme value distribution of both homogeneous and non-homogeneous random fields. Furthermore, it can be extended to higher dimensional random fields without much additional effort. Since random fields in practical problems are mostly 1- or 2-dimensional, and since Farasyn (1997) concentrated on the 1-dimensional case, this thesis focuses mainly on the extreme value distribution of 2-dimensional random fields.

Prior to the analysis, important concepts about random fields, traditional extreme value theory and discretization methods of random fields have been introduced in Chapter 2.

It is shown that traditional extreme value theory is based on Poisson assumptions and the verification of the convergence of the exceedance point-process to a Poisson process may consume much computational effort. On the other hand, the extensions of traditional extreme value theory to higher dimensional random fields are always limited to homogeneous cases.

Since the tube method requires the discretized format of a random field, two

accurate and efficient discretization methods are introduced. The Extension Optimal Linear Discretization (EOLD) method is more accurate but it involves an eigenvalue problem, which may be too large a problem for a large number of random variables. The Ground Motion Model (GMM) method, on the other hand, is more efficient and its accuracy depends on the searching results of an absolute minimum point.

In Chapter 3, the tube method has been studied in detail. It is indicated that the problem of the maxima of a random field is related to the volume of neighborhoods of a sub-manifold embedded on the surface of a unit sphere. To evaluate the approximation of the maxima, Weyl's tube volume formula (1939) cannot be used directly since it involves the intrinsic scalar curvature. By following Weyl's derivations (1939) and introducing Breitung's projection method (1997), an accurate formula for the volume of neighborhoods of a 2D sub-manifold is successfully developed, which is much easier to evaluate. Based on this formula, an approximation of the maxima of a 2D random field is derived. The superior efficiency of this approximation lies in that it only involves integrations along a 2D manifold of the surface of a unit sphere and the calculations of the first two derivatives of the manifold, furthermore, it gives the asymptotic extreme value distribution directly without any assumption and verification. Special formulas corresponding to the extreme value distributions associated with endpoints and boundaries are developed as well, which enlarge the feasibility of the tube method. Finally, a global formula for the extreme value distribution of a 2D random field is given.

The objectives of Chapter 4 have been to verify the accuracy and efficiency of the proposed tube method and its feasibility in practical problems.

- The full analysis procedure of the tube method is outlined. It is shown that, although involving complicated formulas, the tube method is easy to program.

- Simulation methods are used to verify the accuracy and efficiency of the proposed formula. Both of the homogeneous and non-homogeneous examples give satisfactory results. For the homogeneous case, the coincidence between the results of the tube method and those of the simulation is perfect for large thresholds. For the non-homogeneous example, the difference between them is 18% at the threshold of 3. On the other hand, the results of the tube method were obtained after a few minutes on an ordinary PC, in comparison to the several days by the results of the simulation.

- The main factor which affects the quality of the tube method, namely the 'overlap' of the manifold corresponding to the random field, is discussed. It is explained that the overlap is related to the fluctuations of the variance or/and the mean value function of the random field. The tube method is not suitable for a random field with strong fluctuations of the variance or/and the mean value function. But this is not a major problem since those fluctuations in practical random fields are usually weak.

- The proposed formula is compared with the existing approaches for the extreme value distribution of a 2D random field. Both the theoretical comparison and the numerical example show that Vanmarcke's and Adler's formulas are almost the same as the first term of our proposed formula for large thresholds. Therefore, the Vanmarcke's and Adler's formulas are only one part of the tube method for the special situation of a 2D homogeneous Gaussian random field

without boundary and without considering the effect of the second derivatives of the manifold M (equation 3.13).

- The tube method is applied to a practical problem for the extreme value distribution of air pollutant concentrations. The whole procedure, from the expression of the original random field, the discretization of the random field to the application of the tube method is discussed. The results obtained using the tube method are compared with those obtained using Horowitz's method (1980) which is based on traditional up-crossing theory. It is indicated that the tube method can easily be combined with data processing methods and discretization methods of random fields and it is more flexible than traditional methods since it can easily consider the correlation structures and the fluctuations of the variance function of the random field. Although it is not suitable to evaluate the accuracy of the tube method due to lack of samples, it is clear that the results using the tube method are much more reasonable. It is also shown that the expression and the discretization of the original random field are important as well, since they affect tail probability greatly. Among the discretization methods, the EOLD method is the first choice for a comparatively small random field.

In summary, we can make the following conclusions about the tube method in comparison to the existing approaches:

- The proposed tube formula for 2D fields can give the approximation of the extreme value distribution directly and accurately with little computational effort.

- It is suitable for any type of 1D and 2D Gaussian random fields, homogeneous or not.

- It can easily be applied to practical problems and it is flexible enough to consider the probability properties of random fields and to be combined with other methods such as discretization methods.

- It is not suitable for random fields with large domains or/and strong fluctuating variances or mean values. But these are not major problems since large random fields can be divided into small ones and the fluctuations of the variances or the mean values in practical random fields are usually weak.

5.2 Recommendations

Since the tube method is a new computational approach for extremes of random fields, additional work on the following topics would considerably enhance the performance of the method in practical situations.

- **Factors affecting the quality of the tube method.** Factors affecting the quality of the tube method, other than the 'overlap' studied in this work (section 4.3.3), should be investigated. For instance, higher order derivatives of random fields, shape of the domain.

- **Various statistics related to the extremes of random fields.** As mentioned at the beginning of Chapter 1, first-passage and cumulative damage are the two main failure mechanisms considered in probabilistic structural analysis. Statistics such as the cumulative excursion time and the duration of a single

excursion of a random field can be of interest in the assessment of the safety of a structure. Therefore, it is necessary to derive the corresponding formulas for these statistics.

- **Extension to non-Gaussian random fields.** Our present work is limited to a Gaussian random field. Since there also exist non-Gaussian random fields in practical situations, it seems desirable to extend the tube method to non-Gaussian random fields. In section 4.4, we already applied the tube method to the log-normally distributed random field of air pollutant data. Other types of random field should be investigated.

- **Extension to higher dimensional ($k \geq 3$) random fields.** According to section 3.3.5, the focus of the extension of the tube method to k-dimensional ($k \geq 3$) cases lies in the evaluation of the integral (3.79) involved in the tube volume formula. Once the explicit expression of this integral for a higher dimension random field can be found, the calculation of the corresponding extreme value distribution is straightforward.

- **Extreme value distribution of non-differentiable random fields.** The present work in this thesis is dealing only with differentiable random fields. Non-differentiable random fields are also needed to model real-world phenomena such as Brownian motion (Adler, 1981). Unfortunately, this is not a simple problem, since even the discretized format (3.2) of a non-differentiable random field is difficult to obtain (Li and Der Kiureghian, 1993).

- **Extreme value distribution of 2D-responses to nonlinear structural or mechanical models.** The extreme value distributions of responses to linear systems can easily be evaluated, since the responses can be expressed directly and explicitly in terms of system parameters and corresponding input. One example is the earthquake ground motion in the discretization method of Ground Motion Model method (section 2.4.3). Responses to nonlinear system cannot be expressed directly. Approximations of responses can be obtained as illustrated by Farasyn (1997) for the 1D case.

Bibliography

[1] Abramowitz, M. and Stegun, I. A., 1972, *Handbook of Mathematical Functions.* Dover Publications, New York.

[2] Adler, R. J., 1981, *The Geometry of Random Fields.* Wiley, New York.

[3] Belyaev, Yu. K. and Piterbarg, V. I., 1972a, *The Asymptotic Formula for the Mean Number of A-points of Excursions of Gaussian Fields Above High Levels* (in Russian). Bursts of Random Fields, Moscow Univ. Press, Moscow. pp62-89.

[4] Belyaev, Yu. K. and Piterbarg, V. I., 1972b, *Asymptotics of the Average Number of A-points of Overshoot of a Gaussian Field Beyond a High Level.* Dokl. Akad. Nauk SSSR, Vol.203, pp309-313.

[5] Breitung, K., 1990, *The Extreme Value Distribution of Non-Stationary Vector Processes.* Proceedings ICOSSAR '89, 5th International Conference on Structural Safety and Reliability, Vol. II, pp1327-1332.

[6] Breitung, K., 1994, *Asymptotic Approximations for Probability Integrals.* Springer, Berlin.

[7] Breitung, K., Maes, M. A., and Huyse, L., 1995, *The Computation of Maxima of Non-Stationary Gaussian Processes*, Proceedings First Intl. Conference on Engineering Computing and Simulation, Changsha, China, November.

[8] Breitung, K., 1997, *Approximations for the Maximum of Non-stationary Gaussian Random Fields*, unpublished paper.

[9] Burden, R. L., Faires, J. D. and Reynolds, A. C., 1978, *Numerical Analysis*, Prindle, Boston.

[10] Chatfield, C., 1984, *The Analysis of Time Series: An Introduction*, Third Edition, Chapman and Hall, London.

[11] Clough, R. W. and Penzien, P., 1975, *Dynamics of Structures*. McGraw-Hill, New York.

[12] Der Kiureghian, A. and Ke, J. B., 1988, *The Stochastic Finite Element Method in Structural Reliability*, Probabilistic Engrg. Mech., 3(2), pp83-91.

[13] Der Kiureghian, A. and Li, C. C., 1996, *A New Method for Seismic Reliability Assessment of Nonlinear Structures*. Chapter 5 in *Reliability-Based Optimal Aseismic Design of Reinforced Concrete Buildings*. A. H-S. Ang, et al. (Eds.), Final Technical Report, CUREe - Kajima Research Project, Phase 2, pp101-142.

[14] Dwight, H. B., 1961, *Tables of Integrals and Other Mathematical Data*, 4th Edition, MacMillan, New York.

[15] Gumbel, E. J., 1958, *Statistics of Extremes*, Columbia University Press, New York.

[16] Farasyn, I., 1997, *Maxima of Non-Stationary Gaussian Random Fields*, Master Thesis, The University of Calgary.

[17] Horowitz, J., 1980, *Extreme Values from a Nonstationary Stochastic Process: An Application to Air Quality Analysis*, Technometrics Vol.22, pp469-478.

[18] Hoshiya, M., Saito, E., 1984, *Structural Identification by Extended Kalman Filter*, J. of Engrg. Mech., Vol. 110, No.12.

[19] Hotelling, H., 1939, *Tubes and Spheres on n-spaces and a Class of Statistical Problems.* Amer. J. of Mathematics, Vol. 61, pp 440-460.

[20] IMSL, (*International Mathematical Statistics Library)*, 1996, Microsoft.

[21] Kendall, M. G., 1961, *A Course in the Geometry of n Dimensions.* Griffin's Statistical Monographs and Courses.

[22] Kreyszig, E., 1968, *Introduction to Differential Geometry and Riemannian Geometry.* University of Toronto Press.

[23] Larsen, R. I., 1977, *An Air Quality Data Analysis System for Interrelating Effects, Standards, and Needed Source Reductions: Part 4.* Journal of the Air Pollution Control Association, Vol.27, pp454-459.

[24] Leadbetter, M. R., Lindgren, G., and Rootzén, H., 1983, *Extremes and Related Properties of Random Sequences and Processes.* Springer, New York.

[25] Li, J., 1992, *Introduction to Earthquake Engineering* (in Chinese), Earthquake Press of China.

[26] Li, C. C. and Der Kiureghian, A., 1993, *Optimal Discretization of Random Fields.* J. of Engrg. Mech., 119(6), pp1136-1154.

[27] Lin, Y. K., 1967, *Probabilistic Theory of Structural Dynamics*, McGraw-Hill, New York, and Krieger Pub., Huntington.

[28] Liu, W. K., Belytschko, T., and Mani, A., 1986, *Random Field Finite Elements*, Int. J. Numerical Methods in Engrg., Vol.23, pp1831-1845.

[29] Maes, M. A., and Breitung, K., 1996, *Direct Approximation of the Extreme Value Distribution of Non-Homogeneous Gaussian Random Fields.* Proceedings of the 15th Intl. Conference on Offshore Mechanics and Arctic Engineering, Vol.2, pp103-109.

[30] Papoulis, A., 1991, *Probability, Random Variables and Stochastic Processes*, McGraw-Hill, New York, 3rd edition.

[31] Powell, A., 1958, *On the Fatigue Failure of Structures due to Vibrations Excited by Random Pressure Fields,* Journal of Acoustical Society of America, Vol.30, (12)

[32] Rice, S. O., 1944, *Mathematical Analysis of Random Noise.* Bell System. Tech. J., Vol.23, pp 282-332.

[33] Rice, S. O., 1945, *Mathematical Analysis of Random Noise.* Bell System. Tech. J., Vol.24, pp 46-156.

[34] Rubinstein, R. Y., 1981, *Simulation and the Monte Carlo Method.* Wiley, New York.

[35] Patel, N. R., 1973, *Comment on a New Mathematical Model of Air Pollution Concentration.* Journal of the Air Pollution Control Association, Vol.23, pp291-292.

[36] Sólnes, J., 1997, *Stochastic Processes and Random Vibrations*, John Wiley & Sons, New York.

[37] Spanos, P. D. and Ghanem, R. G., 1989, *Stochastic Finite Element Expression for Random Media*, J. of Engrg. Mech., ASCE 115(5), pp1035-1053.

[38] Sun, J., 1991, *Significance Levels in Exploratory Projection Pursuit.* Biometrika, Vol.78, pp759-769.

[39] Sun, J., 1993, *Tail Probabilities of the Maxima of Gaussian Random Fields.* The Annals of Probability, Vol.21, No.1, pp 34-71.

[40] Takada, 1990, *Weighted Integral Method in Stochastic Finite Element Analysis*, Pro. Engrg. Mech., Vol.5, No.3.

[41] Thorpe, J. A., 1979, *Elementary Topics in Differential Geometry*, Springer, New York.

[42] Vanmarcke, E. H., 1983, Random Fields: Analysis and Synthesis, The MIT Press, Massachusetts.

[43] Vanmarcke, E. H. and Grigoriu, M., 1983, *Stochastic Finite Element Analysis of Simple Beams*, J. Engrg. Mech. Div., ASCE, 109(5), pp1203-1214.

[44] Wei, X., 1995, *Dynamic Analysis on Stochastic Structures and Reliability Assessment*, (in Chinese), Master Thesis, Zhengzhou University of Technology.

[45] Weyl, H., 1939, *On the Volume of Tubes.* Amer. J. of Mathematics, Vol.61, pp 461-472.

[46] Yao, T. H.-J. and Wen, Y. K. , 1996, *Response Surface Method for Time-variant Reliability Analysis*, Journal of Structural Engineering, Vol.122, pp193-201.

Appendix A

Simplification of $\psi_0(\beta), \psi_2(\beta)$

$\psi_0(\beta), \psi_2(\beta)$ are defined in equations (3.124) and (3.125) respectively, i.e.,

$$\psi_0(\beta) = \frac{\omega_m}{\omega_n} \int_{\frac{\beta}{|h^*(t)|}}^{\infty} J_0(\theta) f_{\chi_n}(r_n)\, dr_n \tag{A.1}$$

$$\psi_2(\beta) = \frac{\omega_m}{\omega_n} \int_{\frac{\beta}{|h^*(t)|}}^{\infty} J_2(\theta) f_{\chi_n}(r_n)\, dr_n \tag{A.2}$$

Introducing the expressions of $J_0(\theta)$, $J_2(\theta)$ and $f_{\chi_n}(r_n)$ (given in equations (3.26), (3.27), and (3.9) respectively), we have,

$$\psi_0(\beta) = \frac{\omega_m}{\omega_n} \int_{\frac{\beta}{|h^*(t)|}}^{\infty} \int_0^{\arccos \frac{\beta}{r_n |h^*(t)|}} \frac{\sin^{m-1}\theta \cos^k \theta}{2^{\frac{n}{2}-1} \cdot \Gamma(\frac{n}{2})} d\theta \cdot r_n^{n-1} \exp(-\frac{r_n^2}{2}) dr_n \tag{A.3}$$

By changing the order of integrations and inserting the expression of ω_n, equation (3.24), we get,

$$\psi_0(\beta) = \frac{1}{2^{\frac{n}{2}-1} \cdot \pi^{\frac{k+1}{2}} \cdot \Gamma(\frac{m}{2})} \int_0^{\frac{\pi}{2}} \int_{\frac{\beta}{\cos\theta\, |h^*(t)|}}^{\infty} r_n^{n-1} \exp(-\frac{r_n^2}{2}) dr_n \cdot \sin^{m-1}\theta \cos^k \theta\, d\theta \tag{A.4}$$

Using Leibnitz rule (Abramowitz and Stegun, 1972),

$$\frac{d}{dc}\left(\int_{a(c)}^{b(c)} f(x,c)\, dx\right) = \int_{a(c)}^{b(c)} \left[\frac{\partial}{\partial c} f(x,c)\right] dx + f(b,c)\frac{\partial b}{\partial c} - f(a,c)\frac{\partial a}{\partial c} \tag{A.5}$$

We obtain that,

$$-\frac{d\psi_0(\beta)}{d\beta} = \frac{1}{2^{\frac{n}{2}-1}\pi^{\frac{k+1}{2}}\Gamma(\frac{m}{2})}\int_0^{\frac{\pi}{2}} \sin^{m-1}\theta\cos^k\theta\frac{\beta^{n-1}}{\cos^n\theta\cdot|\mathbf{h}^*(\mathbf{t})|^n} \cdot\exp\left[\left(1+\tan^2\theta\right)\left(-\frac{\beta^2}{2|\mathbf{h}^*(\mathbf{t})|^2}\right)\right]d\theta \quad (A.6)$$

Making the substitution,

$$u \rightarrow \frac{\beta^2}{2|\mathbf{h}^*(\mathbf{t})|^2}\cdot\tan^2\theta \quad (A.7)$$

gives,

$$-\frac{d\psi_0(\beta)}{d\beta} = \frac{\beta^k}{(2\pi)^{\frac{k+1}{2}}|\mathbf{h}^*(\mathbf{t})|^{k+1}\Gamma(\frac{m}{2})}\exp(-\frac{\beta^2}{2|\mathbf{h}^*(\mathbf{t})|^2})\int_0^\infty u^{\frac{m-2}{2}}\cdot\exp(-u)du \quad (A.8)$$

Note that,

$$\int_0^\infty u^{\frac{m-2}{2}}\cdot\exp(-u)du = \Gamma(\frac{m}{2}) \quad (A.9)$$

This results in,

$$-\frac{d\psi_0(\beta)}{d\beta} = \frac{\beta^k}{(2\pi)^{\frac{k+1}{2}}|\mathbf{h}^*(\mathbf{t})|^{k+1}}\exp(-\frac{\beta^2}{2|\mathbf{h}^*(\mathbf{t})|^2}) \quad (A.10)$$

Similarly, we can obtain:

$$-\frac{d\psi_2(\beta)}{d\beta} = \frac{\beta^{k-2}}{(2\pi)^{\frac{k+1}{2}}|\mathbf{h}^*(\mathbf{t})|^{k-1}}\exp(-\frac{\beta^2}{2|\mathbf{h}^*(\mathbf{t})|^2}) \quad (A.11)$$

By integrations, we get,

$$\psi_0(\beta) = \int_\beta \frac{d\psi_0(x)}{dx} dx + ce1 \tag{A.12}$$

$$\psi_2(\beta) = \int_\beta \frac{d\psi_2(x)}{dx} dx + ce2 \tag{A.13}$$

in which $ce1$ and $ce2$ are constants. It is clear that we have to find the integration areas first then evaluate $ce1$ and $ce2$.

According to the definition of cumulative distribution function (2.1) , we have,

$$1 - P(\max Z(\mathbf{t}) \geq \beta) = 1 - P(\beta) = F(\beta) \tag{A.14}$$

where $F(\beta)$ is the cumulative distribution function.

Integrating both sides of the above equation with respect to β yields,

$$-\frac{dP(\beta)}{d\beta} = \frac{dF(\beta)}{d\beta} = p(\beta) \tag{A.15}$$

in which $p(\beta)$ is the density function. Since,

$$F(\beta) = \int_{-\infty}^{\beta} p(x)dx = 1 - P(\beta) \tag{A.16}$$

This gives,

$$P(\beta) = 1 - \int_{-\infty}^{\beta} p(x)dx = 1 + \int_{-\infty}^{\beta} \left[\frac{dP(x)}{dx}\right] dx \tag{A.17}$$

Recall the relationship between $P(\beta)$ and $\psi_0(\beta), \psi_2(\beta)$, equation (3.126),

$$P(\beta) = \int_{\mathbf{T}} a_1 \psi_0(\beta) + a_2 \psi_2(\beta)\, d\mathbf{t} \tag{A.18}$$

where a_1, a_2 are the coefficients dependent on t. Integration with respect to β gives,

$$\frac{dP(\beta)}{d\beta} = \int_{\mathbf{T}} a_1 \frac{d\psi_0(\beta)}{d\beta} + a_2 \frac{d\psi_2(\beta)}{d\beta} d\mathbf{t} \tag{A.19}$$

Insertion of the above equation into equation (A.17) results in,

$$P(\beta) = 1 + \int_{-\infty}^{\beta} \left[\int_{\mathbf{T}} a_1 \frac{d\psi_0(x)}{dx} + a_2 \frac{d\psi_2(x)}{dx} d\mathbf{t} \right] dx \tag{A.20}$$

Assume,

$$\int_{\mathbf{T}} a_3 d\mathbf{t} = 1 \tag{A.21}$$

We have,

$$P(\beta) = \int_{-\infty}^{\beta} \left[a_3 + \int_{\mathbf{T}} a_1 \frac{d\psi_0(x)}{dx} + a_2 \frac{d\psi_2(x)}{dx} d\mathbf{t} \right] dx \tag{A.22}$$

Then suppose,

$$a_1 \cdot ce1 + a_2 \cdot ce2 = a_3 \tag{A.23}$$

This gives,

$$P(\beta) = \int_{\mathbf{T}} \left[a_1 \left(\int_{-\infty}^{\beta} \frac{d\psi_0(x)}{dx} dx + ce1 \right) + a_2 \left(\int_{-\infty}^{\beta} \frac{d\psi_2(x)}{dx} dx + ce2 \right) \right] d\mathbf{t} \tag{A.24}$$

Comparing the above equation with (A.18), we obtain,

$$\psi_0(\beta) = \int_{-\infty}^{\beta} \frac{d\psi_0(x)}{dx} dx + ce1 \tag{A.25}$$

$$\psi_2(\beta) = \int_{-\infty}^{\beta} \frac{d\psi_2(x)}{dx} dx + ce2 \tag{A.26}$$

Recall that $P(\beta) \rightarrow 0$ with $\beta \rightarrow \infty$, then according to equation (A.18), it can be concluded that,

$$\psi_0(\beta), \psi_2(\beta) \rightarrow 0, with \beta \rightarrow \infty \tag{A.27}$$

since $\psi_2(\beta)$ is always lower than $\psi_0(\beta)$ for the same β. Then the constants in (A.25) and (A.26) can easily be determined,

$$ce1 = -\int_{-\infty}^{\infty} \frac{d\psi_0(x)}{dx} dx \tag{A.28}$$

$$ce2 = -\int_{-\infty}^{\infty} \frac{d\psi_2(x)}{dx} dx \tag{A.29}$$

(A.25) and (A.26) can be rewritten as,

$$\psi_0(\beta) = -\int_{\beta}^{\infty} \frac{d\psi_0(x)}{dx} dx + ce1 \tag{A.30}$$

$$\psi_2(\beta) = -\int_{\beta}^{\infty} \frac{d\psi_2(x)}{dx} dx + ce2 \tag{A.31}$$

Combining the above equations with equations (A.10) and (A.11), we finally

obtain,

$$\psi_0(\beta) = \frac{1}{2\pi^{\frac{k+1}{2}}}\Gamma\left(\frac{k+1}{2}, \frac{\beta^2}{2\left|\mathbf{h}^*(\mathbf{t})\right|^2}\right) \tag{A.32}$$

$$\psi_2(\beta) = \frac{1}{4\pi^{\frac{k+1}{2}}}\Gamma\left(\frac{k-1}{2}, \frac{\beta^2}{2\left|\mathbf{h}^*(\mathbf{t})\right|^2}\right) \tag{A.33}$$

Appendix B

Verification of $c_2 = \langle \mathbf{h}_{11}^+, \mathbf{h}_{22}^+ \rangle - \langle \mathbf{h}_{12}^+, \mathbf{h}_{21}^+ \rangle = -1$ for the 2D Homogeneous Case

The elements of the metric tensor matrix (3.28) are defined by:

$$\begin{aligned} m_{ij}(\mathbf{t}) &= \mathbf{E}_i(\mathbf{t}) \cdot \mathbf{E}_j(\mathbf{t}) \\ &= \frac{\partial \mathbf{h}(\mathbf{t})}{\partial t_i} \cdot \frac{\partial \mathbf{h}(\mathbf{t})}{\partial t_j} \end{aligned} \tag{B.1}$$

As discussed in section 3.4.4, $m_{ij}(\mathbf{t})$ are not functions of $\mathbf{t}$ for the homogeneous case. This means,

$$\frac{\partial m_{ij}(\mathbf{t})}{\partial t_k} = 0 \tag{B.2}$$

It results,

$$\begin{aligned} \frac{\partial m_{ij}(\mathbf{t})}{\partial t_k} &= \frac{\partial \mathbf{h}(\mathbf{t})}{\partial t_i \partial t_k} \cdot \frac{\partial \mathbf{h}(\mathbf{t})}{\partial t_j} + \frac{\partial \mathbf{h}(\mathbf{t})}{\partial t_i} \cdot \frac{\partial \mathbf{h}(\mathbf{t})}{\partial t_j \partial t_k} \\ &= \mathbf{h}_{ik} \cdot \mathbf{E}_j + \mathbf{h}_{jk} \cdot \mathbf{E}_i \\ &= 0 \end{aligned} \tag{B.3}$$

Then we have,

$$\mathbf{h}_{ik} \cdot \mathbf{E}_j = -\mathbf{h}_{jk} \cdot \mathbf{E}_i \tag{B.4}$$

Similarly, from

$$\frac{\partial m_{kj}(\mathbf{t})}{\partial t_i} = 0 \tag{B.5}$$

we can obtain,

$$\mathbf{h}_{ik} \cdot \mathbf{E}_j = -\mathbf{h}_{ij} \cdot \mathbf{E}_k \tag{B.6}$$

For $i = j$, equation (B.4) results in,

$$\mathbf{h}_{ik} \cdot \mathbf{E}_i = 0 \tag{B.7}$$

According to equation (B.6) and equation (B.7), we have,

$$\mathbf{h}_{ii} \cdot \mathbf{E}_k = 0 \tag{B.8}$$

Let $i = 1$, $k = 2$, the differentiation of equation (B.6) with respect to t_2 results in,

$$\mathbf{h}_{12} \cdot \mathbf{h}_{12} = -\frac{\partial \mathbf{h}_{12}}{\partial t_2} \cdot \mathbf{E}_1 \tag{B.9}$$

Similarly, equation (B.7) results in,

$$\mathbf{h}_{11} \cdot \mathbf{h}_{22} = -\frac{\partial \mathbf{h}_{22}}{\partial t_1} \cdot \mathbf{E}_1 \tag{B.10}$$

Since,

$$\frac{\partial \mathbf{h}_{12}}{\partial t_2} = \frac{\partial \mathbf{h}_{22}}{\partial t_1} \tag{B.11}$$

This gives,

$$\mathbf{h}_{12} \cdot \mathbf{h}_{12} = \mathbf{h}_{11} \cdot \mathbf{h}_{22} \tag{B.12}$$

According to the definition of $\mathbf{h}_{ij}^{+}$ (3.109), we have,

$$\left\langle \mathbf{h}_{11}^{+}, \mathbf{h}_{22}^{+} \right\rangle = \tilde{\mathbf{h}}_{11}^{T} \cdot \mathbf{P}^{T} \cdot \mathbf{P} \cdot \tilde{\mathbf{h}}_{22} \tag{B.13}$$

here T presents inversion.

While,

$$\mathbf{P}^{T} \cdot \mathbf{P} = (\mathbf{I} - \mathbf{E}\mathbf{M}^{-1}\mathbf{E}^{T} - \mathbf{y}\mathbf{y}^{T})^{T}(\mathbf{I} - \mathbf{E}\mathbf{M}^{-1}\mathbf{E}^{T} - \mathbf{y}\mathbf{y}^{T}) \tag{B.14}$$

$$\begin{aligned} = \; & \mathbf{I} - 2\mathbf{E}\mathbf{M}^{-1}\mathbf{E}^{T} - 2\mathbf{y}\mathbf{y}^{T} - \mathbf{E}\mathbf{M}^{-1}\mathbf{E}^{T}\mathbf{y}\mathbf{y}^{T} \\ & - \mathbf{y}\mathbf{y}^{T}\mathbf{E}\mathbf{M}^{-1}\mathbf{E}^{T} + \mathbf{E}\mathbf{M}^{-1}\mathbf{E}^{T}\mathbf{E}\mathbf{M}^{-1}\mathbf{E}^{T} \\ & + \mathbf{y}\mathbf{y}^{T}\mathbf{y}\mathbf{y}^{T} \end{aligned} \tag{B.15}$$

Since,

$$\mathbf{E}^{T}\mathbf{y} = \mathbf{y}^{T}\mathbf{E} = 0 \tag{B.16}$$

$$\mathbf{E}^{T}\mathbf{E} = \mathbf{M} \tag{B.17}$$

$$\mathbf{y}^{T}\mathbf{y} = 1 \tag{B.18}$$

This gives,

$$\mathbf{P}^{T} \cdot \mathbf{P} = \mathbf{I} - \mathbf{E}\mathbf{M}^{-1}\mathbf{E}^{T} - \mathbf{y}\mathbf{y}^{T} = \mathbf{P} \tag{B.19}$$

So equation (B.13) can be rewritten in the form,

$$\begin{aligned} \left\langle \mathbf{h}_{11}^{+}, \mathbf{h}_{22}^{+} \right\rangle &= \tilde{\mathbf{h}}_{11}^{T} \cdot \left(\mathbf{I} - \mathbf{E}\mathbf{M}^{-1}\mathbf{E}^{T} - \mathbf{y}\mathbf{y}^{T} \right) \cdot \tilde{\mathbf{h}}_{22} \\ &= \tilde{\mathbf{h}}_{11}^{T} \cdot \tilde{\mathbf{h}}_{22} - \tilde{\mathbf{h}}_{11}^{T} \cdot \mathbf{E}\mathbf{M}^{-1}\mathbf{E}^{T} \cdot \tilde{\mathbf{h}}_{22} - \tilde{\mathbf{h}}_{11}^{T} \cdot \mathbf{y}\mathbf{y}^{T} \cdot \tilde{\mathbf{h}}_{22} \end{aligned} \tag{B.20}$$

Recall that,

$$\widetilde{\mathbf{H}} = \mathbf{M}^{-1} \cdot \mathbf{H} = \frac{1}{|\mathbf{M}|} \begin{bmatrix} m_{22} & -m_{12} \\ -m_{12} & m_{11} \end{bmatrix} \cdot \begin{bmatrix} \mathbf{h}_{11} & \mathbf{h}_{12} \\ \mathbf{h}_{21} & \mathbf{h}_{22} \end{bmatrix} \tag{B.21}$$

Then we have,

$$\tilde{\mathbf{h}}_{11} = \frac{1}{|\mathbf{M}|} \left(m_{22}\mathbf{h}_{11} - m_{12}\mathbf{h}_{21} \right) \tag{B.22}$$

$$\tilde{\mathbf{h}}_{12} = \frac{1}{|\mathbf{M}|} \left(m_{22}\mathbf{h}_{12} - m_{12}\mathbf{h}_{22} \right) \tag{B.23}$$

$$\tilde{\mathbf{h}}_{21} = \frac{1}{|\mathbf{M}|} \left(m_{11}\mathbf{h}_{21} - m_{21}\mathbf{h}_{11} \right) \tag{B.24}$$

$$\tilde{\mathbf{h}}_{22} = \frac{1}{|\mathbf{M}|} \left(m_{11}\mathbf{h}_{22} - m_{21}\mathbf{h}_{12} \right) \tag{B.25}$$

This gives,

$$\begin{aligned} & \tilde{\mathbf{h}}_{11}^T \cdot \mathbf{E}\mathbf{M}^{-1}\mathbf{E}^T \cdot \tilde{\mathbf{h}}_{22} \\ = \; & \frac{1}{|\mathbf{M}|^2} \left(m_{22}\mathbf{h}_{11}^T - m_{12}\mathbf{h}_{21}^T \right) (\mathbf{E}_1, \mathbf{E}_2) \, \mathbf{M}^{-1} \begin{pmatrix} \mathbf{E}_1 \\ \mathbf{E}_2 \end{pmatrix} (m_{11}\mathbf{h}_{22} - m_{21}\mathbf{h}_{12}) \end{aligned} \tag{B.26}$$

Introducing equation (B.7) and (B.8), we have,

$$\tilde{\mathbf{h}}_{11}^T \cdot \mathbf{E}\mathbf{M}^{-1}\mathbf{E}^T \cdot \tilde{\mathbf{h}}_{22} = 0 \tag{B.27}$$

Similarly, we can get,

$$\tilde{\mathbf{h}}_{11}^T \cdot \mathbf{y}\mathbf{y}^T \cdot \tilde{\mathbf{h}}_{22} = \frac{1}{|\mathbf{M}|^2} (m_{22}\mathbf{h}_{11}^T\mathbf{y} - m_{12}\mathbf{h}_{21}^T\mathbf{y}) \cdot \left(m_{11}\mathbf{y}^T\mathbf{h}_{22} - m_{12}\mathbf{y}^T\mathbf{h}_{12} \right) \tag{B.28}$$

Since,

$$\mathbf{y}^T \cdot \mathbf{E}_i = 0 \tag{B.29}$$

Differentiation with respect to t_j results in,

$$-\mathbf{y}^T \cdot \mathbf{h}_{ij} = m_{ij} \tag{B.30}$$

Therefore we can rewrite (B.28) as,

$$\tilde{\mathbf{h}}_{11}^T \cdot \mathbf{y}\mathbf{y}^T \cdot \tilde{\mathbf{h}}_{22} = \frac{1}{|\mathbf{M}|^2} \left(m_{11}m_{22} - m_{12}m_{21}\right)^2 = 1 \tag{B.31}$$

Making substitution (B.27) and (B.31) into (B.20), we have,

$$\left\langle \mathbf{h}_{11}^+, \mathbf{h}_{22}^+ \right\rangle = \tilde{\mathbf{h}}_{11}^T \cdot \tilde{\mathbf{h}}_{22} - 1 \tag{B.32}$$

Following almost the same steps, we can obtain,

$$\left\langle \mathbf{h}_{12}^+, \mathbf{h}_{21}^+ \right\rangle = \tilde{\mathbf{h}}_{11}^T \cdot \tilde{\mathbf{h}}_{22} \tag{B.33}$$

Finally it can be concluded that,

$$\left\langle \mathbf{h}_{11}^+, \mathbf{h}_{22}^+ \right\rangle - \left\langle \mathbf{h}_{12}^+, \mathbf{h}_{21}^+ \right\rangle = -1 \tag{B.34}$$

for the 2D homogeneous case.

Appendix C

Formulas for $\frac{\partial \mathbf{h(t)}}{\partial t_l}$ and $\frac{\partial^2 \mathbf{h(t)}}{\partial t_l \partial t_j}$ in k-D Case

Since $\mathbf{h^*(t)} = (h_1^*(\mathbf{t}), h_1^*(\mathbf{t}), ..., h_n^*(\mathbf{t}))^T$ are known functions, they should be inputted in program, as well as their derivatives, $\frac{\partial h_i^*(\mathbf{t})}{\partial t_l}$ and $\frac{\partial^2 h_i^*(\mathbf{t})}{\partial t_l \partial t_j}$ $(i = 1, 2, ..., n;\ l, j = 1, 2, ..., k)$.

In order to evaluate $\alpha_i, \mathbf{E}$, $\mathbf{H}$, $\mathbf{M}$, $\mathbf{P}$, c_1, $c_2, \psi_0(\beta), \psi_2(\beta)$ at any specified time, $\frac{\partial \mathbf{h(t)}}{\partial t_l}$ and $\frac{\partial^2 \mathbf{h(t)}}{\partial t_l \partial t_j}$ should be expressed explicitly.

According to:

$$\mathbf{h(t)} = \frac{\mathbf{h^*(t)}}{|\mathbf{h^*(t)}|} \tag{C.1}$$

the derivatives of $|\mathbf{h^*(t)}|$ should be expressed first. We have,

$$\frac{\partial |\mathbf{h^*(t)}|}{\partial t_l} = \frac{1}{|\mathbf{h^*(t)}|} \sum_{i=1}^{n} h_i^*(\mathbf{t}) \cdot \frac{\partial h_i^*(\mathbf{t})}{\partial t_l} \tag{C.2}$$

$$\begin{aligned} \frac{\partial^2 |\mathbf{h^*(t)}|}{\partial t_l \partial t_j} &= -\frac{1}{|\mathbf{h^*(t)}|^3} \left(\sum_{i=1}^{n} h_i^*(\mathbf{t}) \cdot \frac{\partial h_i^*(\mathbf{t})}{\partial t_l} \right) \left(\sum_{i=1}^{n} h_i^*(\mathbf{t}) \cdot \frac{\partial h_i^*(\mathbf{t})}{\partial t_j} \right) \\ &\quad + \frac{1}{|\mathbf{h^*(t)}|} \left(\sum_{i=1}^{n} \frac{\partial h_i^*(\mathbf{t})}{\partial t_l} \cdot \frac{\partial h_i^*(\mathbf{t})}{\partial t_j} + \sum_{i=1}^{n} h_i^*(\mathbf{t}) \cdot \frac{\partial^2 h_i^*(\mathbf{t})}{\partial t_l \partial t_j} \right) \end{aligned} \tag{C.3}$$

Differentiation of equation (C.1) with respect to t_l or, t_l and t_j, results in,

$$\frac{\partial h_i(\mathbf{t})}{\partial t_l} = \frac{1}{|\mathbf{h^*(t)}|} \cdot \frac{\partial h_i^*(\mathbf{t})}{\partial t_l} - \frac{h_i^*(\mathbf{t})}{|\mathbf{h^*(t)}|^2} \cdot \frac{\partial |\mathbf{h^*(t)}|}{\partial t_l} \tag{C.4}$$

$$\begin{aligned}\frac{\partial^2 h_i(\mathbf{t})}{\partial t_l \partial t_j} &= \frac{1}{|\mathbf{h}^*(\mathbf{t})|}\cdot\frac{\partial^2 h_i^*(\mathbf{t})}{\partial t_l \partial t_j} - \frac{1}{|\mathbf{h}^*(\mathbf{t})|^2}\cdot\frac{\partial h_i^*(\mathbf{t})}{\partial t_l}\frac{\partial |\mathbf{h}^*(\mathbf{t})|}{\partial t_j} \\ &\quad -\frac{1}{|\mathbf{h}^*(\mathbf{t})|^2}\cdot\frac{\partial h_i^*(\mathbf{t})}{\partial t_j}\frac{\partial |\mathbf{h}^*(\mathbf{t})|}{\partial t_l} - \frac{h_i^*(\mathbf{t})}{|\mathbf{h}^*(\mathbf{t})|^2}\cdot\frac{\partial^2 |\mathbf{h}^*(\mathbf{t})|}{\partial t_l \partial t_j} \\ &\quad +2\frac{h_i^*(\mathbf{t})}{|\mathbf{h}^*(\mathbf{t})|^3}\cdot\frac{\partial |\mathbf{h}^*(\mathbf{t})|}{\partial t_l}\frac{\partial |\mathbf{h}^*(\mathbf{t})|}{\partial t_j} \end{aligned} \tag{C.5}$$

IMAGE EVALUATION TEST TARGET (QA-3)

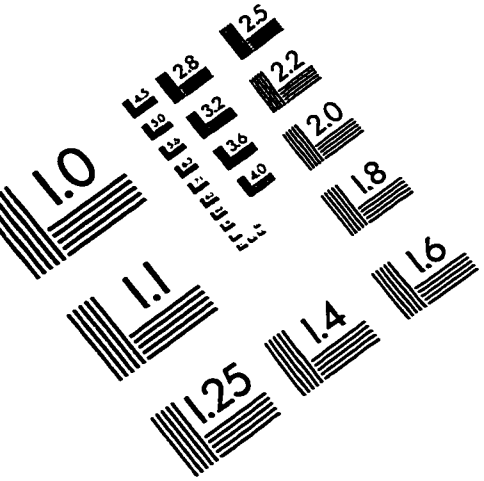

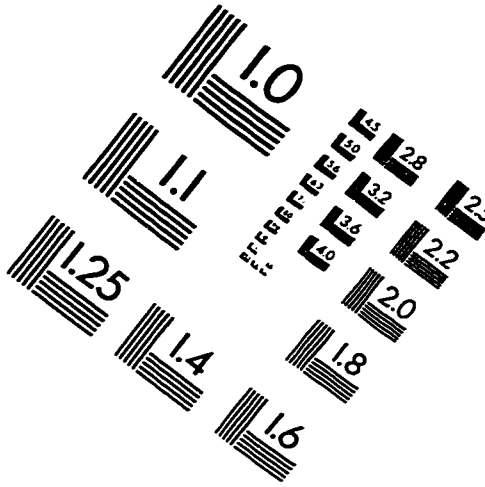

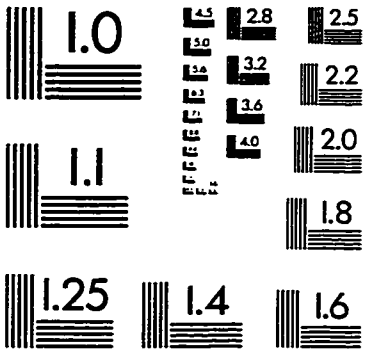

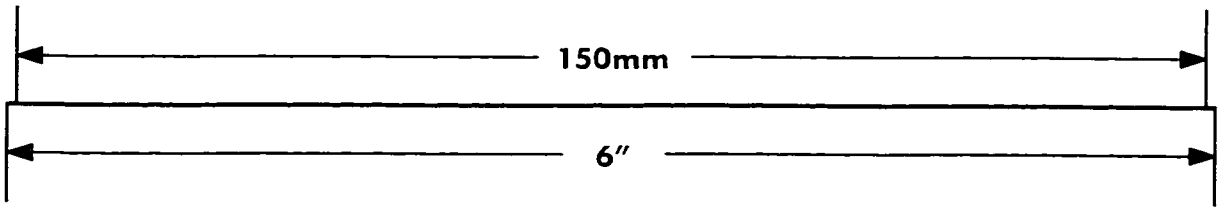

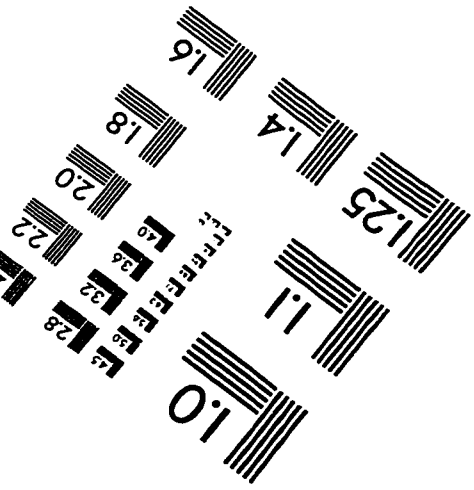

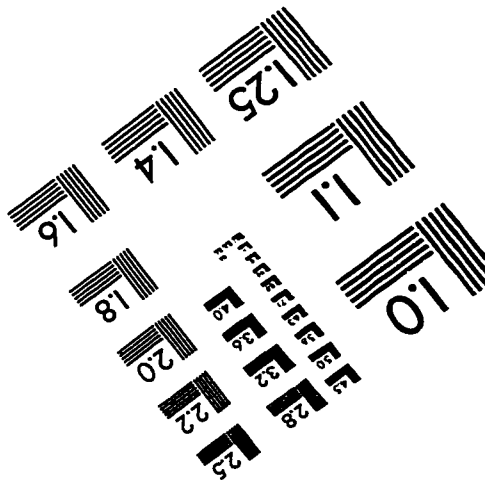

APPLIED IMAGE, Inc
1653 East Main Street
Rochester, NY 14609 USA
Phone: 716/482-0300
Fax: 716/288-5989